Solar Probe:
An Engineering Study

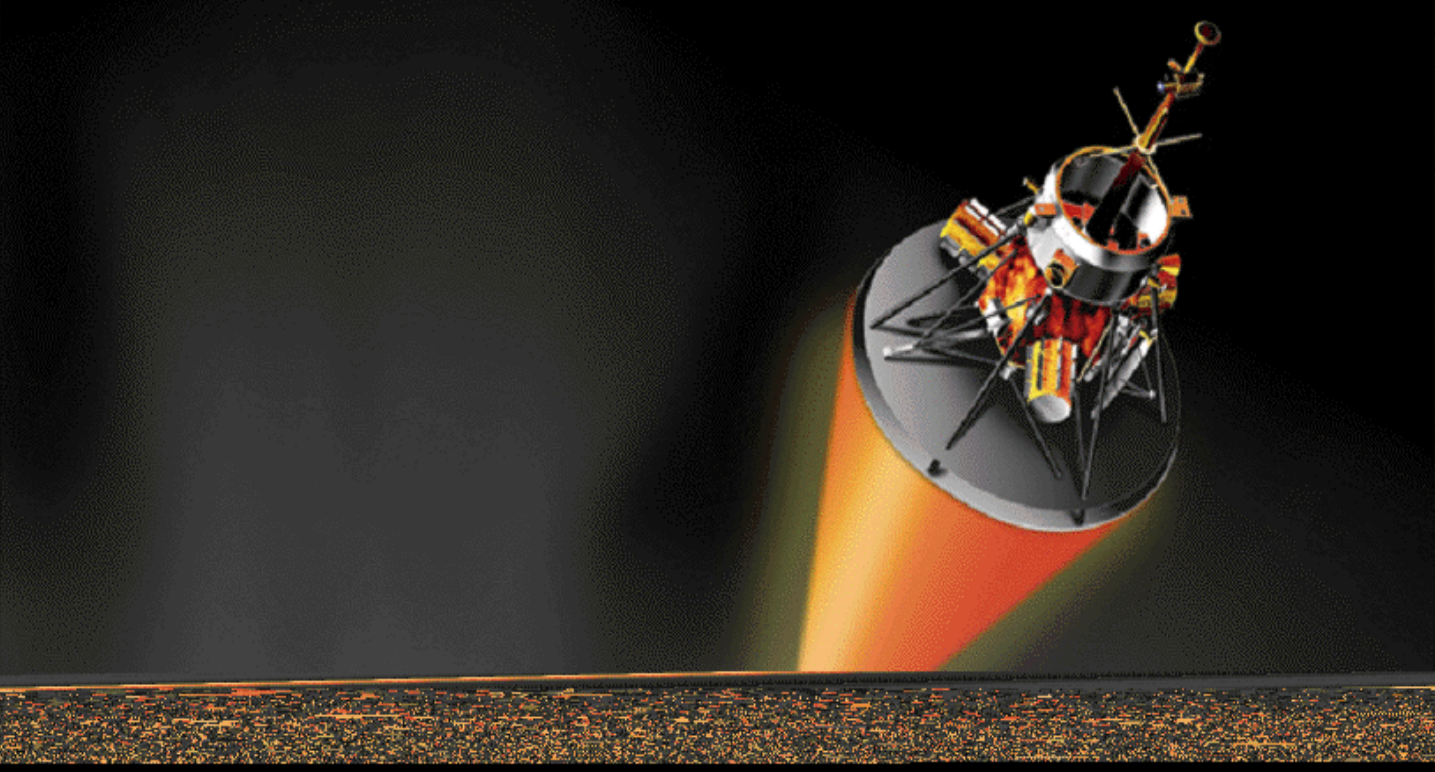

Solar Probe:
An Engineering Study

Submitted to

NASA Goddard Space Flight Center
Living With a Star Program Office
and
NASA Headquarters
Sun-Earth Connection Division
Office of Space Science

November 12, 2002

Prepared by The Johns Hopkins University Applied Physics Laboratory,
Laurel, Maryland, in partnership with the Jet Propulsion Laboratory

Work performed under Contract NAS5-01072

PREFACE AND ACKNOWLEDGMENTS

The NASA Solar Probe mission to the inner frontier of the heliosphere is under study as a part of the Sun-Earth Connection theme within the Office of Space Science. This study was conducted by the Johns Hopkins University Applied Physics Laboratory (JHU/APL) in partnership with the Jet Propulsion Laboratory (JPL) under the sponsorship of the Goddard Space Flight Center Living With a Star Program Office. Participants and their areas of contribution to this study are listed below.

Participants*	Areas of Contribution	Roles in Solar Probe Study
Kenneth A. Potocki, Peter D. Bedini, Neil Murphy (JPL)	Program management	Develop program schedule, cost estimate
Ralph L. McNutt Jr., Barry J. Labonte, Bruce Tsurutani (JPL), Lawrence J. Zanetti	Study science	Assure that mission concept satisfies science requirements
Douglas A. Eng, Douglas Lisman (JPL), Andrew W. Lewin, Laurence J. Frank	System engineering	Develop Solar Probe concept
Yanping Guo, Robert W. Farquhar	Mission design	Define orbit, launch vehicle, propulsion requirements
Steven R. Vernon, Cliff E. Willey, Jennifer R. Tanzman, William E. Skullney	Mechanical engineering	Design spacecraft structure; select materials
David W. Bennett, R. Kelly Frazer, Douglas S. Mehoke, Frank Giacobbe (SWALES)	Thermal engineering	Design Heat Shield; select materials
Carl S. Engelbrecht	Propulsion engineering	Design Propulsion System
Wade E. Radford, Per Uno Carlsson	Power system engineering	Design Power Subsystem
H. Brian Sequeira, Edward F. Prozeller, Robert S. Bokulic	Communications	Develop Ka-band concept
Mark E. Pittelkau, Thomas E. Strikwerda, Steven J. Conard	Attitude Control System and Mission Design	Define attitude control, autonomous operation and propulsion
Paul D. Schwartz, Martin E. Fraeman, Timothy S. Herder, Ark L. Lew, Lloyd A. Linstrom	Command and Data Handling	Design C&DH concept, flight software
Paul H. Ostdiek, James E. Randolph (JPL)	Mission Engineering and Technology	Develop technologies required to enable mission
Edward F. Prozeller, Kenneth P. Klaasen (JPL)	Instrument accommodation	Design Payload accommodation options
Raymond J. Harvey	Mission operations	Develop Integration and Operations
Pazhayannur K. Swaminathan	Dust environment	Develop concepts for spacecraft survival in dust environment
William N. Myers, Jia-Ning Huang, Cheryl L. Reed,	Fiscal and Administration	Provide fiscal and administrative leads
Mary Ann Haug	Program administration	Provide documentation and communications
Heara Lee, Stanley R. Purwin Jr.	Quality assurance	Provide quality assurance

* Except as noted, participants are members of the JHU/APL staff.

EXECUTIVE SUMMARY

Why is the Solar Probe study needed?

Humanity needs to understand how the connections between the Sun and Earth directly affect life and society. The first mission to the planets, Mariner 2 in 1962, revealed a remarkable connection: the Earth is immersed in the outermost material of the Sun, the solar wind. Since then, measurements of the propagation of mass and energy from the Sun to the Earth in the wind have indicated that the Sun is the driving force affecting space weather. The disturbance of electrical power grids, communication systems, aircraft and satellite systems by space weather compels us to examine the origins and sources of the solar wind in the million-degree solar corona with deeper physical understanding.

The innermost heliosphere remains one of the last unexplored regions of the Sun-Earth Connection (SEC). NASA recognizes the importance of a space mission, Solar Probe, to travel to the Sun's corona in a voyage of exploration, discovery, and comprehension. The National Academy of Sciences' Space Studies Board 2002 report, *The Sun to the Earth—and Beyond, a Decadal Research Strategy in Solar and Space Physics*, recommends that the Solar Probe be implemented as soon as possible. The SEC Roadmap 2002–2028 identifies Solar Probe as a mission to implement in the near term.

The Johns Hopkins University Applied Physics Laboratory (JHU/APL) was tasked to perform a conceptual mission design study of the Solar Probe mission. This design study assesses the technical and programmatic feasibility of the selected mission concept to satisfy the Solar Probe science objectives. This report documents the engineering study. Cost methodology and estimates are provided to NASA in a separate document.

How was the Solar Probe study done?

The science investigation was derived from the NASA 1999 Science Definition Team Report, *Solar Probe: First Mission to the Nearest Star*. The fundamental science objectives of the Solar Probe measurements are to understand the heating of the corona and the sources and acceleration of the solar wind. Instrument accommodations were based on strawman instruments that achieve the highest priority science objectives.

The Jet Propulsion Laboratory (JPL) has performed numerous Solar Probe mission design studies over the last 20 years. To ensure that this study took full advantage of these past studies, JHU/APL is teamed with JPL in this effort. JPL has identified many options and trade spaces in the course of its studies. JHU/APL performed a top-down look at the trade space issues, from documented science and solar environmental requirements to engineering solutions, in order to propose a reliable concept to fit the mission.

What did the Solar Probe study find?

An efficient mission design and conservative engineering spacecraft concept are proposed. The concept uses known materials, mature technologies, and redundant design of critical subsystems to enhance the probability of mission success. The report describes a number of specific design recommendations:

1. A mission trajectory has been designed which repeats every 13 months (baseline launch May 2010), has a 3.1-year cruise to the first solar polar pass, and achieves a final 0.02- to 5-AU orbit about the Sun with a period of 4 years.
2. To measure solar wind variability during the solar cycle, two solar passes form the

baseline mission in 7.1 years; a third, optional pass can occur within 11.1 years.

3. A Jupiter Gravity Assist (JGA) trajectory produces a solar polar trajectory with 4-R_S perihelion; an Atlas 551/Star 48B launch vehicle can provide the required lift capability.
4. To improve instrument design and relax spacecraft accommodation issues, the instrument power and mass resources are increased in comparison with the 1999 Solar Probe AO.
5. All instrument data will be acquired, recorded, and transmitted continuously within 0.5 AU (perihelion ± 10 days); additional cruise-mode science data will be transmitted weekly throughout the mission during normal housekeeping and navigation contacts.
6. A Ka-band downlink is used to minimize coronal scintillation and meet data rate goals near perihelion; an X-band downlink supplies redundant backup capability. This data downlink capability will augment the science return.
7. To protect the probe in the 3000-Sun solar intensity at perihelion, the thermal protection system consists of a carbon–carbon cone primary heat shield and a secondary heat shield with low-conductivity, low-mass insulation.
8. Three Multi-Mission Radioisotope Thermal Generators (MMRTGs) will handle the power and heating requirements reliably during the cold (Jupiter flyby) and hot (Solar perihelion) phases of the mission and will allow multiple flybys.
9. Redundant attitude control processors and safehold control will assure that the spacecraft bus stays within the umbra of the thermal protection system during the solar encounter.

Flying a mission to the Sun poses unique challenges. The combined JHU/APL–JPL team has investigated the technologies needed to conduct the proposed mission. A credible risk reduction plan, including fallback approaches for each of the key areas is described. This plan features a concerted pre-Phase A and Phase A risk reduction effort to mature key elements: the thermal protection system material properties and manufacturability; the characteristics of dust impacts and accommodation in the spacecraft design; the efficiency of the Ka-band downlink; MMRTG development through the NASA Nuclear Initiative; and fail-safe attitude control during the solar flybys. Pursuit of this plan would allow overall programmatic and technical risk to be mitigated for mission requirements definition.

How should the Solar Probe study be used?

Our society needs the scientific understanding that Solar Probe will provide. Our scientific leaders advise that the science community is ready for Solar Probe. This design study and its associated risk mitigation plan offer NASA a realistic path to implementing the Solar Probe mission.

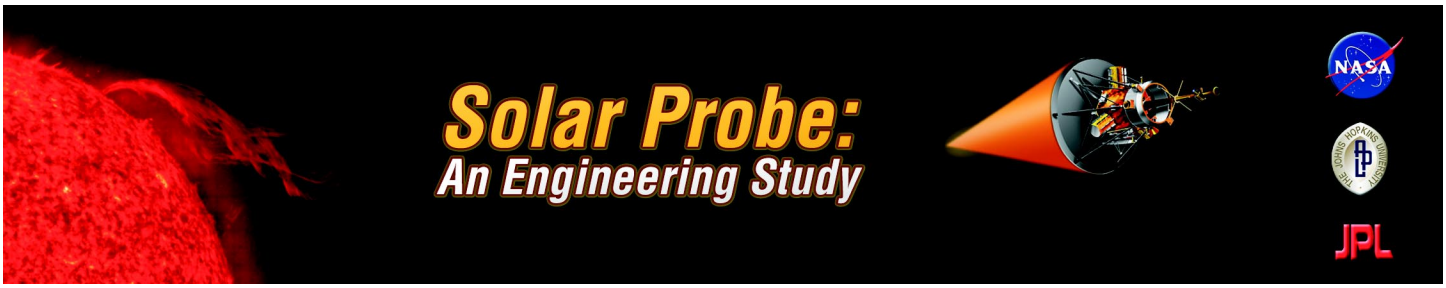

Mission Summary

Launch opportunity every 13 months (Baseline launch May 2010)
Two solar passes (polar, $4R_S$) within 7.1 years; three within 11.1 years
Atlas 551/Star 48B launch vehicle; 713 kg @ $C_3 = 128$ km^2/s^2
JGA trajectory with post-perihelion ΔV for successive passes
3.1-year cruise; 0.02 to 5 AU final orbit with period of 4 years

Measurement Strategy

- Characterize the solar wind within a high-speed stream
- Characterize the plasma in a closed coronal structure and probe the subsonic solar wind
- Image the longitudinal structure of the white-light corona from the poles
- Produce high-resolution images in each available wavelength
- Characterize plasma waves, turbulence, and/or shocks that cause coronal heating
- Determine the differences in solar wind characteristics during maximum and minimum solar activity

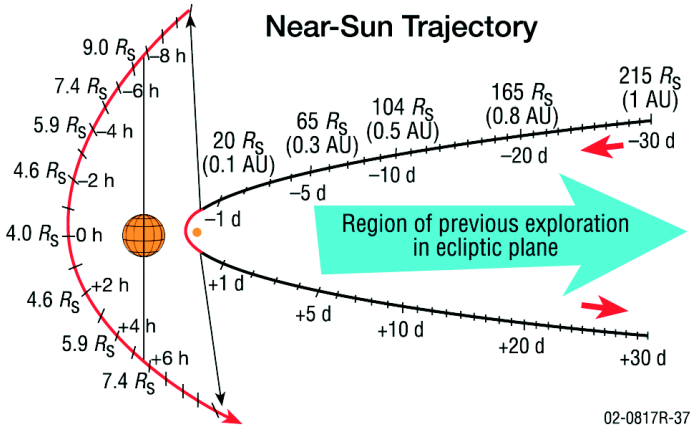

In situ instruments: Solar wind electrons and ion composition, magnetometer, energetic particle composition, plasma waves, and fast solar wind ion detector

Remote-sensing instruments: EUV imager, visible magnetograph–helioseismograph, and all-sky three-dimensional coronograph

Technology Development

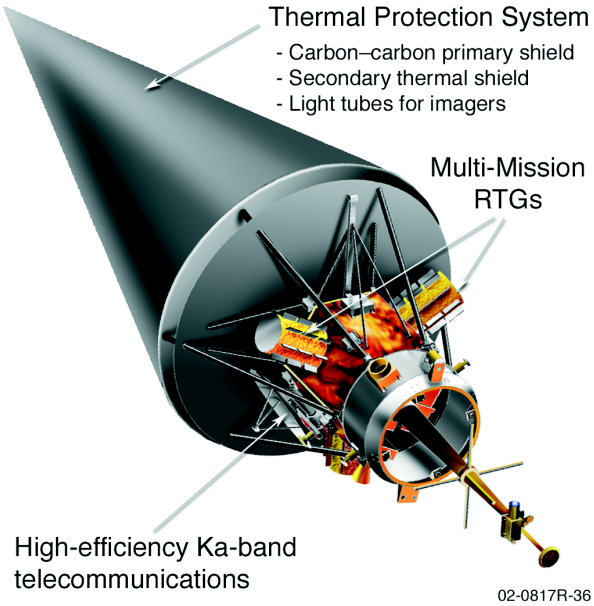

Flight System Concept

- 15° half-angle conical carbon–carbon heat shield
- 3-axis stabilized with 0.2° pointing control and 0.05° knowledge
- RTG power source (three Multi-Mission RTGs supply 330 W at beginning of life)
- Ka-band downlink, X-band uplink using 34-m DSMS dishes
- Data rate: up to 40 kbps real time at perihelion
- Data storage: redundant 128-Gbit stored data
- Instrument payload: 55 kg, 47 W

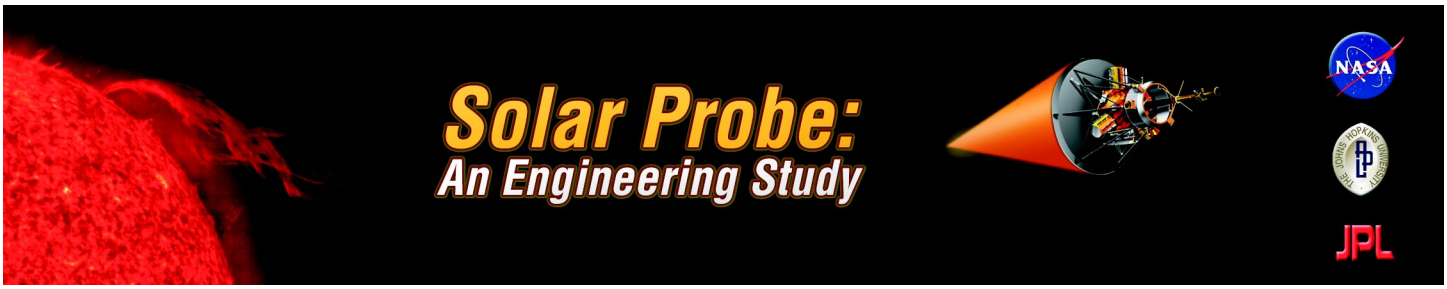

Science Objectives

Category 1

- Determine the **acceleration processes** and find the source regions of the fast and slow solar wind at maximum and minimum solar activity
- Locate the source and trace the flow of energy that **heats the corona**
- Construct the three-dimensional **coronal density configuration** from pole to pole and determine the subsurface flow pattern, the structure of the polar magnetic field, and their relationship with the overlying corona
- Identify the **acceleration mechanisms** and locate the source regions of **energetic particles**; determine the role of **plasma waves and turbulence** in the production of solar wind energetic particles

Category 2

- Investigate **dust** rings and particulates in the near-Sun environment
- Determine the **outflow of atoms** from the Sun and their relationship to the solar wind
- Establish the **relationship between** remote sensing, near-Earth **observations at 1 AU**, and plasma structures near the Sun

Category 3

- Determine the role of **x-ray microflares** in the dynamics of the corona
- Probe nuclear processes near the solar surface from measurements of the **solar gamma rays and slow neutrons**

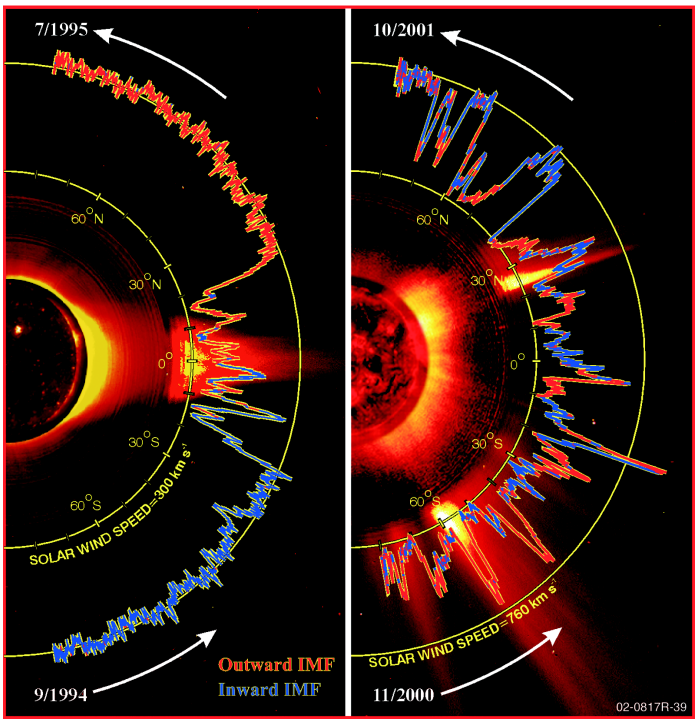

Solar wind observations collected by the Ulysses spacecraft during two separate polar orbits of the Sun, 6 years apart, at nearly opposite times in the solar cycle. Near solar minimum (left) activity is focused at low altitudes, high-speed solar wind prevails, and magnetic fields are dipolar. Near solar maximum (right), the solar winds are slower and more chaotic, with fluctuating magnetic fields. (*Courtesy of Southwet Research Institute and the Ulysses/SWOOPS team*)

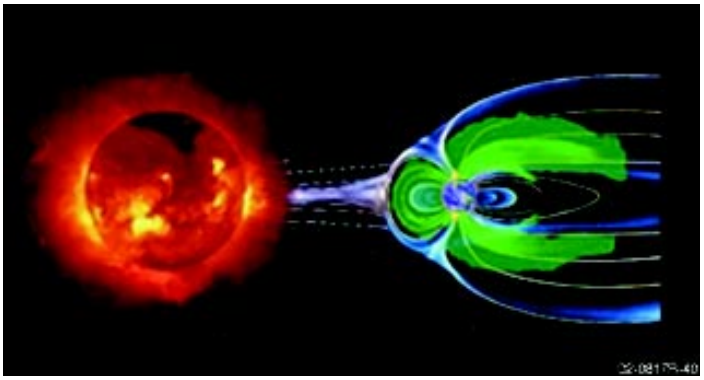

NASA's Sun-Earth Connection Theme seeks to understand our changing Sun and its effects on the solar system, life, and society.

The solar wind is the origin of magnetospheres and of auroras on Earth, and Solar Probe will study the origin of the solar wind.

The Solar Probe mission has been endorsed by the National Academy of Sciences Decadal Survey and the Sun-Earth Connection Theme Roadmap Team.

TABLE OF CONTENTS

1. Mission History 1

2. Solar Probe Engineering Study Charter and Approach 2

3. Science Investigation 3
   - 3.1 Background 3
   - 3.2 Science Objectives 4
   - 3.3 Measurement Strategy 5
     - 3.3.1 Requirements 5
     - 3.3.2 *In Situ* and Remote Sensing Instruments 6
     - 3.3.3 Instrument Resource Allocations 6
   - 3.4 Summary 7

4. Mission Implementation 9
   - 4.1 Mission Requirements 9
   - 4.2 Mission Overview 10
     - 4.2.1 Mission Design Drivers 10
     - 4.2.2 Mission Design 10
     - 4.2.3 Launch Vehicle Selection 12
     - 4.2.4 Mission Concept of Operations 13
     - 4.2.5 Mission Modes 14
     - 4.2.6 Summary 16
   - 4.3 Spacecraft Overview 16
     - 4.3.1 Spacecraft Concept Drivers 16
     - 4.3.2 System-Level Description 19
   - 4.4 Spacecraft Subsystem Descriptions 23
     - 4.4.1 Mechanical Description 23
     - 4.4.2 Thermal Design 27
     - 4.4.3 Telecommunications Subsystem 34
     - 4.4.4 Power 38
     - 4.4.5 Avionics Architecture 42
     - 4.4.6 Data Handling Approach 43
     - 4.4.7 Guidance and Control 46
     - 4.4.8 Propulsion 50
     - 4.4.9 Flight Software 51
   - 4.5 Integration and Test (I&T) 52
     - 4.5.1 Requirements 52
     - 4.5.2 I&T Approach 53
   - 4.6 Ground and Data Systems Overview 55
     - 4.6.1 Requirements 55
     - 4.6.2 Design Approach 55
     - 4.6.3 Summary 57

4.7 Mission Operstions 57
4.7.1 Requirements 57
4.7.2 Approach 57
4.7.3 Summary 59

5. Risk Mitigation 60
5.1 Thermal Protection System (TPS) 60
5.1.1 Primary Shield Assembly 60
5.1.2 Secondary Shield Assembly 63
5.1.3 Light Tubes 64
5.2 Telecommuications 64
5.3 Dust Protection 65
5.4 Attitude Control 66
5.5 Radioisotope Power System 66
5.6 Risk Mitigation Activity Schedule 67

Appendix A: Solar Probe Mass, Power, and Spacecraft Dimensions

Appendix B: References

Appendix C: Acronyms and Abbreviations

LIST OF FIGURES

Figure 1-1. The evolution of the Solar Probe spacecraft design through 1999. 1
Figure 3-1. Solar wind variation over the 11-year sunspot cycle. 3
Figure 3-2. Structure in the solar wind. 4
Figure 3-3. Streamers are related to the slow solar wind. 5
Figure 4-1. Earth quadrature geometry for solar encounters. 11
Figure 4-2. Solar Probe mission trajectory. 11
Figure 4-3. Mission timeline showing optional third solar encounter and relationships of the encounters to the solar cycle. 12
Figure 4-4. Solar encounter trajectory details. 12
Figure 4-5. DSMS coverage near perihelion. 13
Figure 4-6. Solar Probe launch vehicle predicted lift capability. 13
Figure 4-7. Operational concept summary. 15
Figure 4-8. Solar Probe mission modes. 15
Figure 4-9. Solar Probe external view deployed. 19
Figure 4-10. Physical block diagram of the Solar Probe concept. 20

Figure 4-11. Instrument mechanical accommodations. 24
Figure 4-12. Instrument fields of view. 24
Figure 4-13. Spacecraft subsystem mechanical accommodations. 25
Figure 4-14. TPS mounted to spacecraft bus. 28
Figure 4-15. Effect of cone half angle on primary heat shield temperature. 29
Figure 4-16. Effect of cone half angle on carbon mass loss rate. 29
Figure 4-17. Thermal balance for the hot analysis case. 31
Figure 4-18. Hot case thermal analysis results. 32
Figure 4-19. Cold case thermal analysis results. 33
Figure 4-20. Comparison of Ka-band and X-band links during a solar encounter. 35
Figure 4-21. Telecommunications architecture. 36
Figure 4-22. Two-way, noncoherent navigation concept. 38
Figure 4-23. Power system block diagram showing one of the three MMRTGs. 40
Figure 4-24. Empirical RTG decay rate data. 40
Figure 4-25. Solar encounter instrument stored data rates. 45
Figure 4-26. Nominal real-time science data collection profile. 45
Figure 4-27. Solar encounter data collection and storage profile. 46
Figure 4-28. Solar Probe coordinate frame. 47
Figure 4-29. Solar Probe propulsion architecture. 51
Figure 4-30. Aerojet MR-111c 4.0-N rocket engine assembly, shown with axial nozzle. 51
Figure 4-31. Spacecraft integration process. 54
Figure 4-32. Solar Probe ground system architecture. 55
Figure 4-33. Timeline of a 6-month window around a solar encounter. 58
Figure 5-1. Risk mitigation schedule. 67
Figure A-1. Solar Probe Details. A-5

LIST OF TABLES

Table 3-1. Solar Probe sciece objectives. 5
Table 3-2. The strawman science instruments used in planning instrument accommodation. 6
Table 3-3. Comparison of Solar Probe mission configurations. 7
Table 3-4. Resource allocations to science instruments. 8
Table 4-1. Mission requirements derived from AO and SDT documenation. 9

Table 4-2. Solar Probe key design drivers and resulting concept impacts. 17
Table 4-3. Solar Probe total radiation dose. 18
Table 4-4. Hardware redundancy. 21
Table 4-5. Added functional redundancy in Solar Probe concept. 22
Table 4-6. Solar Probe mass summary. 22
Table 4-7. Power summary during solar encounter. 23
Table 4-8. Mechanical subsystem requirements summary. 23
Table 4-9. Spacecraft temperature results of thermal analysis. 33
Table 4-10. Telecommunication subsystem requirements summary. 34
Table 4-11. Power subsystem requirements summary. 38
Table 4-12. Previous JHU/APL contributions to NEPA launch approval process. 41
Table 4-13. Avionics subsystem architecture requirements summary. 42
Table 4-14. Mission Operations Team activities during mission phases. 58
Table 5-1. Subsystem components, heritage, and technology readiness levels (TRLs). 61
Table A-1. Solar Probe Equipment List and Detailed Mass Breakdown A-1
Table A-2. Solar Probe Power Budget. A-3

1. MISSION HISTORY

The idea of a Solar Probe mission dates to the founding of NASA in 1958. The evolution of the mission concept can be thought of as a progression of goals. The first goal, to reach solar orbit, led to the discovery of the solar wind by Mariner II in 1962. The next goal, to sample the solar system inside the orbit of Mercury, was realized in the Helios missions of the 1970s. The ability to launch spacecraft to Jupiter and use the giant planet's gravity field to assist in reaching other locations in the solar system, beginning with Pioneer 11's flight to Saturn, opened opportunities for new types of solar missions. The goal of exploring high latitudes (Page 1975) was reached with Ulysses. Direct flight into the solar corona, the source of the solar wind, became the Solar Probe concept.

The earliest studies of this concept were done in the mid-1970s, with the first major efforts reported in the 1978 Jet Propulsion Laboratory workshops: *A Close-up of the Sun* (Neugebauer and Davies 1978).

The scale, science focus, and spacecraft configuration studied for Solar Probe have been revised at intervals since that time. Initial suggestions included dual spacecraft with different science instruments. The mission was renamed StarProbe during the early 1980s, and became FIRE as a joint United States–Russian mission in the mid-1990s. Figure 1-1 illustrates several of the spacecraft configurations studied in detail and lists their basic elements. The two general concepts have either a conical primary heat shield with steerable high-gain antenna, or a parabolic heat shield/antenna combination. Numerous options have been considered for the spacecraft power source, bus configuration, instrument suite, and mission plan.

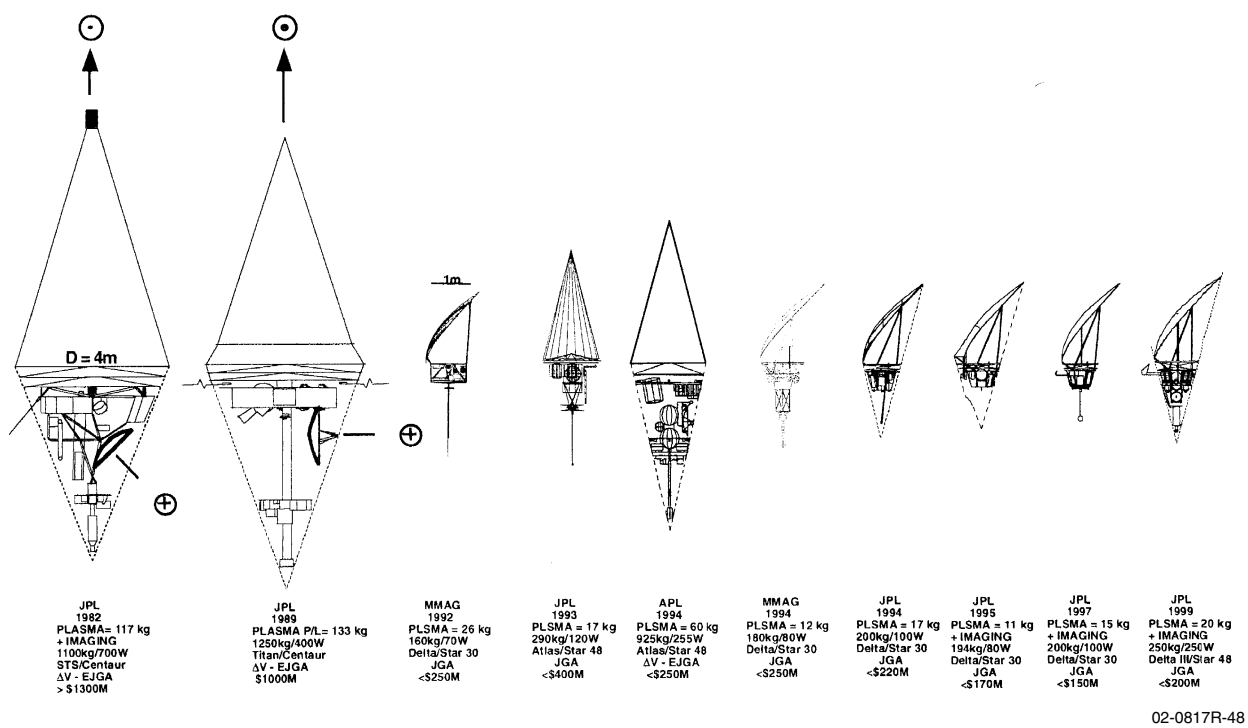

Figure 1-1. The evolution of the Solar Probe spacecraft design through 1999.

2. SOLAR PROBE ENGINEERING STUDY CHARTER AND APPROACH

2.1 Engineering Study Charter

The Johns Hopkins University/Applied Physics Laboratory (JHU/APL) was tasked to perform a conceptual design study of the Solar Probe mission. The study focuses on developing a baseline mission design concept for report to and consideration by the Living With a Star Program at the NASA Goddard Space Flight Center (GSFC) and the Sun-Earth Connection Division at NASA Headquarters.

The study assesses the technical and programmatic feasibility of the selected mission concept to satisfy the Solar Probe category 1 science objectives. These science objectives were identified in a 1999 report of the NASA Science Definition Team, *Solar Probe: First Mission to the Nearest Star* (Gloeckler et al. 1999). Cost and schedule estimates for the mission concept are developed and provided to NASA in a separate document.

2.2 Engineering Study Approach

The Jet Propulsion Laboratory (JPL) has performed numerous Solar Probe design studies over the last two decades. To ensure that this study took full advantage of these past studies, JHU/APL is teamed with JPL in this effort.

The study approach started with a JHU/APL top-down review of the science objectives and instrument accommodation assumptions. Mission requirements and a mission concept were developed. The mission concept includes an orbital trajectory to accomplish the science measurements, a candidate launch vehicle, and a concept of operations.

Using the mission concept and the space environments along the orbital trajectory, several spacecraft concepts were developed. Subsystem trade studies were conducted to evaluate every aspect of these spacecraft concepts and to select the best features for the proposed design. A series of reviews with scientists and engineers outside the study team were used to refine a reliable integrated spacecraft system design.

Important considerations throughout the design are trade studies to characterize technical risk and establish a mitigation plan. The JHU/APL and JPL team has investigated the technologies needed to conduct the proposed mission. Before any technology was included in the baseline design, a credible risk mitigation plan was established, including fallback approaches for each of the key technology areas.

3. SCIENCE INVESTIGATION

3.1 Background

The primary science objective of Solar Probe is "to understand the processes that heat the solar corona and produce the solar wind" (Solar Probe Science Definition Team (SDT) final report, *Solar Probe: First Mission to the Nearest Star*, Gloekler et al. 1999). Since the discovery of the solar wind by Mariner 2, NASA missions have taken two complementary paths toward understanding the origin of the solar wind. The first path measures the properties of the wind *in situ*. Sun-Earth Connection (SEC) missions on this path are Voyager, which, at 86 astronomical units (AU) will soon reach the heliosphere's outer boundary; Ulysses, which is studying the high-latitude heliosphere at 2 AU; and Wind and ACE, which are measuring the solar wind near the Earth at 1 AU. The second path uses remote sensing instruments to analyze the solar corona. SEC missions on this path are SOHO, with a diverse complement of imaging and spectrographic instruments; and TRACE, with very high spatial and temporal resolution imaging of corona structure. These missions will be joined in 2004 by MESSENGER, which will measure the solar wind from Mercury orbit at 0.4 AU; and STEREO, which will combine *in situ* measurements and remote sensing from positions ahead of and behind the Earth in its orbit.

Even so, the innermost heliosphere remains one of the last unexplored regions of the solar system. The closest approach ever made to the Sun, 0.31 AU (67 solar radii R_S), by the Helios spacecraft in the 1970s, is more than twice the outer limit of any remote sensor. The smoothing of solar wind structures, caused by solar rotation and variations in propagation speeds, make detailed connections between the *in situ* and remote sensing measurements impossible. Solar Probe will make measurements *in situ* from the wind regime at 0.5 AU into the coronal volume sampled by remote sensing at 0.02 AU (4 R_S), for the first time providing the physical connections that will allow us to understand the solar processes that govern the solar corona and the solar wind.

Past missions have revealed many aspects of solar wind acceleration (Figure 3-1), but compelling science questions remain unanswered. Coronal holes persist at the solar poles through much of solar cycle. During sunspot minimum, the polar holes are present and the solar wind is well organized, with the fast wind from the polar holes filling much of the heliosphere. The solar

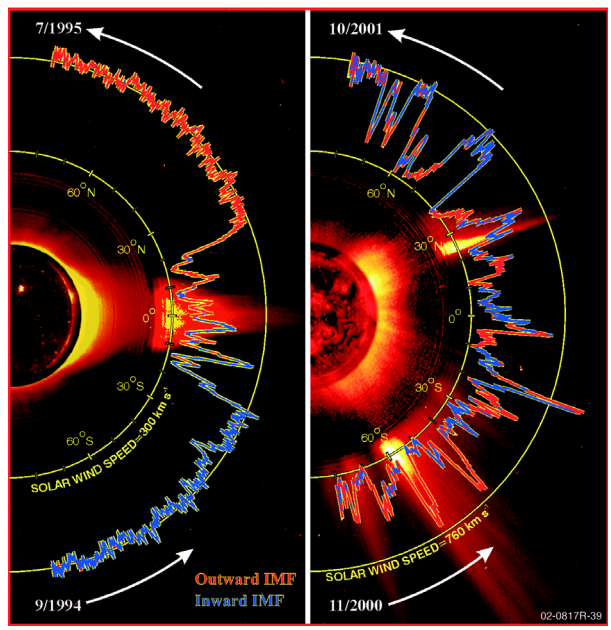

Figure 3-1. Solar wind variation over the 11-year sunspot cycle. Solar coronal images, from SOHO's Extreme Ultraviolet Imaging Telescope (EIT), the Mauna Loa coronameter, and SOHO's Large Angle and Spectrometric Coronagraph (LASCO), show the coronal structure at sunspot minimum (left) and maximum (right). The speed of the solar wind, from Ulysses/SWOOPS, color-coded by the sign of the magnetic field, is plotted over latitude. At minimum, the solar magnetic field is dipolar, with large polar coronal holes and streamers limited to the equator. The heliosphere is dominated by the fast solar wind flowing from the polar holes. At maximum, the dipolar field is gone, streamers are seen over a wide latitude range, and the wind contains a mixture of fast and slow wind intervals.

magnetic fields restructure themselves during the 11-year sunspot cycle. During sunspot maximum, the polar holes are absent, the solar wind is mixed, with fast and slow speed wind seen at all latitudes. As Figure 3-1 shows, the restructuring of the solar magnetic field, modifying the corona and wind, gives important information about the general sources of the fast and slow winds, but the physical processes that accelerate the different wind speeds are not understood.

Observations from SOHO's Ultraviolet Coronagraph Spectrometer (UVCS) imply that the wind acceleration operates over the range of 2 to 10 R_S in coronal holes. The wind flow appears anticorrelated with structures in the coronal holes, as shown in Figure 3-2 (DeForest et al. 2001). Low-density regions have higher temperatures, nonthermal, probably wave motions, and are possibly the source of the fast solar wind (Banjeree et al. 2000). How do the structures of the solar corona, so clearly correlated with the flow of the solar wind, evolve to the smoother wind observed at a distance?

The generation of the slow-speed wind within the streamers is a perplexing problem. SOHO/UVCS observations (Strachan et al. 2002) detected the wind outflow along the outer edges and from the tops of streamers (Figure 3-3). At the same locations, discrete blobs of material are seen moving outward in images from SOHO/LASCO images, but masses are too small to match the solar wind flux (Sheeley et al. 1997). Why does the wind from the streamers not accelerate to the faster speeds seen from coronal holes? Is the boundary between the closed and open magnetic fields at the edges of streamers unstable to wave motions or discrete disconnections that drive the blobs and remove energy from the wind flow?

3.2 Science Objectives

The specific science objectives that drove our engineering study were taken from the 1999 Solar Probe SDT final report (Gloekler 1999). No effort was made to alter the objectives or priorities set by the SDT. The SDT prioritized the specific science objectives necessary to achieve understanding of the processes that drive the solar wind. The resulting prioritized list is given in Table 3-1.

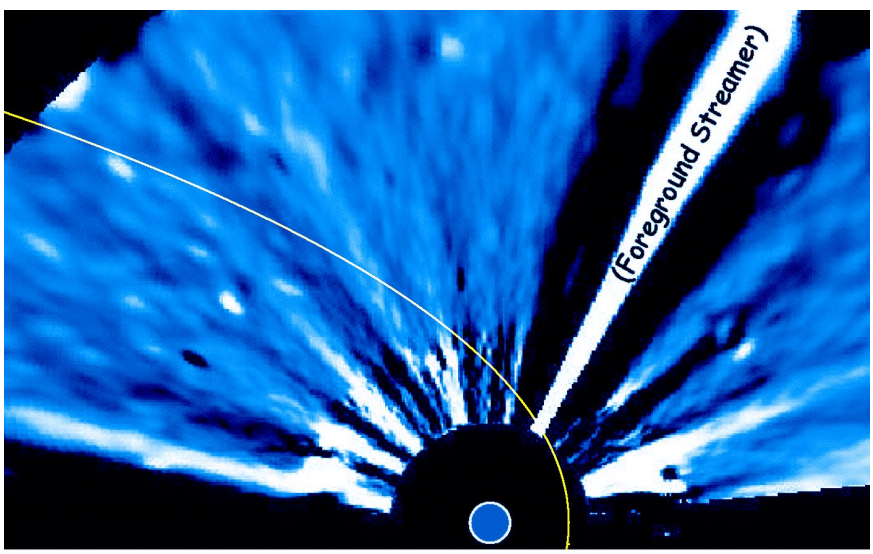

02-0817R-43

Figure 3-2. Structure in the solar wind. Structures observed out to 30 R_S by SOHO/LASCO in polar solar corona holes have densities at least 4 times the background. No corresponding density structures are identified in the solar wind measured by Ulysses/SWOOPS at 2 AU above the poles. Solar Probe will directly sample structure, from the wind into the corona, as it passes to a perihelion of 4 R_S in its orbit (yellow line shows track of solar flyby).

We expect that a revised SDT report must be prepared before any future Solar Probe Announcement of Opportunity (AO). Such a report would account for advances since 1999 in science understanding, instrument technology, mission resources, mission environment, and related space missions. The SEC Roadmap 2002 identifies a number of missions that will

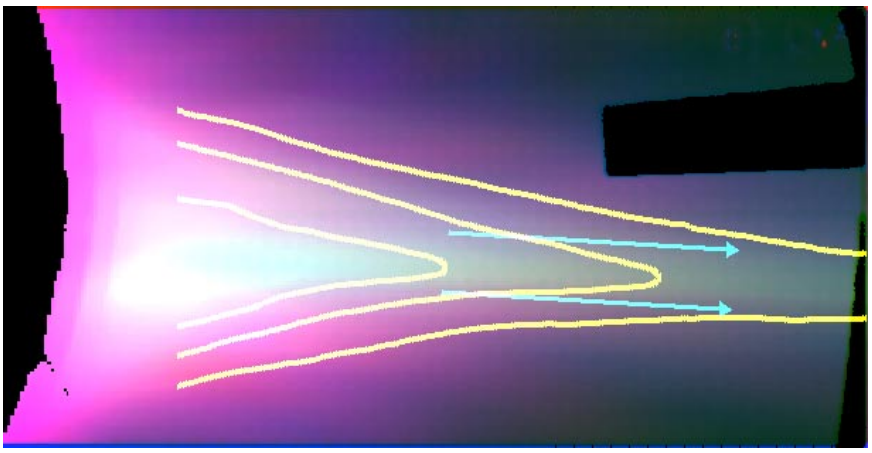

02-0817R-44

Figure 3-3. Streamers are related to the slow solar wind. Images for SOHO/UVCS in O^{5+} (red), neutral hydrogen (blue), and SOHO/LASCO electron scattering (green) of a streamer. Contours of solar wind outflow speeds are plotted at 0, 50, and 100 km/s, increasing outward. Blobs of out-flowing material seen in LASCO movies accelerate along the sides of streamers in the locations show with arrows.

be contemporary with Solar Probe. *In situ* measurements of the inner heliosphere (0.3 to 1 AU) over all latitudes will come from the Solar–Terrestrial Probe (STP) Telemachus, the Living With a Star (LWS) Inner Heliospheric Sentinels, the European Space Agency (ESA) Solar Orbiter, and the joint ESA–Japan Bepi-Colombo. Remote sensing of structure in the solar atmosphere with order-of-magnitude improvements in spatial resolution will come from Solar Orbiter and the STP Reconnection and Micro-scale missions. Solar Probe science will be greatly enhanced by complementary participation in this ensemble.

3.3 Measurement Strategy

3.3.1 Requirements

The science objectives define the basic mission design. The orbital inclination must be 90° for passage through the polar coronal holes. The perihelion, over the solar equator, must be 4 R_S for passage over the poles at 8 R_S, where the fast wind is still showing acceleration. Two perihelion passes are required at different sunspot cycle phases to adequately sample both fast and slow speed wind regimes. Complementary remote sensing instruments are required to provide contemporary context for the *in situ* measurements through the unique range of solar latitudes and distances traversed by the probe.

The SDT established a measurement strategy to accomplish the science objectives. The determination of the source regions and accelera-

Table 3-1. Solar Probe science objectives.

Category 1 Objectives
• Determine the acceleration processes and find the source regions of the fast and slow solar wind at maximum and minimum solar activity. • Locate the source and trace the flow of energy that heats the corona. • Construct the three-dimensional coronal density configuration from pole to pole and determine the sub-surface flow pattern, the structure of the polar magnetic field, and their relationship with the overlying corona. • Identify the acceleration mechanisms and locate the source regions of energetic particles, and determine the role of plasma waves and turbulence in the production of solar wind and energetic particles.
Category 2 Objectives
• Investigate dust rings and particulates in the near-Sun environment. • Determine the outflow of atoms from the Sun and their relationship to the solar wind. • Establish the relationship between remote sensing, near-Earth observations at 1 AU, and plasma structures near the Sun.
Category 3 Objectives
• Determine the role of x-ray microflares in the dynamics of the corona. • Probe nuclear processes near the solar surface from measurements of solar gamma rays and slow neutrons.

tion processes of the solar wind depend on: (1) full knowledge of the plasma state, including magnetic field, composition, distribution functions, and wave spectra; and (2) knowledge of the context of the measurements from remote sensing of the local and global environment. Because the acceleration of the wind is likely to be intimately connected with the heating of the corona, the same measurements are needed to understand the heating processes. Understanding the role of wave–particle interactions in heating and bulk acceleration processes requires rapid measurements of the dominant ions simultaneous with plasma waves. Understanding the acceleration of energetic particles requires simultaneous measurement of those particles (both ions and electrons) and of the plasma waves and properties of the dominant ions at high cadence.

3.3.2 *In situ* and Remote Sensing Instruments

Ideally, the instruments that make the required measurements would be well described and integrated into a spacecraft design. However, to maintain fair competition, the proposals submitted in response to 1999 Solar Probe Announcement of Opportunity were embargoed. For this engineering study, therefore, we based instrument accommodation on a set of strawman instruments that achieve the 1999 AO category 1 Science Objectives (Table 3-2). For efficiencies in operation, we assumed that the instruments would be grouped into two suites. The *in situ* instrument suite comprises five instruments that, taken together, provide all of the *in situ* measurements needed to undertake the science objectives. The remote sensing suite comprises three instruments that provide the context necessary to understand the *in situ* measurements.

Instruments designed to achieve Category 2 and 3 science objectives may be proposed under a future AO, pending resources and/or revised priorities. These could include a dust monitor, a hard x-ray and gamma ray spectrometer, and a neutron spectrometer.

3.3.3 Instrument Resource Allocations

The accommodation of the instruments with respect to fields of view and interference is described in Section 4. Several of the instruments require special accommodation. Because the VMH and EUVI image the solar disk, their view must be through light tubes that penetrate the primary heat shield. The SWICES detects the bulk plasma. Because bulk flow is masked by

Table 3-2. The strawman science instruments used in planning instrument accommodation.

Suite	Instrument	Purpose
In situ	1. Solar wind ion composition and electron spectrometer (SWICES)	Measure distribution functions of the dominant charge states of abundant ions and electrons.
	2. Magnetometer (MAG)	Measure vector DC magnetic field.
	3. Plasma wave sensor (PWS)	Measure AC electric and magnetic fields.
	4. Fast solar wind ion detector (FSWID)	Measure distribution functions of the most abundant ions at high cadence.
	5. Energetic particle composition spectrometer (EPCS)	Measure fluxes of nonthermal electrons and abundant ions.
Remote sensing	1. All sky 3-D coronagraph imager (ASCI)	Image the sunlight scattered from dust and electrons in the volume around the spacecraft orbit to provide local context.
	2. Visible magnetograph–helioseismograph (VMH)	Image the magnetic and velocity fields on the solar surface to provide global context on the magnetic configuration through which the probe will pass.
	3. Extreme ultraviolet imager (EUVI)	Image the thermal emission from the lower corona to provide global context on the coronal topology through which the probe will pass.

the heat shield during some parts of the probe's orbit, a scoop is required to sample the plasma during those times.

The resources available to the science instruments are described in detail Section 4. The significant differences between our study and the mission described in the 1999 Solar Probe AO are summarized in Table 3-3. Specific differences in resource allocations for the science instruments are shown in Table 3-4. As Table 3-4 shows, our study resulted in more resources being made available to the instruments. The additional resources will help to mitigate instrument development risk and will increase the science productivity of the Solar Probe mission.

3.4 Summary

The scientific rationale for the Solar Probe mission is well defined. The critical question is whether the mission can actually be implemented as defined. Section 4 examines the various elements of the Solar Probe mission and spacecraft and defines a feasible and realistic concept for the mission.

Table 3-3. Comparison of Solar Probe mission configurations. Major differences are highlighted in bold.

	1999 AO Mission	2002 JHU/APL Mission
Mission Design		
Launch vehicle	EELV with **Star-48V** third stage	EELV with **Star-48B** third stage
		(Atlas 551 used as baseline; compatible w/ Delta IV)
Launch date	February, 2007	May 2010
Pass 1	October, 2010	August 2013
Gravity assists	Jupiter — June 2008 (10.5 R_J)	Jupiter — August 2011 (7.1 R_J)
Pass 2	January, 2015 **(Earth not in quadrature)**	August 2017 **(Earth in quadrature)**
Radiation TID	88 krad (with RDM = 2)	90 krad (with RDM = 2)
Data collection	**Unavailable from P – 10 to P – 6 days, P + 3 to P + 10 days**	**Continuous for P – 10 through P +10 days (all passes)**
		Cruise mode science capability
Spacecraft Design		
Power	**1 RTG (18 GPHS modules; 300 W BOL)**	**3 MMRTGs (24 GPHS modules total; 330 W BOL)**
		4.5 A-h lithium ion battery
Thermal	**Parabolic** carbon–carbon heat shield	**15° conical** carbon–carbon heat shield
		Aerogel (or carbon mat) secondary shield
	Bus heating with RTG	Bus heating with MMRTGs
C&DH	6-Gbit data storage capability (redundant)	128-Gbit data storage capability (redundant)
ACS	3-axis stabilized	3-axis stabilized
	IMU	IMU
	Star trackers	Star trackers
	Sun sensors	Sun sensors
	Eight 0.9-N thrusters	Sixteen 4-N thrusters
		Reaction wheels
	Pointing accuracy (3σ) = 0.286°	Pointing accuracy (3σ) = 0.2°
	Pointing knowledge (3σ) = 0.057° (inertial hold)	Pointing knowledge (3σ) = 0.057°
	Pointing stability (3σ) = .0057° in 1 s	Pointing stability (3σ) = 0.0057°
Telecom	**Parabolic HGA**	**Steerable 0.8-m HGA (dish on ~30° gimbal)**
		8-W Ka-band SSPA (downlink)
	8-W X-band SSPA (downlink)	8-W X-band SSPA (downlink backup)
	Deep-space transponders	**X-band uplink, noncoherent navigation**
Propulsion	Monopropellant hydrazine	Monopropellant hydrazine
	ΔV = 90 m/s	**ΔV = 150 m/s navigation, 50 m/s targeting burn**

Table 3-4. Resource allocations to science instruments. Instrument resources and science return have increased in comparison with the 1999 AO mission description.

Instrument Resources	1999 AO Mission	Current Study
Power (not to exceed values)		
Instruments	15 W	23 W
Data processing units (DPUs) and low-voltage power converters (LVPCs)		24 W
Mass (not to exceed values)		
Instruments	21 kg	34 kg
DPUs and LVPCs		14 kg
Boom and light tubes		7 kg
Science return (data downlink capability)		
Real-time data rate (at perihelion)	>5 kbps	>25 kbps
Onboard memory	6 Gbit (×2)	128 Gbit (×2)
Data return per perihelion pass	43 Gbits	128 to153 Gbits
Cruise-mode telemetry available		
Incidental benefit of noncoherent tracking for navigation		
One 8-hour contact per week provides 20 Mbits/week		

4. MISSION IMPLEMENTATION

This section describes the general approach to the implementation of the Solar Probe mission. The mission requirements are summarized, and overviews of the mission design and spacecraft design are presented. Finally, the detailed descriptions of the spacecraft subsystems are presented.

4.1 Mission Requirements

The category 1 science objectives identified in 1999 by the Solar Probe Science Definition Team (SDT) (Gloekler et al. 1999) are the basis for the current engineering study, and the mission requirements derive directly from these objectives. The instrument payload accommodated by the mission and spacecraft designs is that presented in the SDT report and described further in the Mission and Project Description (MPD) document (NASA 1999b) and the Solar Probe Announcement of Opportunity (AO) OSS-99-02 (NASA 1999a). Table 4-1 is a listing of the basic mission requirements.

The overarching objective of this study was to develop a viable, affordable, detailed mission concept that maximizes the science return. Accordingly, in addition to the above mission requirements, the study goals included minimizing the cost (without accepting undue risk), maximizing the resources available for the instrument payload, and assuring maximum data downlink throughout the solar passes.

Table 4-1. Mission requirements derived from AO and SDT documentation.

Category	No.	Requirement	Source
Mission	1	Perihelion of 4 ± 0.1 solar radii (R_S)	MPD, p. 21
	2	20-day solar encounter about perihelion	MPD, p. 2
	3	Provide instrument checkout and calibration soon after launch near 1 AU	MPD, p. 2
	4	Accurate post-mission trajectory reconstruction to a few kilometers	MPD, p. 21
	5	Two solar encounters	MPD, p. 2
	6	Orbit inclined 90° to the ecliptic	MPD, p. 19
Mechanical	7	Accommodate all instruments described in AO	MPD, p. 11
	8	Provide light tubes and filter to limit flux to nadir-pointing imagers	MPD, p. 25
	9	Provide retractable boom to minimize interference with several of the *in situ* instruments	MPD, pp. 25, 30, 49
	10	Provide preflight purge to instruments	MPD, p. 49
	11	Solar wind ion & electron spectrometer field of view (FOV) of ±20° boresighted to solar nadir	MPD, p. 30
	12	85° half angle FOV for spacecraft-mounted instruments	MPD, p. 30
	13	Accommodate at least 20.2 kg for instrument mass	MPD, p. 12
Power	14	Provide regulated DC power to instruments between 22 and 36 V	MPD, p. 25
	15	Accommodate at least 13.9 W average power for instrument power	MPD, p 12
	16	Accommodate 100 W peak power; durations less than 50 ms	MPD, p. 25
Thermal	17	Spacecraft temperature range of –20° to 50°C	MPD, p. 28
	18	Spacecraft out-gassing ≤2.5 mg/s during solar encounters	MPD, p. 41
Attitude control system (ACS)	19	Provide 3-axis stabilized pointing during solar encounter and instrument calibrations	MPD, p. 33
	20	0.3° pointing accuracy to solar nadir boresight during the solar encounter	MPD, p. 34
	21	0.05° inertial attitude knowledge during solar encounter	MPD, p. 34
	22	0.005° in 1-s jitter relative to boresight during the solar encounter	AO change list
Command & data handling (C&DH)	23	Capability to handle peak data rates of 112.4 kbps from instrument suites during solar encounter	MPD, p. 12
Communications	24	Maximize real-time telemetry throughout the solar encounter	MPD, p. 17

4.2 Mission Overview

This overview identifies the key drivers of the mission concept and describes how the mission design accommodates them. The selection of launch vehicle and concept of operations is then discussed, along with a summary of the mission modes.

4.2.1 Mission Design Drivers

Based on the above mission requirements and the stated study goals, three fundamental features of the Solar Probe mission emerge as the key mission drivers:

- Polar orbit with perihelion 4 R_S from the center of the Sun
- Multiple passes of the Sun within one solar cycle
- Real-time data downlink during the passes

4-R_S Polar Orbit. The science objectives require that measurements be made at high solar latitudes, over the poles, and in the corona at a distance of 4 R_S from the Sun's center. Using established methods of propulsion, the only way to meet these requirements is to use a Jupiter gravity assist trajectory. Supplying sufficient power to the spacecraft at Jupiter (at 5 AU from the Sun) and within the orbit of Mercury (0.3 AU) has not been accomplished with solar panels, but can easily be achieved by incorporating traditional nuclear power sources.

Associated with the 4-R_S flyby is the need to harbor the instruments in the harsh solar environment of the Sun's corona. A thermal protection system must be capable of withstanding the extreme temperatures while rejecting enough heat to maintain the spacecraft at normal operating temperatures. Precautions must be taken to account for the uncertain dust environment and to keep the spacecraft shielded from the Sun as the spacecraft passes through perihelion at over 300 km/s.

Multiple Solar Passes. The science objectives of Solar Probe as defined by the SDT require sampling the solar wind in the corona at times of high and relatively low solar activity, preferably near solar maximum and minimum. This requirement, coupled with the fact that the spacecraft will spend a relatively short time in the corona due to its great speed, led to the conclusion that at least two passes of the Sun should be made. With the current mission design, Solar Probe enters a 0.02 × 5 AU heliocentric orbit that provides a first pass in 3.1 years, allows two passes in 7.1 years, and a third pass within 11.1 years.

Real-time Downlink. Although the system design is robust, and minimizing risk was a key factor in the various subsystem trade studies performed, the environment in the corona is harsh and uncertain, and there is some chance that the spacecraft may encounter a catastrophic event on any given pass of the Sun. As a result, another important driver is the capability to provide real-time return of the science data. Designing the mission for Earth to be in quadrature when the spacecraft is at perihelion creates the optimum geometry to downlink the data (Figure 4-1). Ka-band is used because coronal scintillations make such transmission difficult with X-band telecommunications.

4.2.2 Mission Design

The Solar Probe mission design uses a direct Jupiter gravity assist (JGA) to achieve a polar heliocentric orbit with the desired perihelion. The first solar pass occurs 3.1 years after launch, and a modest ΔV maneuver after this pass retargets the spacecraft into a final orbit with solar passes possible every 4 years. The 4-year period produces the same optimum communications geometry for all perihelion passes. Three passes are possible within an 11-year solar cycle. The mission profile used for this study assumes a launch in May 2010, but is available every 13 months; Figure 4-2 shows the mission trajectory for the 2010 launch design; Figure 4-3 shows a mission timeline.

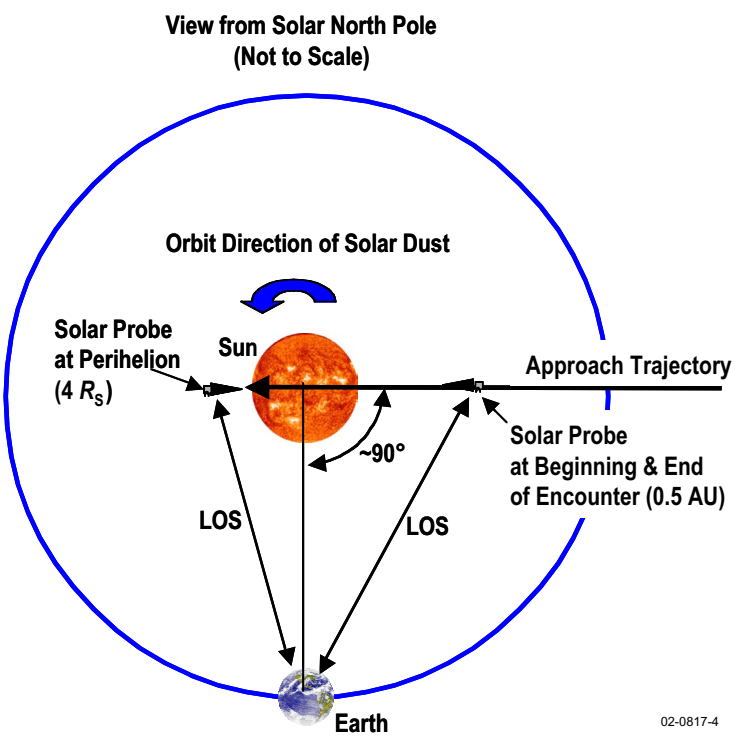

Figure 4-1. Earth quadrature geometry for solar encounters.

Launch. The 20-day launch window opens May 26, 2010. The maximum required launch energy C_3 is 128 km²/s², and the declination of launch asymptote (DLA) ranges from –11.2° to –14.0°. The probe will be launched during the daytime from Cape Canaveral Air Force Station (CCAFS), Florida.

Jupiter Flyby. The mission design utilizes the gravity of Jupiter to lose enough angular momentum to achieve a 4-R_S perihelion. At the same time, the spacecraft makes a 90° plane change to enter into a polar heliocentric orbit. Depending on the launch date, the Jupiter flyby occurs August 23 to 28, 2011. The closest approach to Jupiter is at 7 Jupiter radii (R_J) with a flyby speed of 26 km/s. A southward Jupiter flyby approach has been chosen rather than a northward approach because the required launch energy is lower.

Solar Encounter. The southward Jupiter approach results in a solar pass from the north along an orbit that is 90° inclined from the ecliptic plane and flies by the Sun at a speed of 308 km/s, as shown in Figure 4-4. Its closest

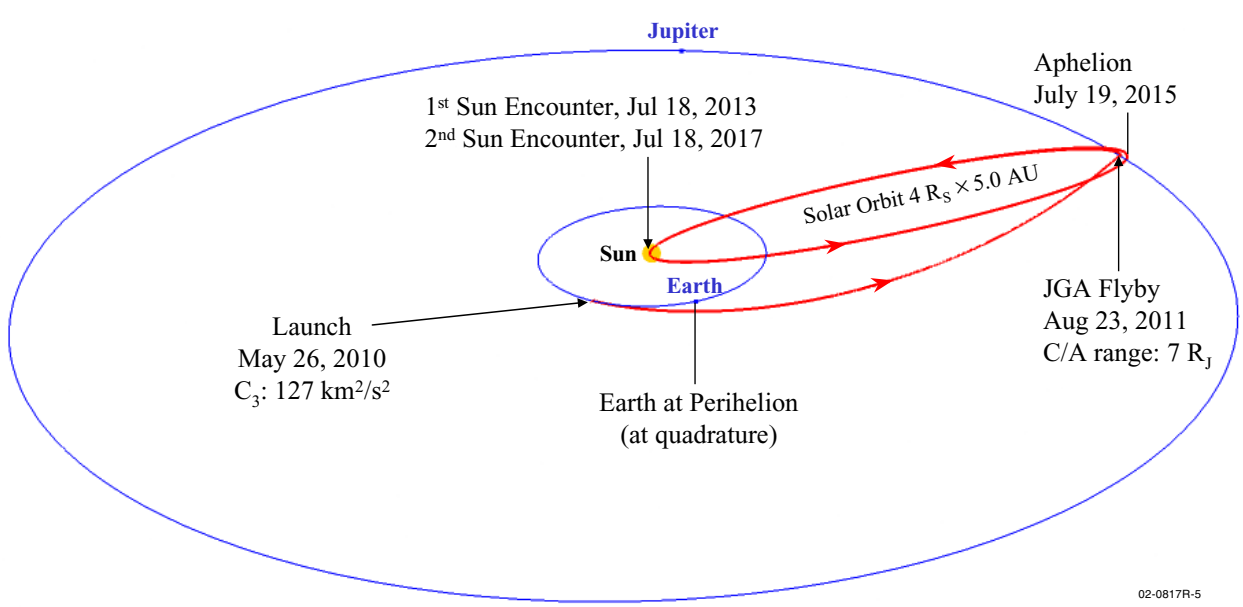

Figure 4-2. Solar Probe mission trajectory.

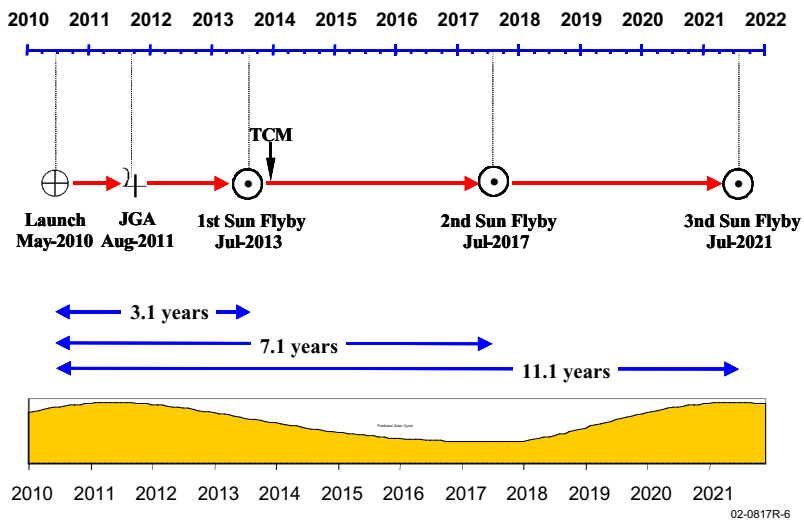

Figure 4-3. Mission timeline showing optional third solar encounter and relationships of the encounters to the solar cycle.

approach to the Sun is 3 R_S from the surface near the equator, and the pole-to-pole flyby takes place within a solar distance of 9 R_S in a period of 14 hours. The solar distances at 30 days and 10 days before and after perihelion are 1 AU and 0.5 AU, respectively.

Both the solar encounter date and the orbit inclination are selected to allow continuous real-time data transmissions to Earth during the solar passes. As the spacecraft passes the Sun at closest approach, Earth is in quadrature, positioned 90° from the Sun–probe line to the west of the Sun. This configuration allows the spacecraft simultaneously to point its antenna toward Earth and its thermal shield toward the Sun and it avoids direct impact from dust particles that circulate near the Sun in an east–west direction. The perihelion time is selected to have simultaneous access to the Probe from two Deep Space Mission System (DSMS) stations, Goldstone and Madrid (Figure 4-5).

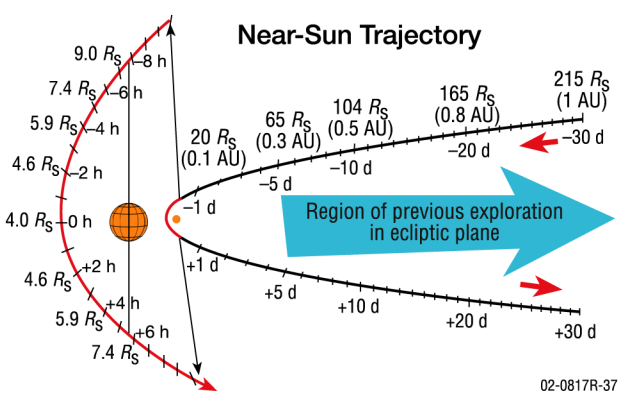

Figure 4-4. Solar encounter trajectory details.

A re-targeting burn will be performed after the first solar flyby to adjust the orbital period so that successive solar passes occur every 4 years with the same favorable quadrature geometry. A ΔV of 50 m/s is required for a burn performed 22 days after perihelion, when the spacecraft is 0.8 AU from the Sun.

ΔV Requirement. The onboard ΔV requirement is moderate. No deterministic ΔV is needed for achieving the first solar flyby, and only 50 m/s is required for targeting successive solar flybys. A ΔV budget of 150 m/s was estimated to correct for launch vehicle dispersion, guidance, and navigation errors. An additional 25 m/s was included for additional margin, resulting in a total onboard capability of 225 m/s, excluding the separately budgeted attitude control propellant.

4.2.3 Launch Vehicle Selection

The required C_3 for the Solar Probe trajectory is 128 km²/s². Two expendable launch vehicles (ELVs) can deliver this C_3 and satisfy regulatory constraints related to the use of radioisotope thermoelectric generators (RTGs): the Atlas V 551 and the Delta IV 4040H-19. The baseline for this study is the Atlas V 551 with the Star 48B third stage, although the design

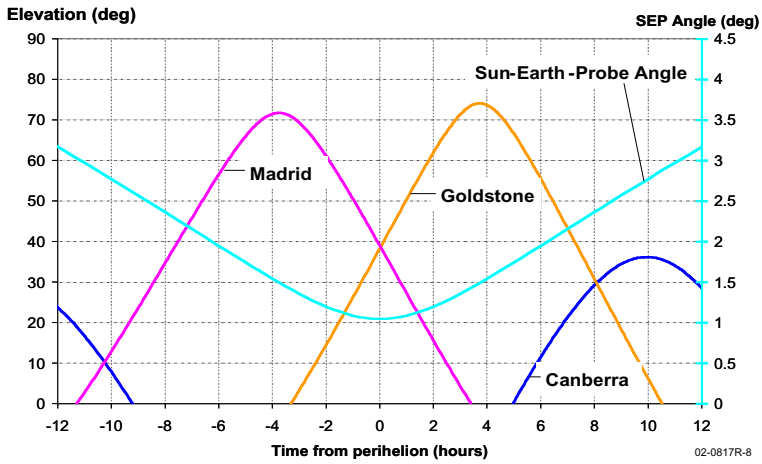

Figure 4-5. DSMS coverage near perihelion.

could easily support the use of the Delta IV. The Atlas V/Star 48B has an adequate predicted lift capability of 713 kg, and its current advertised cost is lower than that of the Delta. Figure 4-6 shows the lift capability of the two launch vehicle options.

The spin-stabilized Star 48B third stage was selected over the 3-axis stabilized Star 48V largely because a spin-stabilized upper stage is preferable from a range safety perspective for launches carrying nuclear payloads.

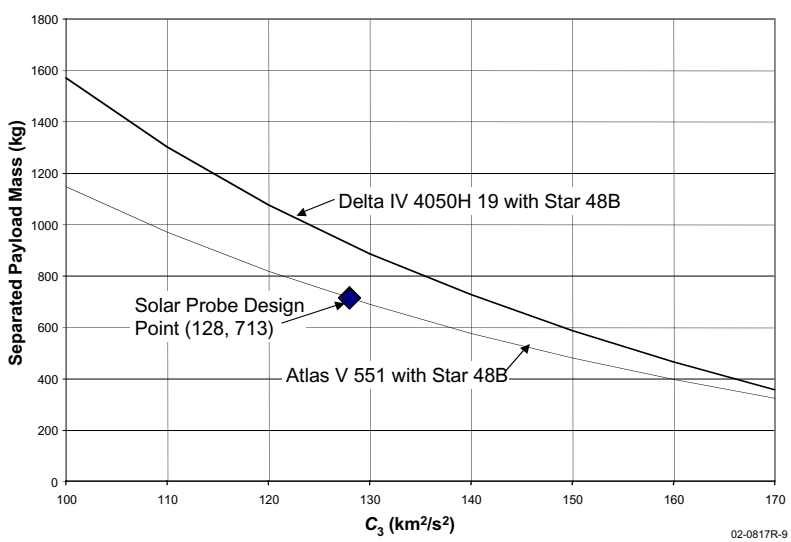

Figure 4-6. Solar Probe launch vehicle predicted lift capability.

4.2.4 Mission Concept of Operations

Launch and Early Operations. Solar Probe will be launched from the Cape Canaveral Air Force Station within a 20-day launch window on a two-stage ELV with a Star 48 third stage. Except for the propellant budgeted for navigation correction, the entire ΔV necessary for achieving the Jupiter flyby will be supplied by the launch vehicle. For the first- and second-stage fly-out, the spacecraft will be 3-axis stabilized by the launch vehicle. For the third-stage fly-out, the stage will be spin-stabilized at approximately 60 rpm.

Upon separation from the third stage, Solar Probe will perform a despin maneuver and assume a 3-axis stabilized orientation with the medium-gain antenna (MGA) and high-gain antenna (HGA) pointed toward Earth. The MGA will be the primary antenna used for communications for early checkout and cruise. The first 90 days of the mission is allocated for early orbit checkout of the spacecraft, which can easily be supported by 8-hour contact periods 3–4 times per week.

Outbound Cruise. After the initial checkout is completed, the number of required contacts is reduced to one 8-hour contact per week. The spacecraft remains 3-axis stabilized with the HGA and MGA pointed toward Earth. A slow spacecraft rotation will be introduced about the antenna axis to minimize the cumulative angular momentum effects of solar pressure torque.

Jupiter Gravity Assist. Beginning 30 days before the Jupiter encounter, contacts will increase to 3–4 per week to allow analysis, execution, and evaluation of a navigation burn planned for 21 days prior to the flyby. This burn will provide final corrections necessary to assure that the gravity assist will target the spacecraft for the desired 4-R_S perihelion solar encounter.

Inbound Cruise. From 1 month after the Jupiter flyby until 3 months before the solar pass, the spacecraft returns to cruise mode and reduces contacts to one per week. At this time, contacts again increase to 3–4 per week to perform necessary instrument calibrations and test spacecraft modes planned for the encounter. At a distance of approximately 0.8 AU, the spacecraft must change attitude to point the thermal protection system (TPS) toward the Sun. Communication with Earth is maintained by a single-axis antenna arm and gimbal that controls the MGA and HGA position and attitude. Freedom to point the antenna in the other axis will be attained by rotating the spacecraft about the *Z*-axis (symmetric about the thermal shield).

Solar Encounter. At 0.5 AU, 10 days prior to perihelion, the solar encounter phase begins, and ground contact becomes nearly continuous. The spacecraft will accommodate continuous data streams from the instruments except during brief momentum management maneuvers lasting less than 1 minute and no more frequent than every 20 minutes. All science data are recorded redundantly on two solid-state recorders (SSRs). A portion of the science data is transmitted in real time. During the encounter, the data rate will support at least 25 kbps. Spacecraft autonomy will maintain proper attitude for science collection, adjust the HGA, and rotate the spacecraft to maintain communications with Earth. An extensive autonomous fault protection system assures a safe spacecraft attitude in the event of any single hardware or software failure.

Post Encounter. The solar encounter phase ends 10 days after perihelion, and retrieval of non–real-time science data from the recorders begins. The spacecraft must maintain the TPS pointed toward the Sun until 20 days after perihelion, when a retargeting burn of 50 m/s ΔV establishes the 4-year orbital period and guarantees quadrature for successive solar encounters. This maneuver will be performed while maintaining contact with the ground.

After the retargeting burn, the spacecraft returns to its cruise attitude configuration and resumes downlinking the recorded science data. Downlinking the entire 128 Gbits of potential data will take approximately 60 days from the end of the encounter. The spacecraft remains in cruise mode with weekly contacts until preparation for the second solar encounter, which will be operationally identical to the first encounter. Figure 4-7 summarizes operational concept as a timeline.

Cruise Mode Science. An additional capability of Solar Probe is collection of science data during the cruise phases. Since weekly contacts are planned to support navigation and spacecraft health and maintenance, science data can be continuously recorded and downlinked weekly. The spacecraft power and command and data handling (C&DH) systems support instrument operation throughout cruise. Approximately 22 Mbits of science data per week could be telemetered to the ground during these phases.

4.2.5 Mission Modes

Figure 4-8 shows the Solar Probe mission modes and mode transitions. These modes help define groupings of spacecraft functionality useful for operations planning, fault protection system development, software development, and guidance and control (G&C).

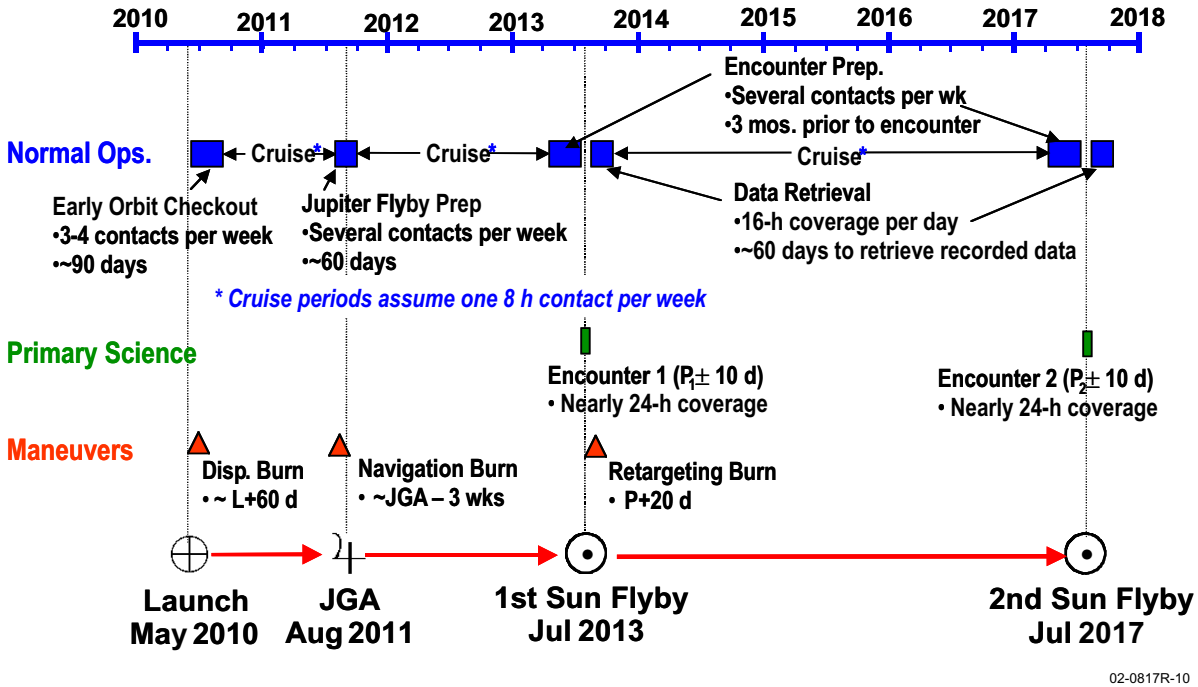

Figure 4-7. Operational concept summary.

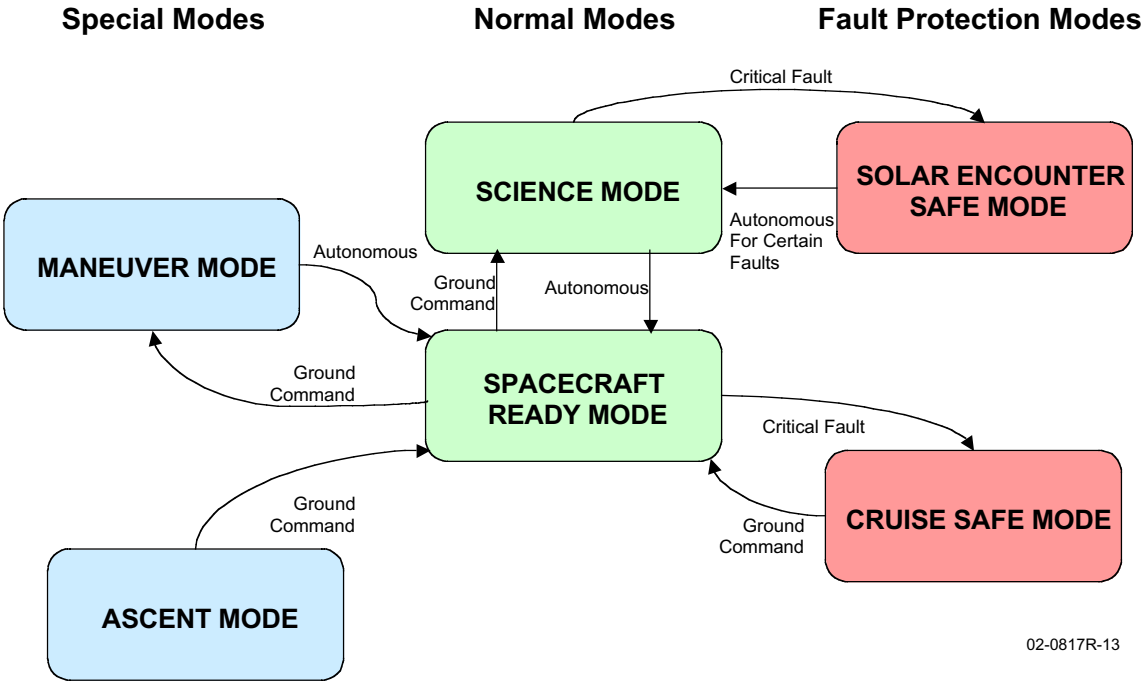

Figure 4-8. Solar Probe mission modes.

Ascent Mode. While the spacecraft is in the fairing, all systems not required for initial deployment are powered off and the RTGs operate at a low power level. After initial fly-out, onboard timers activate G&C components and the transmitter. After deployment, the spacecraft

autonomously performs a despin maneuver and points the antennas toward Earth. The spacecraft remains in Ascent Mode until a ground command is received.

Spacecraft Ready Mode. The standard mode outside of solar encounter periods is Spacecraft Ready Mode, wherein the spacecraft has full functionality and its attitude is normally 3-axis stabilized with the HGA/MGA pointed toward Earth.

Maneuver Mode. A ground command initiates transition to Maneuver Mode, which is used to perform ΔV maneuvers both for navigation corrections and for the retargeting burn. Its specialized functionality is isolated from the other modes to prohibit accidental maneuvers. Transition out of this mode is made autonomously after completion of the maneuver sequence.

Science Mode. The normal mode during solar encounters and instrument calibrations is Science Mode, in which the instruments capture data and are on the 1553 data bus schedule. In this mode, the TPS points toward the Sun and autonomous functions assure the safety of the spacecraft.

Cruise Safe Mode. One of the two safe modes for Solar Probe, Cruise Safe Mode is used in the event of a fault while the spacecraft is in Spacecraft Ready Mode. Nonessential loads are powered off, and the spacecraft points its antennas toward the Sun using digital Sun sensors. Farther than 3 AU, this is sufficient to capture Earth within the MGA beamwidth. At closer distances, a small step-stare search pattern will be used to get the MGA to capture Earth. At distances less than 2 AU, a widebeam low-gain antenna (LGA) can also be used to reestablish communications. Cruise Safe Mode operates on software isolated from the operational software and is triggered by the onboard fault protection system.

Solar Encounter Safe Mode. This second safe mode is only used during the solar encounters, and is triggered by fault protection logic active when the spacecraft is in Science Mode. An independent processor in the attitude interface unit (AIU) takes control of the G&C functions using a solar horizon sensor to maintain the spacecraft in a safe attitude. Depending on the fault, the primary systems or redundant systems will take over, and promotion back to science mode will be autonomously performed. For some critical faults, ground intervention may be required and mode transition would be from the ground.

4.2.6 Summary

The Solar Probe mission design puts the spacecraft in a favorable position to achieve the science objectives. The short cruise time from launch to first solar encounter and the final orbital period allows for two passes in 7 years, and possibly three coronal measurements within a single 11-year solar cycle. Quadrature geometry optimizes the downlink of science data during the encounters, making it unnecessary to rely solely on the transmission of recorded data after the passes.

4.3 Spacecraft Overview

4.3.1 Spacecraft Concept Drivers

The Solar Probe spacecraft concept was constrained by several significant design drivers and defined many of the subsystem approaches. Most of the design drivers are based on the extreme environments the spacecraft will encounter during the mission. Table 4-2 and the paragraphs below summarize the key design drivers and reference the appropriate subsection of this report where the resulting subsystem concept is discussed in more detail.

Solar Thermal Flux. The intense solar flux of 400 W/cm^2 at perihelion is the most challenging spacecraft design driver. This heat input is

Table 4-2. Solar Probe key design drivers and resulting concept impacts.

Requirement	Resulting Environment	Concept Impacts	Subsection
4 R_S perihelion mission	Solar flux ~ 400 W/cm^2	• New heat shield development • Light tubes for nadir imagers	4.4.2
	1% chance of ≥100-μm dust impact	• Dust shield	
	Solar scintillation near perihelion	• Ka-band downlink	4.4.3
	Coronal lighting near perihelion	• Alternative ACS safing sensor	4.4.7
	93-krad total dose (100 mils) because of Jupiter flyby	• Radiation-tolerant electronics	4.4.5
≥2 solar encounters (>7.2-year mission life)		• Radioisotope power source • Redundant systems	4.4.4, 4.3.2
Pointing accuracy of 0.2° Inertial knowledge 0.05° Jitter of 0.005° in 1 s		• Star tracker • High-precision inertial measurement unit (IMU)	4.4.7
Maximize science return		• 128-Gbit recorder • Ka- and X-band downlink	4.4.3, 4.4.5
Mass loss rate ≤2.5 mg/s		• 15° conical carbon–carbon heat shield • Reaction wheels	4.4.2, 4.4.7

managed by a thermal protection system (TPS) that shadows the spacecraft bus and instruments from the direct solar flux. This TPS consists of primary and secondary thermal shields and light tubes to allow nadir-pointing remote sensing instruments to safely collect images while rejecting additional flux that could damage them.

Solar Dust. Remote sensing instruments have observed dust near the Sun at latitudes of ± 30° from the equator with a generally a counterclockwise orbit when observed from the Solar north pole. Based on remote observations of the solar dust, an expected solar dust flux density model was developed based on the work of Mann (2001). Using this dust flux density model, the spacecraft was designed to withstand a single impact of a particle of 100-μm diameter per pass, plus additional impacts of smaller dust particles. Due to the relative velocities of the spacecraft and dust particles, impact velocities as high as 400 km/s are likely. The design includes a mass allocation for shielding of critical components, and the reaction wheels and thrusters are sized to accommodate torques imposed by these impacts.

Solar Scintillation. The effects of solar scintillation have been well characterized based on mission data provided by the NEAR-Shoemaker spacecraft during solar conjunction as well as earlier by Magellan and Galileo. During the NEAR mission, at solar conjunction, measurable telemetry losses were experienced using X-band transmission once the angle between the Sun, Earth, and the spacecraft came within 2.3°. For Solar Probe near perihelion, this angle will be less than 2.3° for several hours, and an X-band downlink was not considered reliable to meet the real-time telemetry goal of 25 kbps during this most critical time in the mission. Ka-band transmission was selected as the baseline because it is relatively unaffected by the solar scintillation and could meet the 25 kbps goal during the solar encounter.

Coronal Lighting. Expected coronal lighting near the Sun is currently an important environmental uncertainty and can have significant consequences for maintaining attitude control. Excessive coronal lighting can increase background noise and degrade the ability of the star tracker to detect star constellations needed to determine the spacecraft attitude. Coronal lighting conditions can be estimated using data from remote sensing instruments currently in orbit at a distance of 1 AU. This information may be enough to provide some characterization of the

lighting environment; however, uncertainty will remain until a mission near the Sun is performed. To accommodate this uncertainty, the Solar Probe concept incorporates two star trackers, facing approximately orthogonal directions, and a high-precision IMU. Additionally, the concept incorporates a safing sensor that detects the edge of the solar horizon if the star trackers have been blinded for an extensive period.

Radiation Environment. The Solar Probe ionizing radiation environment consists of three components: electrons and protons trapped in the Jovian magnetosphere, solar protons during solar maximum conditions, and gamma rays from the RTG fuel. Table 4-3 provides the ionizing dose behind 100 mils of Al spacecraft shielding using one-dimensional slab geometry. In this table, the Divine–Garrett model for a Jovian pass with minimum approach of 7 R_J was used to calculate the radiation dose near Jupiter (Divine and Garret 1983). The JPL-91 solar proton flux model (Xapsos et al. 1996) was used at the 95% confidence level to estimate the dose contribution for the period of the mission during solar maximum conditions. The RTG gamma ray flux was derived from measurements of the Cassini RTGs.

Both the relatively high total dose and the large initial dose at the Jupiter flyby affected the overall concept. All electronics devices for this mission are selected to be radiation tolerant to the total dose defined in Table 4-3. As a precaution, unnecessary radiation-sensitive components, including the redundant integrated electronics module (IEM) and star tracker, will be turned off while the spacecraft passes through Jupiter's radiation belts to minimize radiation effects.

Table 4-3. Solar Probe total radiation dose. The Jupiter flyby radiation is the most significant component of the total mission radiation dose.

Component	Margin	Dose with Margin (krad Si)
Jupiter pass (Divine–Garrett model)	×2	79
RTG gamma (scaled Cassini data)	×1.5	4
Solar protons (JPL-91 model)	×3	9.7
Total		**93**

Multiple Solar Encounters. The current mission requirement is to conduct two solar encounters. This design provides scientists the opportunity to collect data over different periods of the solar cycle. Solar Probe incorporates hardware with an expected design life to accommodate 2 or more encounters. In addition, this design incorporates significant redundancy, discussed in Section 4.3.2.4, to ensure mission success. Accommodating multiple solar encounters also constrained the primary power source for the mission. A radioisotope power source was considered the only practical alternative to operate for more than 7 years in a widely varying solar flux environment of 0.02 to 5 AU.

Pointing and Jitter. The pointing accuracy requirement for Solar Probe was driven by two different sources. The remote-sensing, solar-nadir-pointing instruments require an absolute pointing capability of 0.3° and attitude knowledge of 0.05°. Selection of Ka-band combined with the antenna dish size of 0.8 m resulted in an HGA pointing requirement of 0.2°. The AO also specified a jitter requirement of maintaining boresight within 0.005° in 1 s during the solar encounter. The combination of these requirements drove the selection of attitude determination sensors to a star tracker and a high-precision IMU. For attitude control, the selection of reaction wheels provides both very good attitude pointing control and low jitter.

Maximum Science Return. The principal goal in development of this Solar Probe concept was to the maximize science return of the mission. Due to constraints in transmitter power and the size of the HGA, real-time telemetry was limited to 25–60 kbps and could not meet the science data needs alone. As an alternative, therefore, the concept incorporates redundant 128-Gbit SSRs easily capable of duplicate recording of all the science data taken over the

entire solar encounter. With this concept, the function of the real-time telemetry is to provide an important contingency capability and further increase the potential science data return.

Maximum Spacecraft Mass Loss Rate. The 1999 AO specified a maximum mass loss rate of the spacecraft materials of ≤2.5 mg/s during the solar encounter to ensure that spacecraft charging and mass loading do not adversely affect the sensitive particle measurements being taken. At perihelion, this requirement is a significant driver; it limited the materials and maximum temperature of the TPS, defining the primary shield concept as a tall conical carbon–carbon structure. This requirement was also interpreted to include all spacecraft mass loss including propellant, which led to the selection of reaction wheels over thruster attitude control to minimize the propellant exhaust expelled into the environment during sensitive particle science measurements.

4.3.2 System-Level Description

Solar Probe is a 3-axis stabilized spacecraft designed to operate in environments from 0.02 to 5 AU from the Sun and in close proximity to Jupiter (7 R_J). The concept is illustrated in Figure 4-9 in deployed configuration; spacecrat dimensions are shown in Appendix A. The most prominent feature is the TPS, with its large 2.7-m diameter carbon-carbon conical primary shield and a low conductivity secondary shield attached at the base. This TPS protects the spacecraft bus and instruments within its umbra during solar encounter. The TPS is attached to the bus via 12 struts. The spacecraft bus accommodates all instruments specified in the 1999 AO, including a retractable boom for several of the

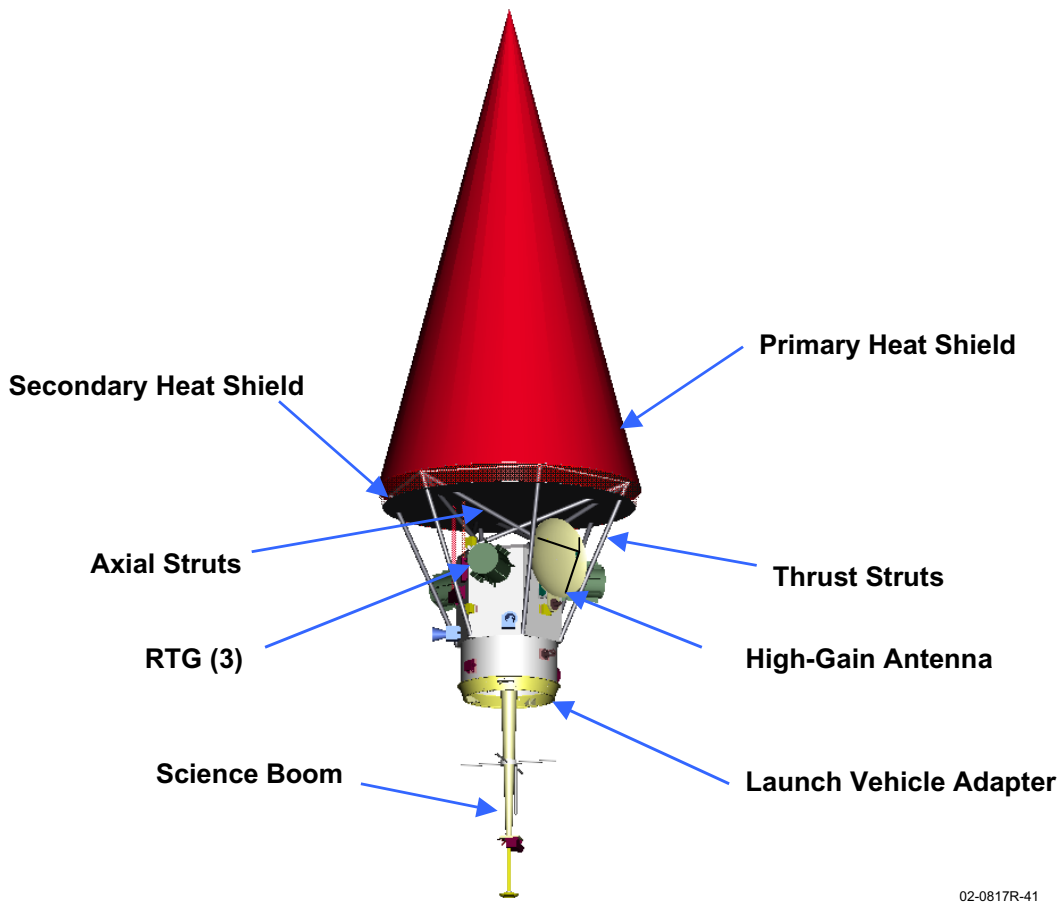

Figure 4-9. Solar Probe external view deployed.

in situ instruments as well as the fail-safe solar horizon sensor. A hexagonal/cylindrical bus accommodates the spacecraft subsystems and provides an efficient mechanical structure to handle launch loads and integrate with the launch vehicle. The RTGs are placed high on the bus to help minimize the diameter of the TPS and are positioned for integration with the spacecraft via access doors in the fairing. The propellant tank is central to the bus, and most of the electronics boxes are mounted on the bottom deck with the telescoping boom.

The architecture for the Solar Probe concept (Figure 4-10) is derived from previous JHU/APL missions, including NEAR, TIMED, STEREO, and MESSENGER. The dual IEMs are a central feature of these designs. They provide a highly mass- and volume-efficient packaging solution for the command and data handling hardware, attitude control processor, and communications electronics. The instruments are grouped into remote sensing and *in situ* suites, each with a dedicated data processing unit (DPU) and power converter. Commands and data are routed throughout the spacecraft through a redundant digital 1553 bus. Some attitude control components require an analog interface. The attitude interface unit (AIU) converts the analog and digital signals and provides the necessary interface to these components.

4.3.2.4 Fault Protection

Solar Probe fault protection was driven by several factors. First, considerable uncertainty remains in the solar encounter environments affecting attitude control. Maintaining attitude control and recovering rapidly from faults affecting the ACS are critical to spacecraft

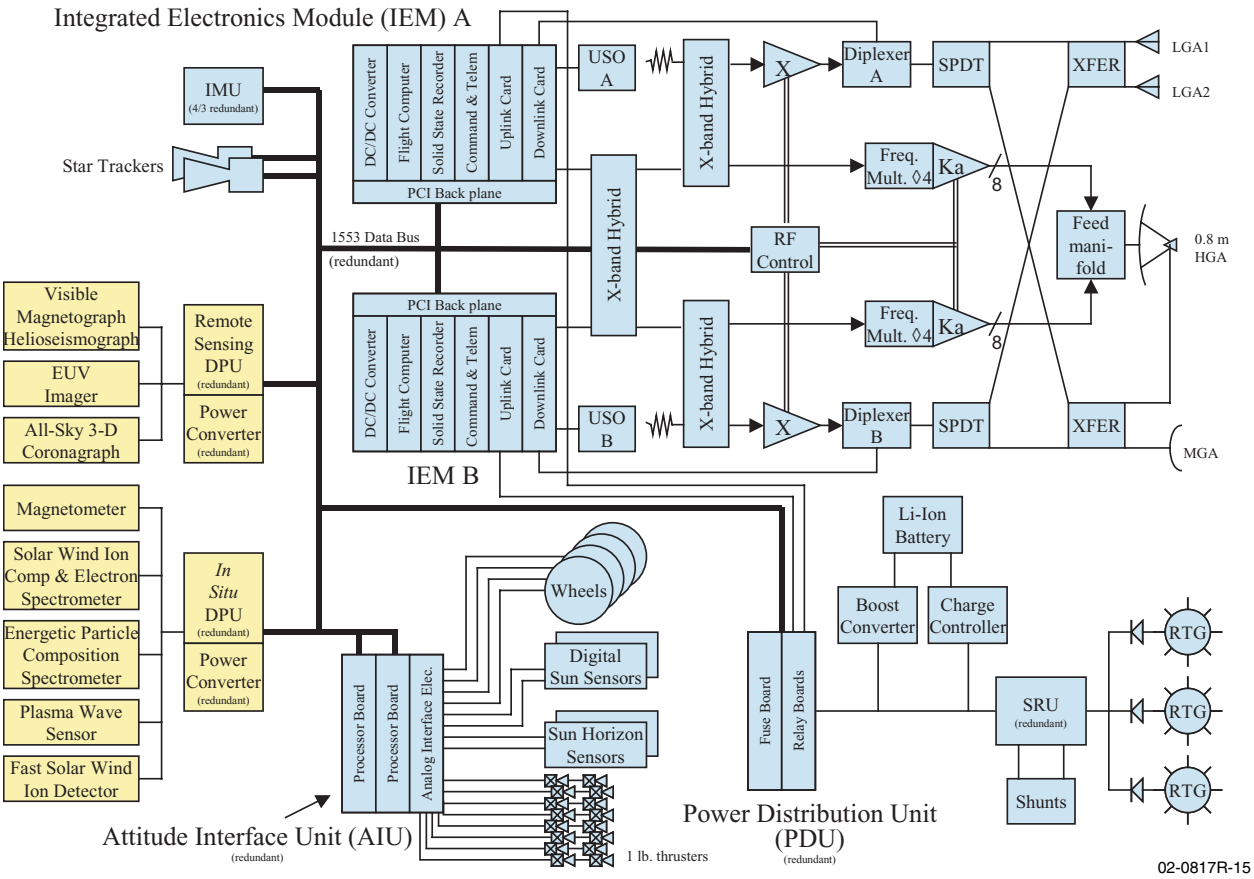

Figure 4-10. Physical block diagram of the Solar Probe concept.

survival. Second, critical aspects of the science data collection occur over relatively short periods. The flight through the coronal holes for each encounter lasts only 14 hours. These considerations drive the spacecraft to having significant onboard autonomy and hot backup systems during the solar encounters.

The plan for two encounters, with a potential for three or more, also drives hardware selection and redundancy considerations. Solar Probe incorporates redundancy in virtually all subsystems. The primary single-point failure that remains is the RTG, for which it is prohibitively expensive to fly a spare unit. Even with a failed RTG, however, a degraded mission is possible with the remaining two units. All other spacecraft systems are either redundant in their design or redundant units are flown. Hardware redundancy is summarized in Table 4-4.

Years of space flight history have shown that random failures constitute only a portion of mission failures. Many anomalies have common causes or stem from design or manufacturing flaws; two identical, redundant units can both fail. As a result, Solar Probe took more of a "belt and suspenders" approach; the design incorporates many areas of functional redundancy that allow the spacecraft to either fully or partially recover the mission using different (functionally redundant) hardware, even if both redundant units fail. Solar Probe functional redundancy is highlighted in Table 4-5.

4.3.2.4 Resource Allocations

Mass Allocations. Table 4-6 shows the mass summary for Solar Probe. Mass is summarized for the instruments and each major subsystem and is compared against the maximum launch mass of 713 kg. The mass estimate shows the current estimate of the mass at launch. The growth allowance represents the allowable percentage growth of that subsystem based on the maturity of components within that subsystem. The instruments were provided a generous mass growth allowance of 40%. Generally, new or modified hardware on the spacecraft was given a 20% growth allowance, and components that would be procurements of existing hardware were given 10% growth allowance. The not-to-exceed (NTE) mass represents the mass with the growth allowances incorporated.

Table 4-4. Hardware redundancy.

Functional Area	Hardware Redundancy	Comments
C&DH processing	2 processors	• Hot spare during solar encounter • G&C processing on same unit
G&C processing	2 full-function processors 2 safing processors	• Hot spare during solar encounter • C&DH processing on same unit • Different safing processors and algorithms
Attitude determination (cruise)	2 star trackers Sun sensors	• 1 star tracker turned off during Jupiter flyby
Attitude determination (solar encounter)	2 star trackers Solar horizon sensor	• Both star trackers on • Solar horizon sensor always on
Attitude control	4 reaction wheels	• Three needed for 3-axis control
Propulsion	16 thrusters	• Redundant coupled pair in each axis
Data bus	Redundant 1553 bus	
Data storage	2 SSRs	• 1 recorder turned off during Jupiter flyby • Science data duplicated on each recorder during solar encounter
Telecommunications	2 uplink cards 2 downlink cards 2 LGAs MGA & HGA 2 X-band solid-state power amplifiers (SSPAs) 2 Ka-band SSPAs	• Both receivers on at all times • Either MGA or HGA can be used for cruise communications • Redundancy in X- or Ka-band to either MGA or HGA

Table 4-5. Added functional redundancy in Solar Probe concept.

Functional Area	Primary System Failure	Functional Redundancy	Mission Impact
G&C processing	G&C software fault	Different AIU processor with independent G&C software	• Reduced pointing capability until new software loaded • Unable to execute ΔV maneuvers
Attitude determination (cruise)	Star tracker	IMU – temporary Sun sensors	• Maintaining communications with ground more complex
	IMU	Star tracker Sun sensors	• No significant impact
Attitude determination (solar encounter)	Star tracker	IMU – temporary Solar horizon sensor	• Eventual loss of HGA pointing capability
	IMU	Star tracker	• Reduced pointing capability
Attitude control	Reaction wheels	Thrusters	• Increased propellant usage • Sublimation requirement may not be met
Data storage	SSRs	Real-time telemetry	• Reduced science data
Telecommunications	Ka-band downlink	X-band downlink	• Potential real-time data loss near perihelion
	X-band downlink	Ka-band downlink	• No significant impact
	HGA	MGA	• Reduced real-time data during solar encounter • Longer data retrieval times
Power	Battery hardware	RTG power alone	• Increased probability of need to power cycle instruments • Unnecessary hardware turned off during maneuvers

Table 4-6. Solar Probe mass summary.

Subsystem	Mass (kg)	Growth Allowance	NTE Mass (kg)
Instruments	39.70	40%	55.58
Telecomm.	16.92	20%	20.30
G&C	40.58	19%	48.24
Power	95.80	20%	114.96
Structure	85.60	20%	102.72
Thermal control	148.80	28%	190.96
C&DH	14.41	20%	17.30
Propulsion	21.83	11%	24.42
Harness	21.55	20%	25.86
Dust shield	12.00	20%	14.40
Total dry mass	497.19	24%	614.73
Maneuver propellant	63.10		63.10
ACS propellant	6.00		6.00
Trapped propellant	1.37		1.37
GN_2	0.60		0.60
Total expendables	71.07		71.07
Total wet	**568.26**		**685.80**
Max launch			713.00
Reserves			27.20
Total dry mass growth margin			**29%**

Propellant masses are estimated based on the required ΔV and ACS propellant assuming the maximum launch mass of 713 kg. Mission reserves represent unallocated mass that can be applied to the overall system growth margin. A more complete listing, with mass breakdown of individual components, is given in the master equipment list (Appendix A).

Power Summary. Loads imposed during the solar encounters drive the spacecraft power required for the mission. Basically, during this part of the mission, all subsystems and instruments are active. In addition, because of the extreme solar pressures and solar dust impacts, frequent momentum management maneuvers will be needed, requiring additional power for the thrusters.

Table 4-7 summarizes the power required during the solar encounter and compares it with the power available with the three RTGs for each solar encounter. As shown, significant margin in average power is available for both solar encounters. Occasionally, transient peak loads, mostly from occasional thruster firings and reaction wheel torques, will exceed the power provided by the RTGs alone. A 5 A-h battery incorporated as secondary power source easily accommodates these transient loads. A more detailed breakdown of power usage during the mission is provided in Appendix A.

Table 4-7. Power summary during solar encounter.

Subsystem	Average Estimated Power During Solar Encounter (W)	Growth Allowance (%)	NTE Average Power During Solar Encounter (W)	Transient Peak Loads (W)
Instruments	39.2	20	47.0	100.0
Power	25.6	17	30.0	30.0
Guidance & control	66.8	10	73.5	191.6
Propulsion	9.5	10	10.5	46.8
Telecommunications	26.1	18	30.8	30.8
C&DH	47.8	10	52.6	52.6
Harness losses	3.2	14	3.7	6.8
Total average power	218.2	14	248.0	458.6
Power available 1st encounter (W)			293.7	
Power reserves 1st encounter (W)			45.7	–164.9
Power growth margin 1st encounter			35%	
Power available 2nd encounter (W)			273.9	
Power reserves 2nd encounter (W)			25.9	–184.7
Power growth margin 2nd encounter			26%	

4.4 Spacecraft Subsystem Descriptions

4.4.1 Mechanical Description

4.4.1.1 Requirements

In the development of the Solar Probe concept, several requirements constrained and drove the mechanical configuration. In addition to the mechanically related mission requirements described in Section 4.1 (Table 4-1, requirements 7–13), several requirements were derived to support the selected mission implementation and are included in Table 4-8.

4.4.1.2 Instrument Accommodation

Instrument mounting locations are shown in Figure 4-11. The solar wind ion composition and electron spectrometer (SWICES) and all-sky coronagraph imager (ASCI) are located on the $+X$ side of the spacecraft, allowing them to point in the velocity direction. The energetic particle composition spectrometer (EPCS), visible magnetograph–helioseismograph (VMH), and extreme ultraviolet imager (EUVI) are located towards the $-X$ side to help balance the configuration. The design incorporates a retractable boom that accommodates the magnetometer, plasma wave sensor (PWS), and fast solar wind ion detector (FSWID). The instrument boom is capable of extending from 1.5 to 5 m relative to the bottom of the spacecraft bus. The boom will extend and retract during the solar encounters to match the maximum bus standoff distance available within the protective umbra of the TPS. All instruments are located with a clear FOV as defined in the AO (Figure 4-12).

Table 4-8. Mechanical subsystem requirements summary.

Requirement	Mechanical Implementation
Accommodate instruments as defined in AO	• Mount in locations with clear FOVs • Provide retractable boom for in situ instruments
Package instruments and subsystems within TPS protective umbra	• Compact design (0.95 m bus diameter) • RTGs mounted high under TPS
Provide single-axis HGA range of motion of 0° to 33° off of the nominal $-Y$ boresight and maintain it within protective umbra	• Single-axis gimbaled HGA with two joints and extension arm
Meet interface requirements of Atlas V or Delta IV	• Spacecraft fits well within 5-m fairing dimensions • STAR 48B stage integration straightforward • Low center of gravity offsets
Support TPS, propulsion RTG launch loads, and transfer into launch vehicle adapter	• Thrust struts provided to support TPS • Brackets designed to support RTG and propulsion tank

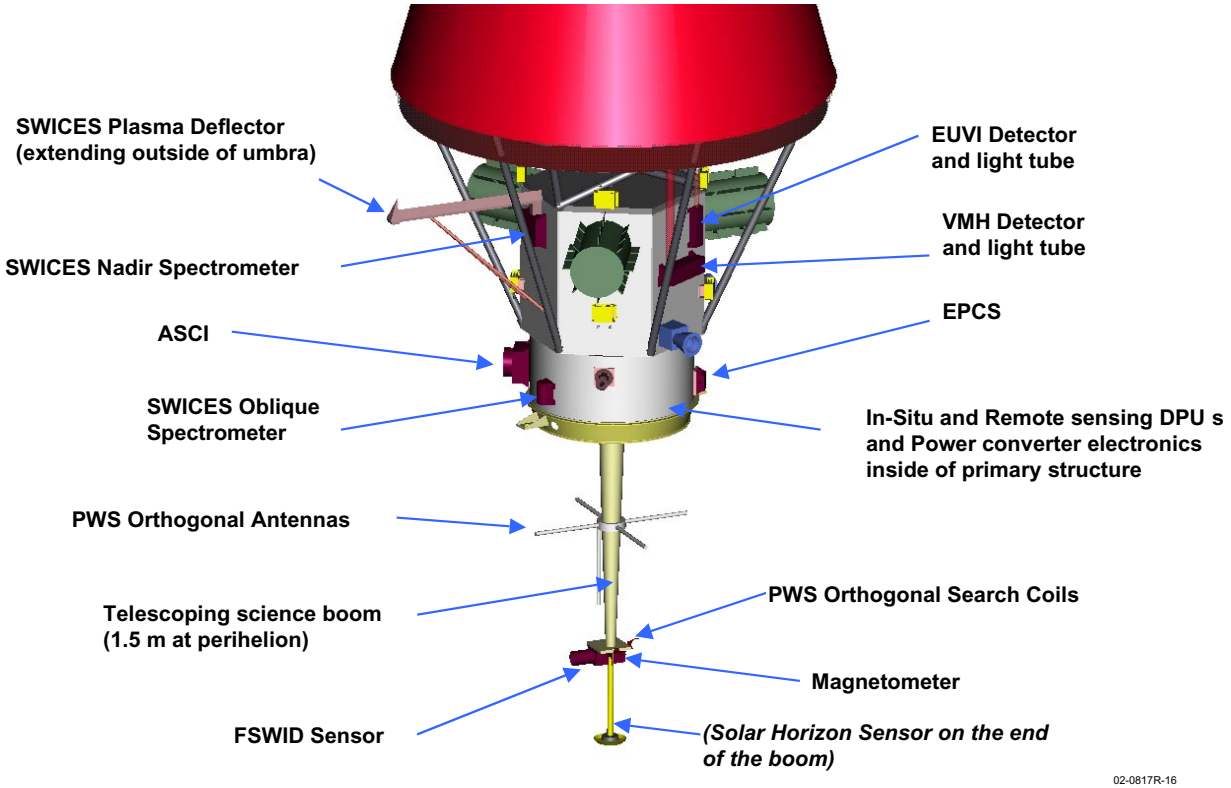

Figure 4-11. Instrument mechanical accommodations.

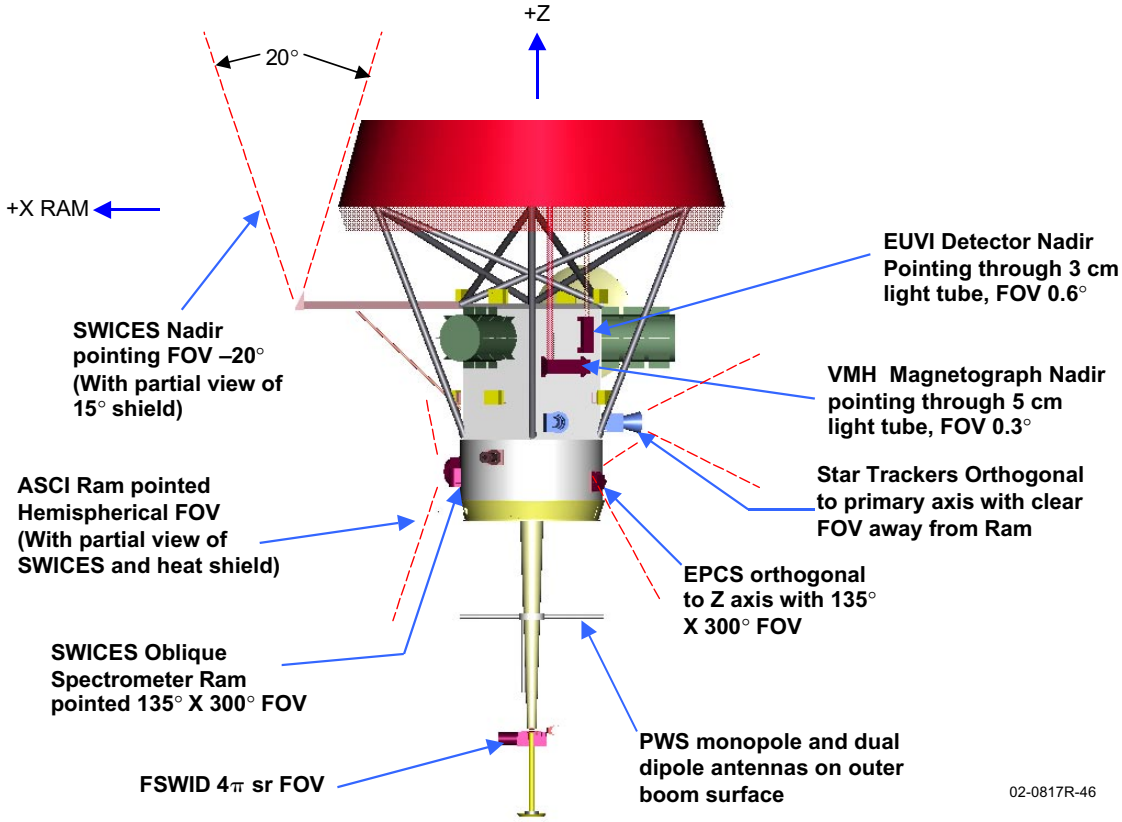

Figure 4-12. Instrument fields of view.

4.4.1.3 Subsystem Accommodation

Major spacecraft subsystem locations are shown in Figure 4-13. Most of the subsystem electronics fit within the interior of the hexagon panel structure. The RTGs are mounted externally to provide adequate view of radiator surfaces to space for cooling. The RTGs also need to be accessible for installation through fairing doors while on the launch pad. The New Horizons mission to Pluto is using a similar arrangement for its single RTG and has shown that this type of mounting is strictly required to do installation on the pad through the fairing doors. Major components of the propulsion system include the Centaur diaphragm tank and four rocket engine modules (REMs). Plumbing is routed inside the structure and allows removal of side panels. The structure can also be integrally assembled with the propulsion system so stainless steel tubing runs can be welded in place from the tanks to the thrusters.

All subsystems fit within a 16.5° umbra provided by the TPS at perihelion. Nominal umbra at perihelion is 14.5° with 2° allocated to account for misalignments and attitude control errors. The diameter of the primary heat shield (2.7 m) is driven by the need to provide umbra shadow over the RTGs.

Antenna placements are defined by mission orientation, with the HGA, MGA, and one LGA pointing along the –*Y*-axis toward Earth. Another LGA is on the opposite side to supply spherical antenna coverage for tumble recovery. A gimbaled joint for the HGA and MGA assembly provides single-axis rotation in the *Y-Z* plane for Earth tracking. A second rotation joint allows the HGA to move out from the bus, allowing the full

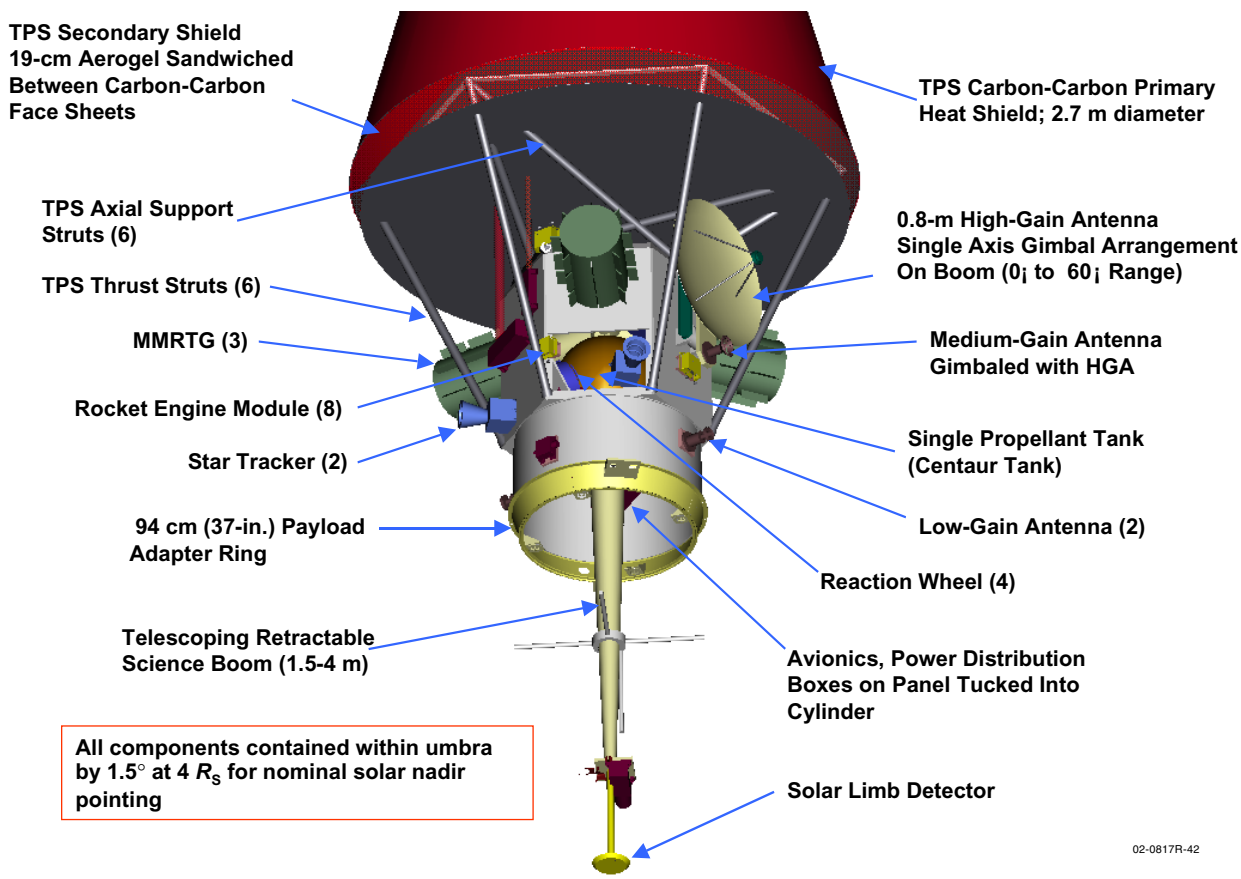

Figure 4-13. Spacecraft subsystem mechanical accommodations.

0° to 33° of rotational freedom necessary to maintain contact throughout the solar encounter while keeping the heat shield pointed toward solar nadir. Drive components for the antenna system use off-the-shelf stepper motors that have very accurate pointing capability, are highly reliable, and have heritage on numerous programs. A launch restraint mechanism attaches the HGA to the structure and will be commanded for a one-time release on orbit.

4.4.1.4 Bus Mechanical and Structural Design

The primary structure for the spacecraft bus uses low-mass aluminum honeycomb panels and machined aluminum construction typical of recent JHU/APL spacecraft. Detailed structure design methodologies, materials, and attachments draw heavily from past and current programs and take advantage of new technology that minimizes mass while maintaining low technical, cost, and schedule risk. Panels are designed for easy removal to facilitate access to subsystem and instruments inside the structure. The panels also provide good thermal conduction and electromagnetic compatibility (EMC) grounding for electronics and instruments.

The primary structure also has very efficient load paths to carry subsystems, instruments, and the TPS. The two main structural components are the cylindrical launch adapter and the hexagonal equipment module. This structure is sized to carry the launch loads and meet launch vehicle stiffness requirements. The single Centaur propulsion tank mounts to the base of the hexagon with brackets and efficiently transfers load directly into the adapter ring. The launch vehicle adapter ring is a one-piece aluminum 7075-T73 machined ring forging typical of most launch adapters and provides a very high strength factor of safety. The hexagon consists of structural panels with 1.0 to 1.5 mm aluminum face sheets bonded to lightweight aluminum honeycomb core. Interconnection of panels is made with aluminum clips that are integrally bonded to the panels. This design has tremendous flexibility and can be modified late in the schedule to accommodate changes in instrument and subsystem interfaces.

Loads from the TPS are efficiently transferred from the strut system into the launch vehicle adapter. After achieving orbit, the thrust struts are baselined to be thermally decoupled from the spacecraft body to limit heat transfer from the heat shield into the bus during solar encounters. Options include simply disconnecting the strut from the bus or ejecting the strut altogether. The latter approach may be advantageous because it may reduce possible FOV or thruster impingements. A more detailed design of the TPS support system is needed, along with further FOV study, to determine which approach (if any) is needed to decouple the thrust struts from the bus after launch.

4.4.1.5 Thermal Protection System Structural Analysis

Initial structural analysis was performed to aid in the design of the TPS and its interface to the spacecraft bus. This analysis was the structural driver in meeting both Atlas V and Delta IV launch environments.

The quasi-static limit load factors, sinusoidal vibration environment, flight acoustics, payload separation shock, ascent pressure profile, and frequency requirements of both vehicles were considered. Positive margins of safety will be demonstrated for all load conditions and combinations, and appropriate factors of safety will be designed into all structural components. A finite-element model of the primary shield, secondary shield, and struts was developed in NASTRAN.

The primary shield consists of six plies of carbon–carbon in a two-dimensional quasi-isotropic layup (0, +60, –60) with a thickness of 0.8 mm. An internal ring stiffener was added at the middle of the conical shield to alleviate

local modes in the primary shield while minimizing added mass. This stiffener is a 1 × 1 in. square closed section, with a wall thickness of 0.5 mm. The material is a two-dimensional warp-aligned 5:1 carbon–carbon that achieves a high elastic modulus in the longitudinal direction and is the same material being used for the struts. The 12-strut arrangement contains six struts for thrust loads and six for lateral loads. Each strut is 5 cm in diameter and 0.5 mm thick, a geometry that balances thermal and structural requirements. The total mass of the shield arrangement is 121 kg.

The TPS was designed to withstand thrust loads of 20 G and lateral loads of 12 G, but it is primarily a stiffness-driven design. Secondary structure mode frequencies must be above 35 Hz to avoid undesirable coupling with launch vehicle modes and/or large fairing-to-spacecraft relative dynamic deflections. The NASTRAN finite element model of the heat shield assembly attached to the spacecraft bus calculates a primary structural mode of 49.8 Hz, demonstrating compliance with this requirement.

4.4.1.6 Spacecraft Handling

Handling of Solar Probe during test requires the TPS to be removed from the spacecraft for shipment to the launch site. JHU/APL has existing containers and fixtures from previous missions that would accommodate both the TPS and the bus to meet the handling requirements. A custom lift fixture for the TPS will attach at the midpoint stiffening ring and allow easy integration onto the spacecraft.

4.4.1.7 Summary

The mechanical concept meets all mission and derived requirements and represents a robust design with an overall low technical risk. Additional definition of the mechanical design will require interaction with the instrument teams.

4.4.2 Thermal Design

4.4.2.1 Requirements and Drivers

The Solar Probe thermal design presents a unique thermal design challenge set by the extreme environmental requirements (Table 4-1, requirements 1, 17, and 18). The spacecraft components and instruments must be kept between –20° and +50°C, the propulsion system between 10° and 40°C. These temperatures must be maintained over extreme solar flux environments from 4 R_S to 5 AU. In addition, the thermal system needs to reject excess heat provided by three multi-mission RTGs mounted to the bus structure, on average 248 W of internal thermal dissipation, and a scoop connected with the solar wind ion composition and electron spectrometer that is exposed directly to the solar flux.

An important design constraint in developing a thermal protection system was to limit the outgassing of all the thermal components to ≤2.5 mg/s. This can be a very limiting constraint when developing thermal shields to operate in maximum solar fluxes of 400 W/cm^2.

4.4.2.2 Thermal Protection System (TPS)

The spacecraft must be shielded from solar heating during the near-Sun mission phases. The thermal control design approach incorporates a TPS that shields the spacecraft from the Sun at distances closer than 0.8 AU. At 4 R_S, the solar radiation is 400 W/cm^2, 3000 times stronger than it is at the Earth. The TPS consists of a primary shield, secondary shield, and light tubes, and it is integrated to the spacecraft by 12 struts. The primary shield consists of a high-aspect-ratio cone that keeps the peak system temperature below 2200 K. The secondary shield provides the bulk of the thermal insulation between the primary shield and spacecraft bus. The light tubes limit incident flux to the two nadir-pointing imaging instruments. The struts provide support and stiffness

during launch and during the mission. Half of the struts, which are included to support the TPS only for launch loads, will be thermally decoupled after launch.

The TPS concept is shown in Figure 4-14. In this depiction, six of the struts are not shown, since they will be thermally decoupled after launch, and the light tubes are integrated within the primary shield and secondary shields.

The primary shield is a 15° half-cone that is always pointed toward the Sun when the spacecraft is closer than 0.8 AU and is constructed completely of carbon-carbon composites. It is 2.7 m in diameter with a 0.8-mm skin thickness. As noted above, a primary mission science requirement is to have a minimal effect on the local plasma density. This is accomplished with a 15° half-angle cone, which has a small area projected to the Sun but a large total surface area. The effect of cone half angle on primary heat shield temperature is shown in Figure 4-15. The resulting TPS carbon-carbon outgassing rate as a function of cone angle is shown in Figure 4-16. Mass loss rates are below the required value of 2.5 mg/s for cone half angles up to 22°. However, the uncertainty in the design values and the increasing sensitivity with temperature argue for a conservative approach. Therefore, the 15° cone half angle was chosen for the design study.

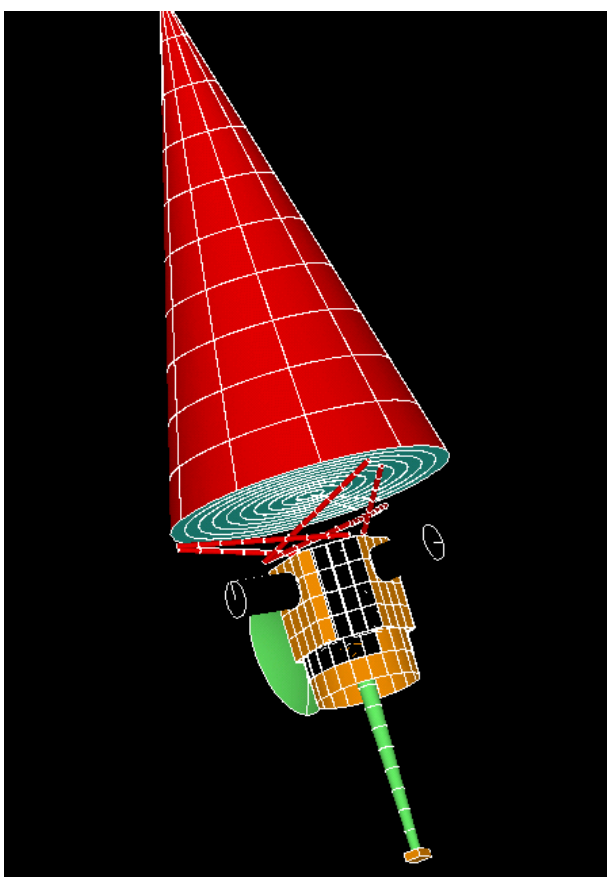

02-0817R-17

Figure 4-14. TPS mounted to spacecraft bus.

The objective of the secondary shield is to limit the heat flow between the primary shield and the spacecraft bus; also, separating the secondary shield from the spacecraft bus allows the thermal energy to radiate into space. The secondary shield consists of a thick, low-density, low-conductivity material contained by carbon-carbon face sheets that provide support. It closes off the base of the cone formed by the primary shield. The current concept calls for a 20-cm thickness. The hot side shield temperature reaches the same level as the primary shield, but the cold side drops to between 500 and 600 K. The secondary shield is separated from the spacecraft bus by 0.5 m. The remaining spacecraft insulation consists of the high-temperature multilayer insulation (MLI) on the top surface of the bus.

Two material choices are available for the secondary shield. Both carbon–carbon aerogel and spun carbon fiber batts represent modifications of existing technologies requiring some development (Frazer 2002). A critical feature of the TPS is that the planned development work continue on both materials. The design values for the secondary shield density and conductivity assume 0.06 g/cm^2 and 0.1 W/m K, respectively.

The aerogel technology is currently being developed by Southern Research Institute (SRI). SRI efforts have been conducted using in-house funding and are limited in temperature. Present conductivity measurements support values as low as

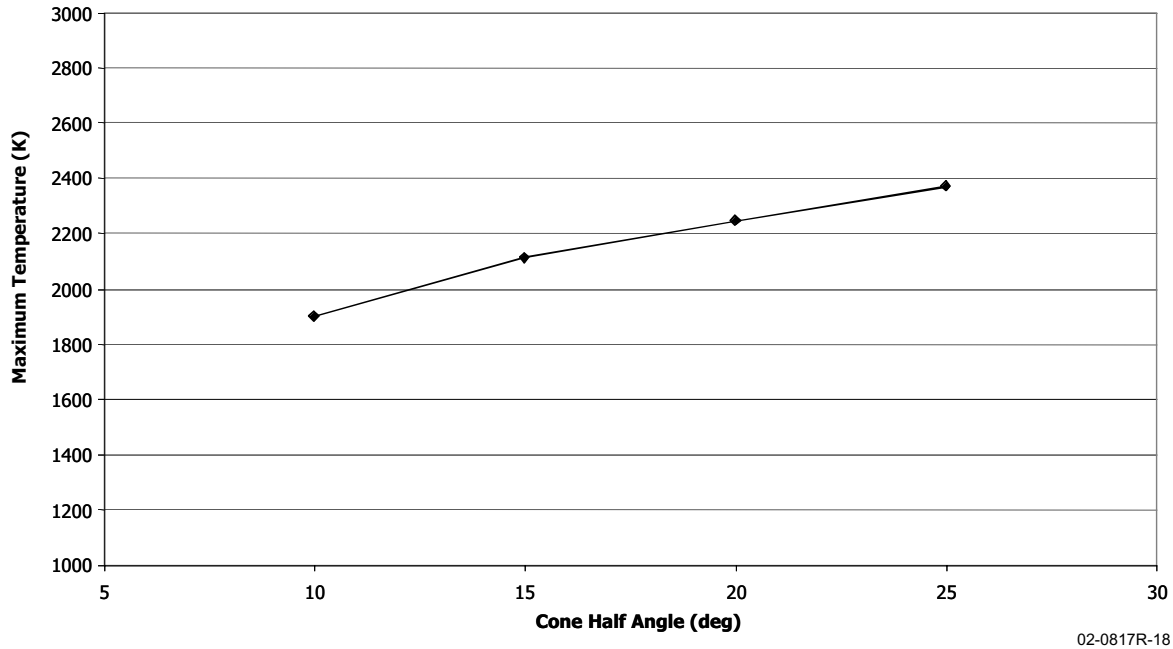

Figure 4-15. Effect of cone half angle on primary heat shield temperature.

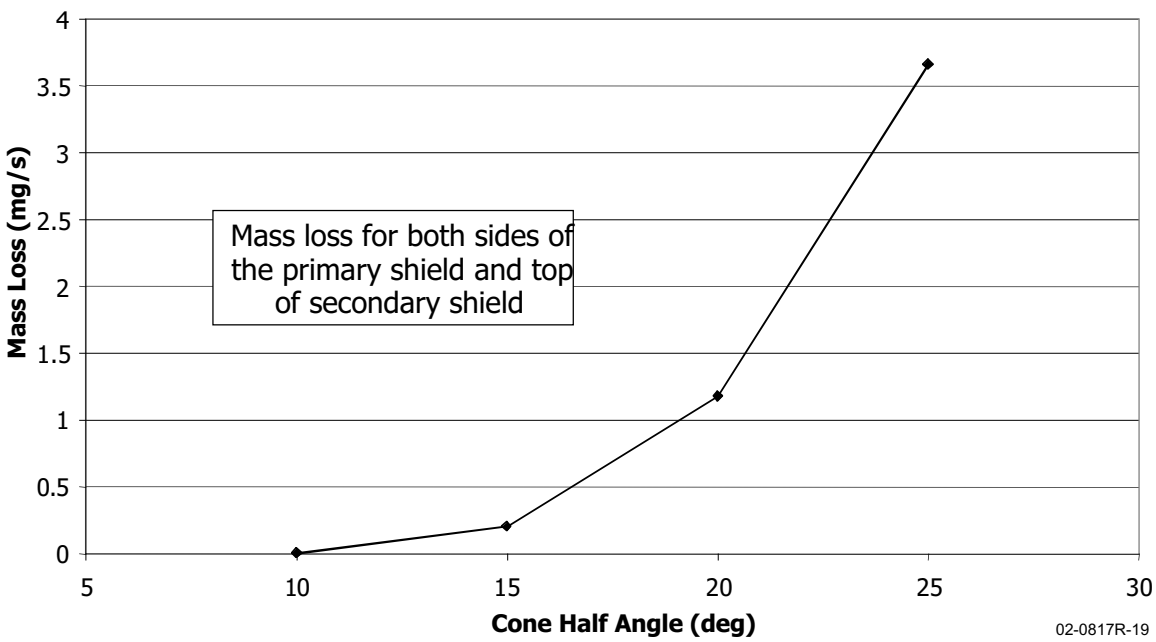

Figure 4-16. Effect of cone half angle on carbon mass loss rate.

0.04 W/m K. Of concern at higher temperatures are the microstructural changes that affect both the conductivity and density. Studies indicate that these changes are relatively constant to 2300 K. As part of the risk mitigation effort, SRI will continue their work in high-temperature aerogels, which will include material reformulation and fabrication studies and high-temperature material property testing.

The other possible choice of material for the secondary shield is carbon fiber batts. The

Applied Science Laboratory has proposed to develop this material. Spun fibers of approximately 1-μm diameter are fabricated into materials with bulk densities of approximately 0.05 g/cm^2. The fiber orientation and density mean the bulk of the heat transfer will be by radiation. Bulk conductivity values are calculated from radiation theory at about 0.02 W/m K. The analysis is supported with testing on similar material systems. Risk mitigation efforts include fabrication of the fibers into 20-cm bats and material property testing after exposure to 1 G and vibration environments.

Two carbon–carbon light tubes are integrated at the top to the primary shield and run through the secondary shield, stopping at the bottom carbon-carbon face sheet. Maintaining a gap between the instruments and the light tubes is necessary to limit conductive thermal flux into the bus.

4.4.2.3 Thermal Modeling and Analysis

The baseline thermal design was modeled and analyzed (Giacobbe 2002) for both the hot case at 4 R_S from the Sun and at 5 AU during aphelion. All the analyses assume steady-state conditions at the given Sun distance. The absorptivity-to-emissivity ratio (α/ε) of the primary shield was assumed to be 1 and represents an uncoated carbon–carbon surface. The conductivity of the carbon–carbon was modeled as a function of temperature. There are six support struts. Each strut is 1.7 m long, with a 5-cm diameter and a 0.5-mm wall thickness. The bus structure is primarily covered with MLI thermal blankets with 1.13 m^2 surface area exposed as radiators.

The thermal analysis of the light tubes (Lee and Lee 2002) shows that the spacecraft heat input comes both from direct solar radiation down the tube and re-radiation from the sides of the tube. The direct insolation is about 23 W. The secondary radiation from the tube ranges from 1 to 25 W depending on the length of the tube. There is less re-radiation at larger spacings between the light tube end and the spacecraft deck. However, optical issues also drive baffle design and will affect light tube analysis. A 75-W light tube heat input was assumed for the study.

A thermal scoop associated with the solar wind ion composition and electron spectrometer is also included to deflect local particles toward the instrument apertures. For this study, we assumed that the instrument team would design the scoop and be responsible for limiting thermal input into the bus. However, the scoop can have a significant thermal impact on the spacecraft thermal balance. The scoop is also made of carbon–carbon, with the exposed portion reaching the same temperatures seen by the primary shield. Without thermal shielding, the heat input from the scoop will raise the spacecraft temperature by several hundred degrees C. Analysis indicates the heat input can be reduced to acceptable levels with a 10-cm-thick, hemispherical, aerogel shield. Thermal isolation at the mounting interface remains a critical issue. Because the instrument scoop is critical and because the test efforts for the scoop and the primary shield are similar, we recommend that the spacecraft design team take a larger role in scoop design and fabrication.

The spacecraft bus structure consists of a hexagonal honeycomb panel structure mounted to the cylindrical launch vehicle adapter. The shadow of the TPS protects all spacecraft and spacecraft-mounted components from direct solar input. The RTGs are mounted to three of the sides of the hexagonal structure and are thermally isolated. The spacecraft support electronics are mounted near the bottom of the hexagonal structure and in the adapter section. Electrical power not required by the spacecraft is rejected directly to space with two shunt panels that are thermally isolated from the spacecraft. The propulsion section is thermally tied to the space-

craft bus to eliminate the need for separate heaters on the tanks, lines, and thrusters. While reducing heater power, this configuration requires the bus temperature to be kept above 10°C. Although the design includes the option of using a variable-conductance heat pipe/radiator system to reduce the heat leak during the cold part of the mission, the current analysis does not include this feature because the design is feasible without it. An option for a variable-conductance heat pipe system represents additional margin in the spacecraft design.

Key features of the thermal design and the thermal balance for the hot case are illustrated in Figure 4-17. Although over 3400 W is transferred from the primary shield to the secondary shield, most of this heat is radiated to space. Less than 25 W is transferred from the TPS to the spacecraft bus, and most of this comes from the

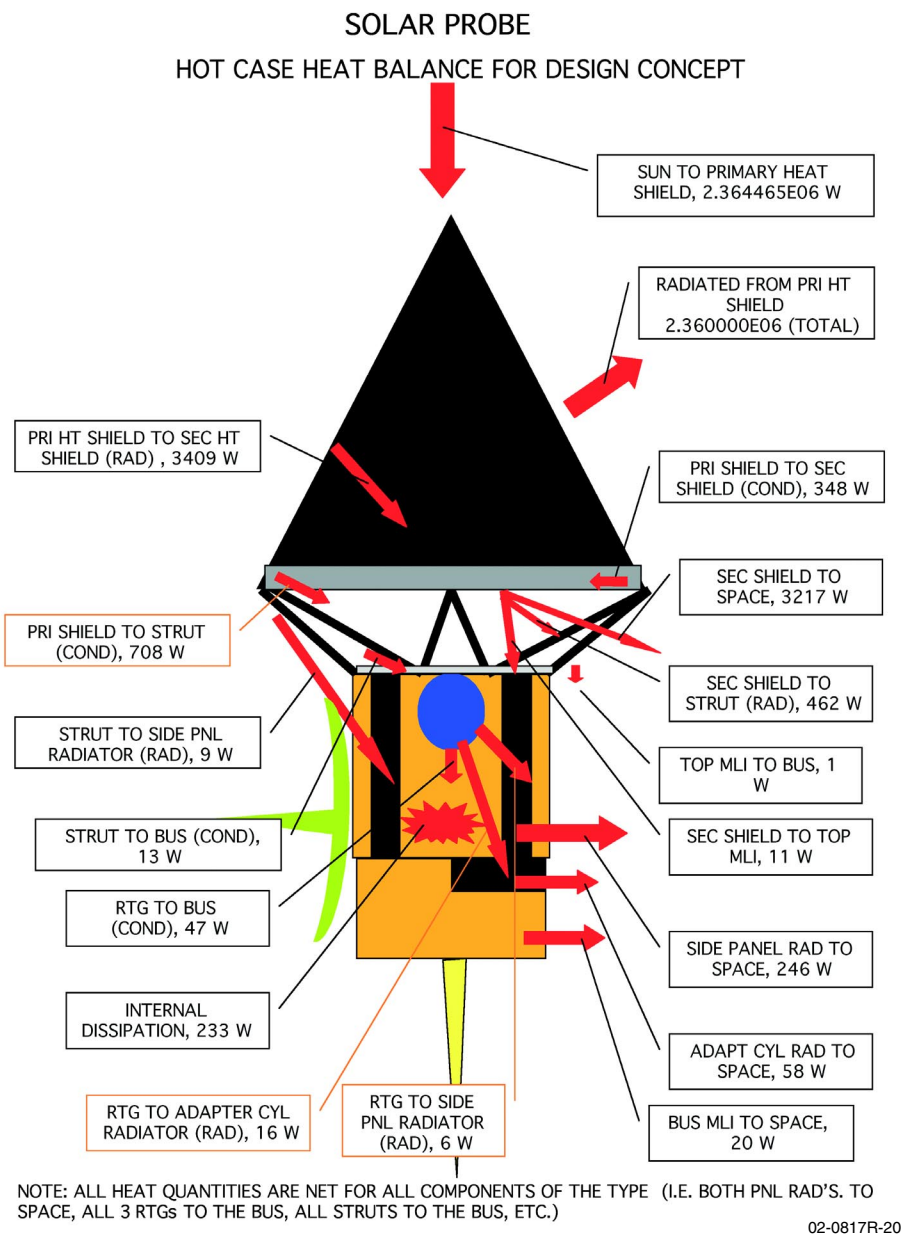

Figure 4-17. Thermal balance for the hot analysis case.

TPS support struts. The spacecraft is effectively isolated from the primary shield by the secondary shield, the low-ε surfaces on the secondary shield, and the spacecraft MLI. Internal dissipation provides the bulk of the heat input to the spacecraft, and the RTG provides the second-largest heat input. The RTG is assumed to be thermally isolated, but the actual heat flow can be tailored based on the conductivity of the mount and the needs of the system.

Hot case temperature analysis results are illustrated in Figure 4-18 and shown in Table 4-9. Results for the baseline concepts indicate the spacecraft bus temperatures will be maintained within the required temperature limits.

Cold case temperature analysis results are illustrated in Figure 4-19 and shown in Table 4-9. The results show acceptable temperatures at 5 AU. Spacecraft bus temperatures ranges from –16 to 17°C, with the propulsion tanks 5°C. If required by the final spacecraft design, the propulsion system temperatures could be raised with the use of a variable-conductance heat pipe to limit the heat loss from the spacecraft in the cold case. The cold case temperatures include the replacement heater power to keep the bus

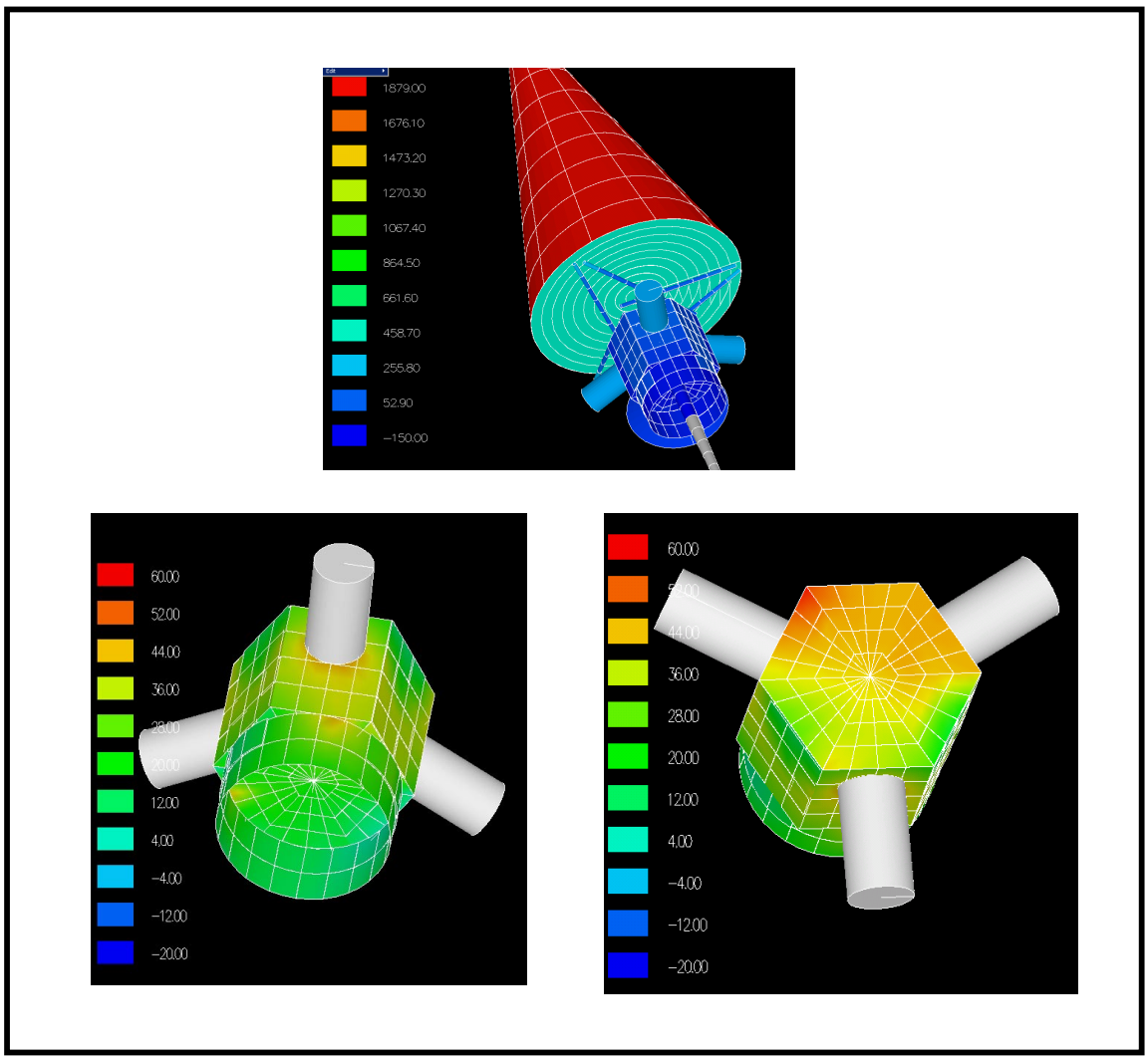

Figure 4-18. Hot case thermal analysis results.

02-0817R-21

Table 4-9. Spacecraft temperature results of thermal analysis.

Spacecraft Location	Hot Case Temp. (°C)	Cold Case Temp. (°C)
Primary shield	1879	–167
Secondary shield	440 to1879	–160
Struts	237	–112
Top deck MLI	88	–36
Top deck	53	–13
Hex structure	16 to 37	–17 to 8
Adapter structure	8 to 27	–16 to 17
Bottom deck	9 to 41	–13 to 3
Propellant tank	42	5 to 6
HGA	–18	–35

dissipation at a near-constant 248 W. Heater power in the cold case is moved to the propulsion system components to raise their local temperature during the cruise phase.

4.4.2.4 Summary

The thermal concept defined meets the mission requirements with reasonable technology risks. An advantage of the MMRTG power source is the ability to use the waste heat to help maintain spacecraft bus temperatures at large solar distances without the need for additional heaters. There are identified technology risks in the implementation of the thermal protection system. Section 5, Risk Mitigation, discusses the next technical development activities, which will

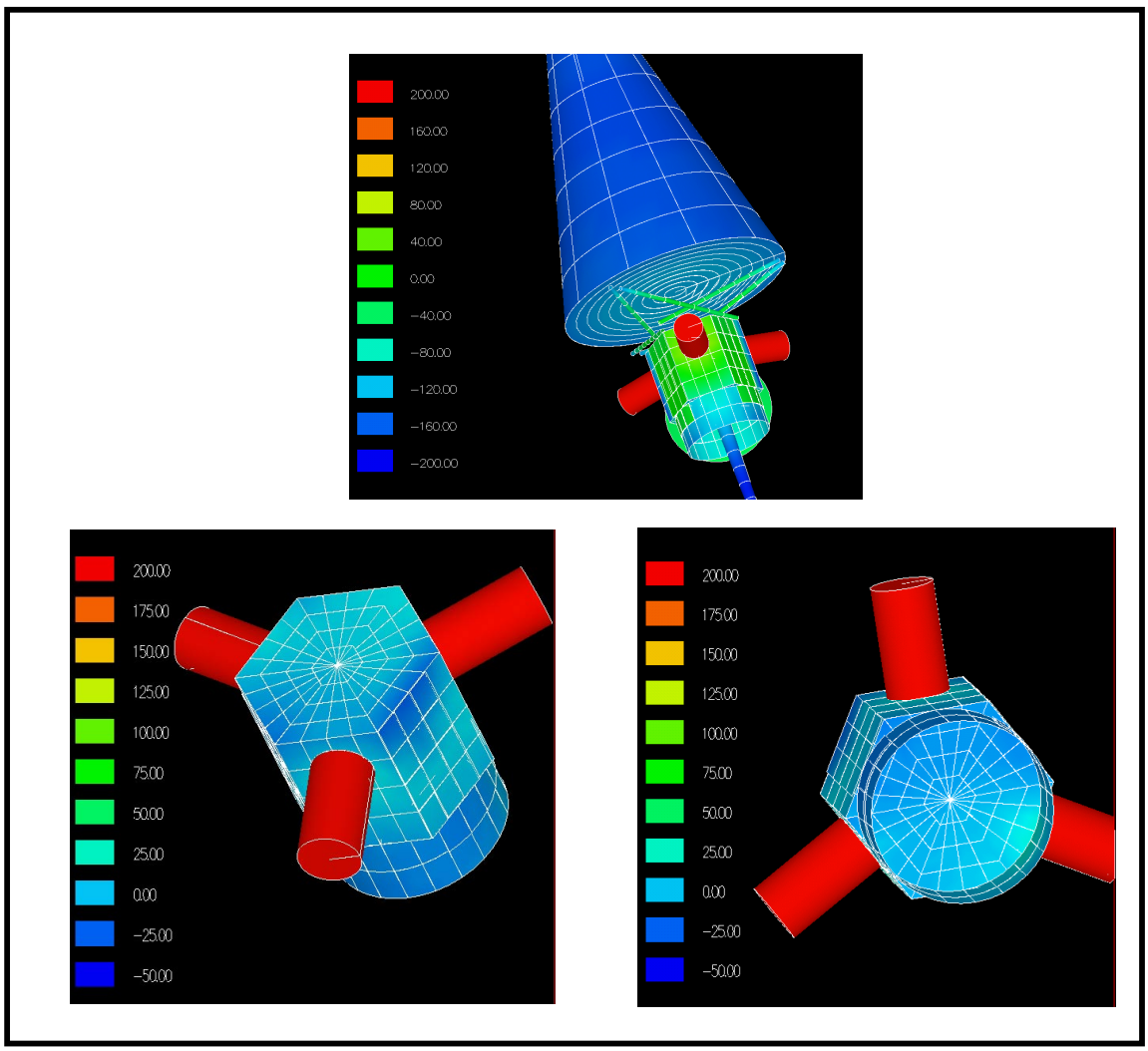

02-0817R22

Figure 4-19. Cold case thermal analysis results.

reduce risk by fabricating and demonstrating a prototype design early in development.

4.4.3 Telecommunications Subsystem

4.4.3.1 Requirements and Constraints

Several requirements and constraints drove the Solar Probe telecommunications design. The primary drivers and resulting implementation are summarized in Table 4-10.

4.4.3.1. Design Considerations

Downlink Frequency Considerations. One of the most important considerations in selecting the telecommunications architecture was the need to provide real-time telemetry near perihelion. As Solar Probe approaches perihelion during a solar encounter, the Earth is in quadrature with the Probe–Sun line, and the elongation (Sun-Earth-Probe or SEP) angle is approximately 1°. Conjunction experiments with other probes show that X-band and S-band communication links are affected adversely at small elongation angles. For example, a study of the NEAR-Shoemaker spacecraft as it underwent a superior conjunction in early 1997 showed measurable degradation of command and telemetry links at X-band for elongation angles below 2.3° (Bokulic and Moore 1999). On the downlink and at an elongation angle of 1.1°, the ground station successfully recovered only 3% of the telemetry frames transmitted by the spacecraft at 1104 bps, and 0% of the same when transmitted at 39.4 bps. The predicted telemetry margins were 6 dB at 1104 bps and 19 dB at 39.4 bps if solar effects were ignored. For elongation angles greater than 2.3°, the ground station recovered in excess of 99.7% of the transmitted frames at 1104 bps. The published literature characterizes such degradation as a scintillation loss. Earlier studies on the Magellan (Webster 1994) and Galileo (Beyer et al. 1996) spacecraft produced similar conclusions.

Table 4-10. Telecommunication subsystem requirements summary.

Requirement	Impact
Maximize science return over the mission	128 Gbit baselined
Maximize real-time telemetry throughout a solar encounter	≥ 25 kbps baselined
Solar corona effects (scintillation) on radio wave propagation	Ka-band data downlink
Extreme speed of the spacecraft	X-band command uplink
Limited size of TPS to shadow the antennas	0.8-m antenna diameter
Tight power constraints associated with an RTG-powered mission	8-W Ka-band transmitter

A model of radio wave propagation in turbulent media (Armstrong and Woo 1980; Koerner 1984) generates similar conclusions about frequency dependence of such degradation and predicts that Ka-band links will be significantly more resistant to corona scintillation effects than X-band and S-band links. Improvements in link performance at Ka-band have been confirmed by simultaneous transmission of telemetry on X-band and Ka-band links during solar conjunctions with Mars Global Surveyor (MGS) (Morabito et al. 2000); Deep Space 1 (DS-1) (Morabito et al. 2001); and Cassini (Morabito et al. 2002).

According to models developed from the data (Armstrong and Woo 1980), scintillation loss varies inversely as the square of the frequency. The frequency ratio of a Ka-band frequency to X-band frequency for a given DSMS channel is 3.8:1, and consequently, the model predicts that Ka-band enjoys a 11.6-dB advantage over X-band with respect to scintillation loss. Poor weather does erode some of the advantages of Ka-band, but even under 90% weather conditions, only a Ka-band system can meet real-time telemetry goals near perihelion. For this reason, the Solar Probe concept is baselined to use a Ka-band downlink during critical periods of solar encounters.

An X-band system has advantages when solar scintillation is absent. An X-band system, when taking advantage of the 70-m DSMS antennas, will actually outperform a Ka-band system, which is limited to the 34-m DSMS antennas for the foreseeable future. In addition, X-band is relatively insensitive to weather as compared with Ka-band, offering additional flexibility. X-band also offers the benefit of greater technological maturity and flight heritage. And finally, an X-band system has a wider beam for a given antenna size than Ka-band, making pointing budgets more forgiving. For these reasons, it was considered advantageous to carry an X-band downlink in the baseline design, as well as a Ka-band downlink.

Figure 4-20 shows the performance of the baseline telecommunications concept during a single-day solar encounter. The graph assumes an 8-W RF transmitter for X- and Ka-band. The X-band transmission is received using the 70-m antenna, and the Ka-band transmission is received using the 34-m antenna. Both are shown for clear weather conditions (cumulative distribution [CD] = 0.1, 0.9), and we further show Ka-band at 90% condition. In all cases, the calculated data rates were achieved with a link margin of 3 dB. Scintillation losses and varying elevations of ground track stations are included in the calculations.

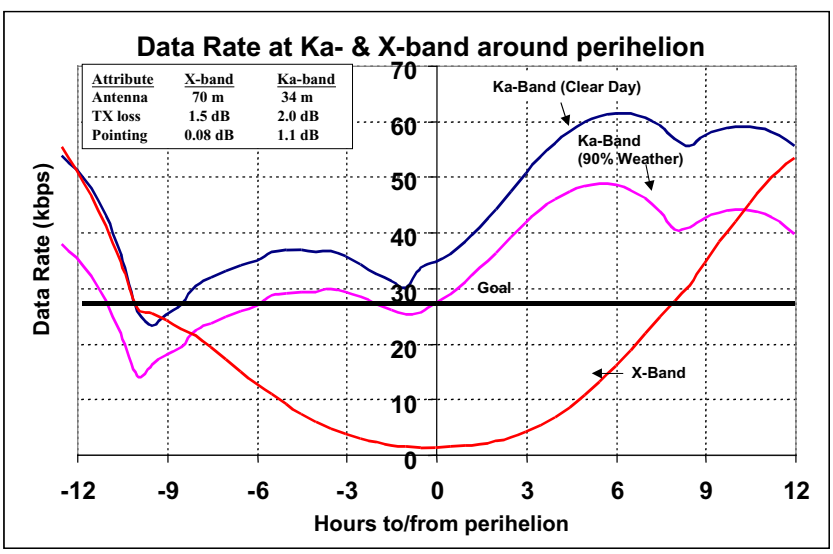

Figure 4-20. Comparison of Ka-band and X-band links during a solar encounter.

Over the range of weather (CD = 10% to 90%), the Ka-band link comfortably meets the minimum data rate over the entire primary science period, albeit with slight deterioration of link margin from 3 to 2.45 dB during the early part of the solar encounter. Figure 4-20 further shows that the X-band link outperforms the Ka-band link except during the 24-hour (critical science) period around perihelion. Outside of this period, the data rate exceeds 45 kbps and is less susceptible to variations in weather and elevation angle.

To reduce the sensitivity of link performance to month of arrival, our architecture utilizes science telemetry links at both X- and Ka-bands. Provision for both frequencies using the same antenna aperture comes at the expense of somewhat reduced performance for X-band. Nevertheless, the reduced X-band data rates outside the single day around perihelion remain comparable to those of the Ka-band link but are less sensitive to weather.

Command Link Considerations. The desire for simplicity and the extreme speed of the spacecraft at perihelion drive the choice of uplink frequency. The spacecraft reaches a top speed of 308 km/s, at which the angular separation between transmitting and receiving line of sight is nearly 3.5 beamwidths of a 34-m antenna if both links are at Ka-band. However, the spacecraft speed is under 100 km/s for all but 2 days of the orbit, and the corresponding angular separation is approximately 1.3 beamwidths at Ka-band and one-half beamwidth at X-band.

Consequently, an X-band command link was selected. The uplink allows a command rate of 500 bps with a link margin of 16 dB when spacecraft speed is 100 km/s. Alternatively, separate 34-m assets could be used for Ka-band telemetry and commanding, but this option requires that the spacecraft carry a Ka-band receiver, which is less desirable because of technological immaturity and lack of heritage in interplanetary missions. Besides, the low data rate associated with commanding diminishes the need for Ka-band. The X-band configuration chosen utilizes receiver hardware with strong flight heritage from the TIMED and CONTOUR programs.

4.4.3.2. Baseline Implementation

The selected telecommunications architecture is shown in Figure 4-21. The telecommunication subsystem features bidirectional communications at X-band through all of the spacecraft's antennas: two LGAs, one MGA, and one HGA. In addition, it includes a telemetry link at Ka-band via the HGA. Although the HGA affords the best link, it sets an upper bound for the total pointing error relative to the spacecraft-to-Earth line of sight at 0.2°. The telecommunication subsystem utilizes the LGAs and the MGA to accommodate communication with the Earth during cruise. The LGA and MGA designs have prior flight heritage.

Two LGAs were incorporated into the design for emergencies that could occur early in the mission or when mission events preclude pointing of the MGA and HGA. The LGAs are mounted 180° apart; each provides angular coverage of 45° (±22.5°) and peak gain of 10.75 dBi at the X-band downlink frequency, and, for a 5-W transmitter, a telemetry rate that exceeds 10 bps into a 70-m ground station for spacecraft-to-Earth distances of less than 2 AU. Each allows a command rate of at least 31.25 bps with over a 6-dB margin under the same conditions on the uplink.

The primary antenna used during the cruise portion of the mission is the MGA, which is a single MGA with angular coverage of 10° (±5°) and gain of 20.4 dBi at the X-band downlink frequency. For an onboard 5-W transmitter, the link supports a data rate of 10 bps with 3-dB margin into a 70-m ground station at spacecraft-to-Earth distances up to 6 AU (the maximum distance

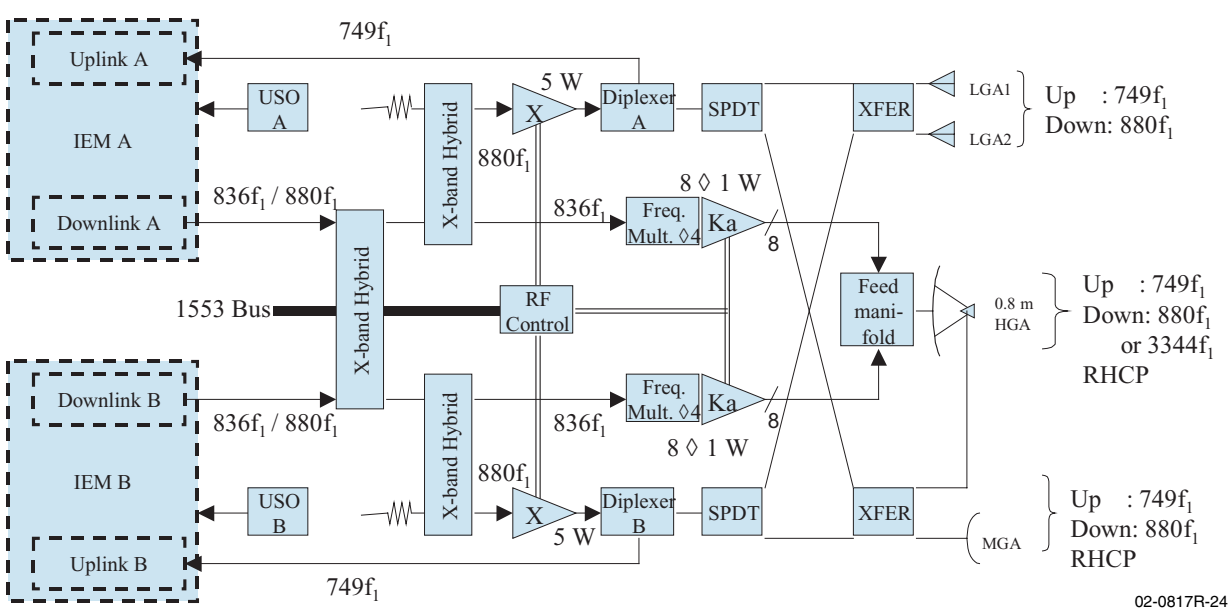

Figure 4-21. Telecommunications architecture.

from Earth in the current mission design). Under these circumstances the command rate is at least 125 bps with over 6-dB of link margin. The baseline design facilitates MGA pointing by having the MGA mounted on the gimbal that points the HGA.

The HGA is the preferred aperture for communications transactions during the solar encounter and data retrieval phases of the mission, including all of the science telemetry. The main reflector is 0.8 m in diameter and utilizes a dichroic subreflector to transmit a right-hand circularly polarized wave at Ka-band. A horn behind the subreflector provides bidirectional communications at X-band. Umbra size (and ultimately lift mass), constrains the size of the main reflector and the focal length of the optics ($f/D \leq 0.4$).

Figure 4-21 shows how the antennas just described connect to the spacecraft electronics. The spacecraft's transmitter section consists of a pair of downlink cards, each within its own integrated electronics module (IEM); four solid-state power amplifier (SSPA) modules, two at X-band and two at Ka-band; a pair of ultrastable oscillators (USOs); and a distribution network to couple signals between the SSPAs and any of the available antenna apertures. We envision that prime power is applied to only one of the four SSPAs to enable either X-band or Ka-band communications on the telemetry link. Both frequency bands are serviced by block-redundant SSPAs. The output from either of the X-band SSPAs may be steered to any of the antennas through a network of single-pole-double-throw (SPDT) and transfer (XFER) switches, which are themselves configured for redundant operation. A frequency quadrupling circuit drives the input of each bank of Ka-band SSPAs.

The downlink card starts with the same design basis as those flown on TIMED and CONTOUR. However, it must be enhanced to support turbo-encoding to take advantage of the reduced signal-to-noise ratio (S/N) at which these DSMS links can operate.

The uplink card is the same as that under development for the New Horizons mission. The transceiver was selected based on the uplink and downlink cards rather than a transponder because of the ease of integration brought about by consolidating the baseband and RF modulation functions within the same enclosure as the IEM. The USOs are also based on CONTOUR/New Horizons heritage; we start with that design and provide enhancements that lower mass and prime power consumption and improve immunity to irradiation.

4.4.3.3. Noncoherent Navigation

Instead of standard Doppler tracking techniques using a transponder, Solar Probe's communications system includes features for making accurate Doppler measurements with a transceiver. This approach eliminates the need to carry a transponder. For an RTG-powered spacecraft such as Solar Probe, this design provides a significant and needed reduction in required spacecraft power.

An approach was developed and demonstrated on CONTOUR that allows accurate Doppler measurements to be made with a simple transceiver and a moderately stable oscillator (Jensen and Bokulic 1999). The approach involves a measurement of the ground station's uplink carrier frequency by the spacecraft, which provides results to the ground station via telemetry. The ground station combines the information from telemetry with measurements of the spacecraft's downlink carrier frequency to obtain a Doppler measurement that has the same precision as one obtained with a coherent transponder. A conceptual drawing of the approach is shown in Figure 4-22. This navigation approach to Doppler tracking with a transceiver does not require any new equipment at the ground stations. The technique impacts ground operations because the observed Doppler

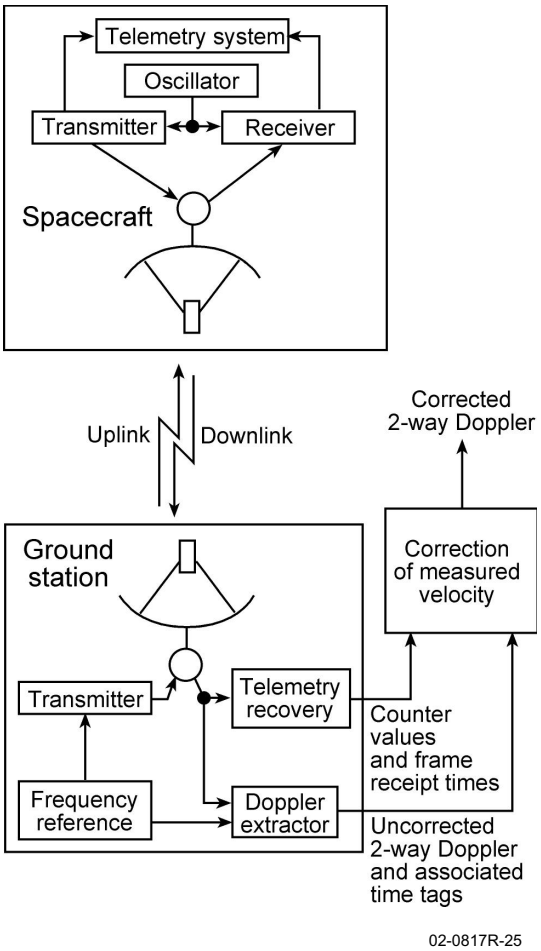

Figure 4-22. Two-way, noncoherent navigation concept.

frequencies must be corrected by telemetry prior to their use in orbit determination. Extensive tests (Jensen and Bokulic 2000) demonstrated that this noncoherent telemetry-assisted technique makes velocity measurements with a precision of ≤0.1 mm/s for 1-min measurement intervals. Thus use of a lighter-weight, lower-power-consumption transceiver yields results equivalent to those obtainable from a coherent technique with a transponder.

4.4.3.5 Summary

The telecommunications subsystem meets all the mission requirements. The continuous high downlink data rate throughout the perihelion passages is critical to ensure a successful science mission and is accommodated by implementing a Ka-band downlink. A unique advantage is the opportunity for telemetry of Cruise-Mode science data return during the contacts for noncoherent navigation. Some technology development is needed to implement a high-efficiency Ka-band system; the work plan is detailed in Section 5, Risk Mitigation.

4.4.4 Power

4.4.4.1 Requirements

Requirements that drive the design of the power subsystem are set by the extremes of the Solar Probe orbit and its dual solar encounters (Table 4-1, requirements 1, 3, 14-16). The impacts on the power subsystem design are summarized in Table 4-11.

4.4.4.2 Primary Power Source Selection

Several candidate sources for primary power were considered. Solar power was ruled out early in the trade-offs because of the mission's wide extremes in the solar environments. Currently, no spacecraft with solar panels has flown beyond the 2.1 AU reached by NEAR, and no spacecraft has been conceived to fly closer than

Table 4-11. Power subsystem requirements summary.

Requirement	Impact
Provide reliable spacecraft power to the spacecraft over the entire mission	Solar panels impractical; chose multi-mission radioisotope thermal generator (MMRTG) as primary power source
Extremely low solar flux at 5.0 AU aphelion	
Intense solar flux at 4-R_S perihelion	
Multiple orbits and solar encounters encompassing over 7 years design life	Three MMRTGs for end-of-mission power level
Maximum average power required, driven by the solar encounter of 248 W	
Maximum peak power required, driven by the solar encounter when propulsion is active (momentum management) or when the reaction wheels are providing large torques to slew or compensate for dust impacts. The total power could theoretically peak to 458 W	Lithium ion battery secondary power source for extended peak loads

the 0.3 AU planned for MESSENGER. Solar Probe will spend about 10 days inside of 0.3 AU during each solar encounter. On the basis of the power required and the mass constraints, we determined that using batteries alone for power during this period would be impractical.

The only other mature space power sources are radioisotope sources. The RTG design that has been flown for the past 25 years is no longer produced and will not be available to support Solar Probe. However, plans are for two radioisotope sources to be available to support a 2010 Solar Probe mission: the multi-mission RTG (MMRTG) and the Stirling radioisotope generator (SRG).

The MMRTG is has essentially the same basic design as previously flown RTGs but is smaller, carrying eight general purpose heat sources (GPHSs) rather than 18. Transfer of the heat generated by the radioisotope units to electrical energy is essentially the same as in previous RTG designs. Each MMRTG is specified to provide at least 110 W BOL (beginning of life) spacecraft power per unit.

The other possibility, use of SRG power sources, offers the advantage of significantly better efficiencies than RTGs and would require less plutonium to supply the same power. SRGs are currently being developed at NASA Glenn Research Center, and development is scheduled to support a 2010 launch. Currently SRG designs have no flight heritage. However, development and testing of prototype units at NASA Glenn look promising. An SRG is baselined for the Mars 2007 Lander.

The MMRTG option was selected as the current baseline, primarily because the technical risk is lower than that for the SRG option. The MMRTG design is basically a repackaged version of flight-proven RTG technology. In addition, we had some concerns about whether the SRG, with its moving electronic parts, would meet the electromagnetic compatibility and interference (EMC/EMI) requirements of the sensitive plasma wave instrumentation that Solar Probe will carry. This decision can be revisited in the future and reevaluated as the MMRTG and SRG designs mature.

4.4.4.3 Secondary Power Source Selection

Because potentially large transient peak power loads were identified during the study, a secondary power source was considered necessary. High transient peaks will come primarily from reaction wheels, thrusters, and some of the instruments. Most of these peaks are less then 1 s in duration, but during momentum management and ΔV maneuvers, significant power draws could last for several minutes.

These potential peak power loads are likely to last too long for reliance on a capacitor bank alone, which is typical for RTG-powered missions. A small battery, on the order of 4.5 A-h, would be more than adequate to handle these transient peak power loads. A lithium ion battery was chosen based on its high energy density and predicted availability in the next few years. Lithium ion power sources have been under significant development in recent years, and the risk of going to this technology was considered low.

4.4.4.4 Power System Implementation Description

A block diagram of the power system components is shown in Figure 4-23. The system consists of three MMRTGs, a shunt regulator unit (SRU), external shunts, battery charger, boost converter, battery, and a power distribution unit (PDU). The three MMRTGs provide total power of 330 W BOL. Power available decays to 274 W at the end of the mission. Figure 4-24 shows power decay from earlier RTG missions.

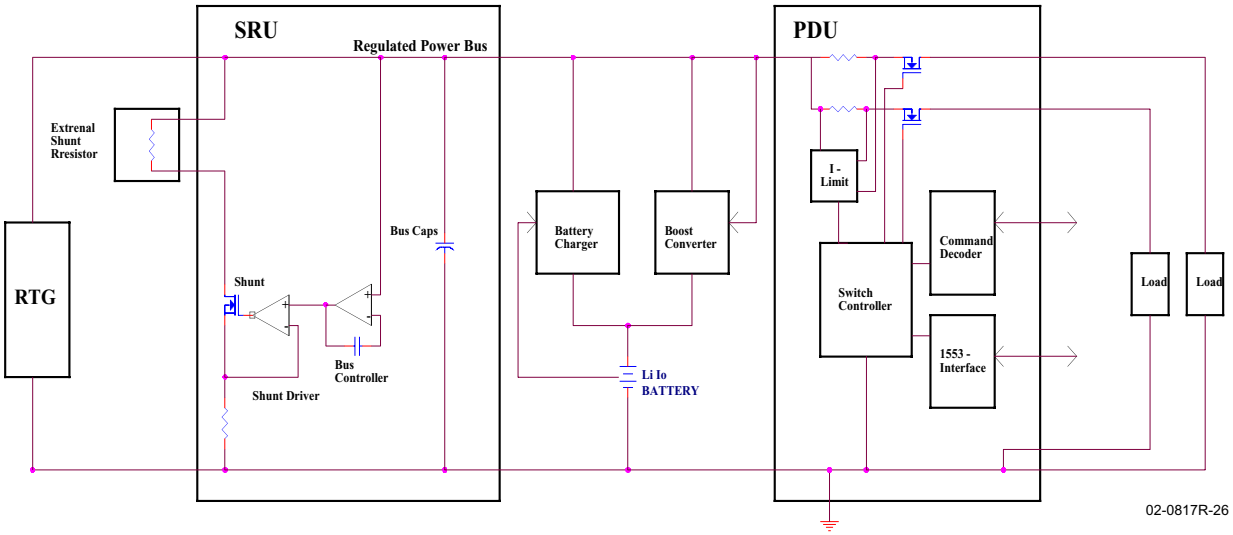

Figure 4-23. Power system block diagram showing one of the three MMRTGs.

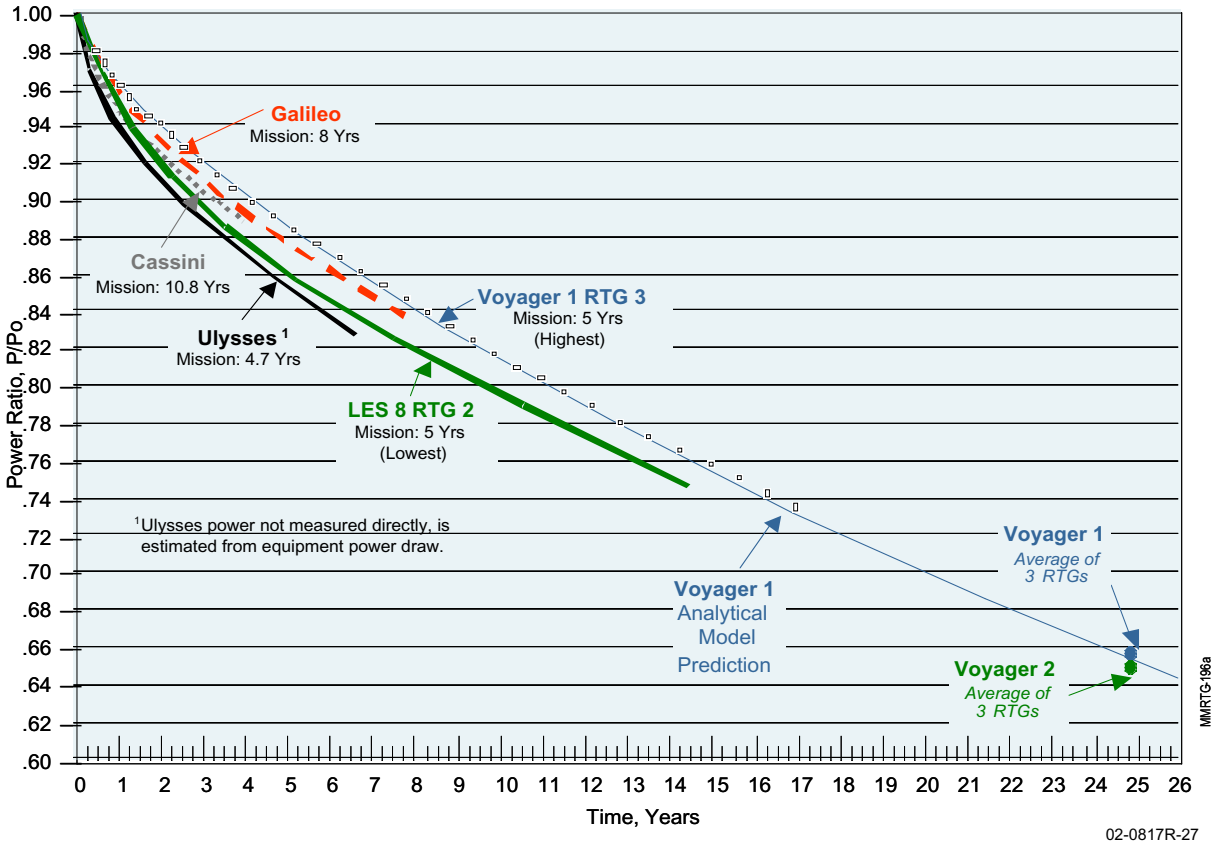

Figure 4-24. Empirical RTG decay rate data.

RTG power will also degrade some during launch. On the launch pad the unit is cooled with forced air. At the instant of liftoff, the air flow stops and the unit is enclosed in the launch vehicle fairing for much of the lift phase. As a consequence, the radiator plates of the MMRTGs heat up and the power output decreases. Soon after the fairing is ejected, xenon gas will be vented and the MMRTGs will radiate thermal energy to space, which will allow the RTG units

to reach normal operating efficiency in approximately 8 hours. The spacecraft design will limit required power loads during launch, and initial maneuvers will be conducted after adequate power margin is available.

The SRU controls power to the spacecraft using resistive shunts to dissipate unneeded power and a small capacitor bank to provide an even flow of current to the spacecraft. As discussed earlier, a lithium ion battery provides secondary power to accommodate peak loads. The battery is charged and controlled by the battery charger when there is surplus power, so that the battery is kept fully charged throughout the mission. When the load power exceeds the MMRTG output, the bus voltage drops. The boost converter monitors the bus voltage, and at 29 V it begins to take energy from the battery to keep the bus voltage at 29 V. The PDU provides relays and switches controlling loads to various subsystems.

4.4.4.5 Experience with RTG-Powered Spacecraft

An RTG-powered spacecraft must cross significant hurdles to get approval for flight. The National Environmental Policy Act (NEPA) process to approve RTG-powered spacecraft launches is very involved. Nonetheless, RTGs are used for a number of space missions. JHU/APL has experience in obtaining launch approval on multiple projects that used RTGs and is quite familiar with the NEPA process. We are currently developing the required documentation for the New Horizons project, and we have assisted/developed the NEPA documents for Aerospace Nuclear Safety Programs since 1971. These include Voyager, Pioneer, Galileo, Ulysses, Mars Pathfinder, Cassini, Mars 2001 and Mars 2003. JHU/APL's previous experience with the NEPA approval process is summarized in Table 4-12.

4.4.4.6 Summary

The power subsystem meets all requirements derived for this mission with a low technical risk for implementation. The availability of the MMRTG is governed by activities beyond the scope of the Solar Probe project, as detailed in Section 5, Risk Mitigation. However, the current development schedule the Department of Energy has released for the MMRTG meets our

Table 4-12. Previous JHU/APL contributions to NEPA launch approval process.

Mission	Flight RTG Units	No. Radio-isotope Heater Units	Year Launched	JHU/APL Contributions
Galileo	F-1, F-4	Over 100	1989	Response analysis of light-weight radioisotope heater units (LWRHUs) to inadvertent Earth reentry during Venus-Earth-Earth gravity assist (VEEGA); technical review of General Electric (GE) analysis; arc-jet tests of GPHS, graphite impact shell (GIS), and LWRHU to simulate reentry.
Ulysses	F-3		1990	Technical review of GE analysis; wind tunnel tests of GPHS, GIS, and LWRHU.
Mars Pathfinder	N/A	3	1996	Response analysis of LWRHUs to solid rocket motor (SRM) fires.
Cassini	F-2, F-6, F-7	117	1997	Response analysis of LWRHUs to inadvertent Earth reentry during Venus-Venus-Earth-Jupiter gravity assist (VVEJGA); preliminary GPHS reentry safety assessment, GPHS motion studies; technical review of Lockheed Martin Astronautics analysis; answer Interagency Nuclear Safety Review Panel (INSRP) inquiries, launch contingency effort.
Mars 2001	N/A	3	2001 (lander cancelled)	Issued nuclear risk assessment for draft environmental impact statement (DEIS); issued preliminary safety analysis report (PSAR) (Tetra Tech NUS, Inc. [TtNUS]); tested SRM fires.
Mars 2003	N/A	Up to 22 total	2003 (planned)	Issued "quick-look" nuclear risk study; reviewed databook (TtNUS); reviewed STAR 48 breakup system design.

2010 launch date schedule. The lithium ion battery technology is maturing rapidly and is currently being used in other space applications. It is expected to be one of the standard battery technologies available within the Solar Probe development time frame.

4.4.5 Avionics Architecture

The Solar Probe avionics architecture is illustrated in the system block diagram in Figure 4-21 and described in the following sections.

4.4.5.1 Requirements

The requirements that most affect the Solar Probe avionics subsystem architecture are summarized in Table 4-13. They result from the need to ensure successful science mission against the risks and uncertainties in the extreme spacecraft environment (Table 4-1, requirements 1, 3, 23, and 24).

4.4.5.2 Data Bus

The initial selection for the baseline Solar Probe data bus is a 1553B bus. This data bus is a standard configuration with significant flight heritage. Performance of the 1553 bus is more than adequate to handle spacecraft data traffic, as well as the instrument peak data rates defined in the AO of 112 kbps. As the Solar Probe project develops, this selection will be revisited in a formal trade study.

4.4.5.3 Integrated Electronics Module (IEM)

Solar Probe uses an IEM architecture for housing most of the avionics hardware. This approach is consistent with previous APL spacecraft programs and will take advantage of extensive use of heritage hardware. Each IEM includes the flight processor, SSR, command and telemetry card, telecommunications uplink and downlink cards described in Section 4.4.3, and power conditioning. Solar Probe accommodates two IEMs fully cross-strapped for redundancy.

Table 4-13. Avionics subsystem architecture requirements summary.

Requirement	Impact
Maximize science return during each solar encounter	Redundant 128-Gbit SSRs
Provide a fault-tolerant architecture with adequate redundancy to ensure mission success	Dual IEM plus dual AIU with backup attitude control function
Survive high-radiation environment introduced by the Jupiter flyby	Qualify to 100 krad total dose

Command and Data Handling (C&DH), G&C, and spacecraft fault protection functions will be performed in a single (240-MIPS) radiation-hardened RAD750 processor. The system architectures developed for the CONTOUR and MESSENGER spacecraft provides significant heritage for developing the Solar Probe IEM electronics.

Each Solar Probe IEM will include a 128-Gbit SSR board based on the 64-Gbit data recorder currently being developed for the New Horizons mission. The New Horizons SSR design uses 1-Gbit flash memory integrated circuits that are physically stacked to form each of the 16 independently powered 4-Gbit memory banks. The New Horizons SSR board control logic enhances system fault tolerance and survivability by maintaining an EEPROM map of bad memory blocks and substituting functional memory blocks for failed portions of the SSR memory. JHU/APL successfully tested the 1-Gbit flash memories at the New Horizons SSR total dose limit of 40 krad while operating the memories at a 10% duty cycle.

The proposed Solar Probe SSR board will form sixteen 8-Gbit memory banks by stacking four (currently available) 2-Gbit flash memories. Minor modifications to the New Horizons SSR flash memory control field-programmable-gate-array (FPGA) logic will be required to accommodate the larger memories, but the SSR architecture and most of the control electronics will be essentially unaltered. Tests will be conducted to verify proper operation of the 2-Gbit memories at a total dose limit of 100 krad while

operating at a 10% duty cycle. Since the SSR board does not have to be powered during the Jupiter flyby, turning the SSR off near Jupiter remains an option if additional (total dose) margin is required. An alternative Solar Probe SSR design that stacks eight 1-Gbit memories to form each memory bank can be considered if total dose testing of the 2-Gbit flash memories is not totally successful.

During a solar encounter, both IEMs will be powered and each IEM will process uplink command messages, detect and correct spacecraft fault conditions, and record all instrument science data (i.e., redundant recording of all science data). The primary (selected) IEM processor will perform all G&C control functions and will serve as the spacecraft data bus controller. If a critical fault condition is detected in the primary IEM, data bus controller and G&C functions can be quickly switched to the redundant IEM processor without rebooting. During non-critical mission periods, the redundant IEM may be turned off to reduce spacecraft power bus loading.

4.4.5.4 Attitude Interface Unit (AIU)

Redundant AIUs housed in a single chassis provide all required interfaces between the 1553B data bus and the attitude system sensors (horizon sensors, digital solar aspect detectors [DSADs]) and actuators (reaction wheels, thrusters). Unlike the IEM processors, the AIU processors will operate in a standby redundant mode, with only one unit powered at any time. The selected AIU serves as a backup attitude control processor, running a simplified control algorithm that will take over attitude control functions should a critical attitude error occur during a solar encounter. The Solar Probe AIUs are similar in concept and complexity to the RTX-2010–based NEAR AIUs; each consists of a processor board, dedicated attitude system interfaces, and power conditioning electronics. The current AIU baseline design includes a RAD750 processor that offers the benefit of a common design with the IEM processor, but alternative, lower-power processors will be considered.

4.4.5.5 Instrument Data Processing

Because no instrument teams were working with us during this study, we had to assume an instrument data processing architecture. Based on recent experience on several other JHU/APL spacecraft programs, we assumed that the *in situ* and the remote sensing instrument suites would each have their own DPU acting as a remote terminal on the spacecraft data bus. All instrument science and housekeeping data and all instrument commands will be transferred between the DPUs and the IEMs over the redundant 1553B spacecraft data bus, which can easily accommodate the maximum planned instrument data rate of 112 kbps.

4.4.5.6 Summary

The avionics subsystem meets all the requirements with a robust and low-risk implementation. The issue of radiation hardness of the SSRs is detailed in Section 5, Risk Mitigation. Aside from that issue, the subsystem can be implemented within current technical capability.

4.4.6 Data Handling Approach

4.4.6.1 Requirements

The Solar Probe data handling subsystem is the coordinated operation of the onboard data store and telecommunications. The requirements for data handling are to maximize both the quantity and the reliability of the science data return (Table 4-1, requirements 23 and 24). The hardware elements of the data handling system were described in Sections 4.4.3 and 4.4.5. Here we focus on the operational approach.

4.4.6.2 Data Management Approach

The primary objective of the Solar Probe data management approach was to maximize both the quantity and the reliability of the science data

return. The spacecraft design provides a large, redundant data storage capability as well as a limited-bandwidth, continuous real-time link.

Each of the two 128-Gbit SSRs is sized to hold an entire 20-day solar encounter's worth of planned science data with margin. Although Solar Probe maintains a continuous real-time downlink during the encounter, this link plays a backup role, ensuring a scientifically significant data return even in the event of a catastrophic failure in the harsh near-Sun environment. The redundant recorders capture all science data, and real-time data paths and redundant X- and Ka-band downlink capability ensure maximum probability of returning prioritized mission science data.

The encounter science data collection profile is broken into three phases as follows:

- Primary: –10 days to –1 day; +1 day to +10 days
- Critical II: –24 hours to –8 hours; +8 hours to +24 hours
- Critical I: –8 hours to +8 hours

The total data rate increases as Solar Probe approaches the Sun and decreases as the spacecraft recedes, reflecting the criticality and uniqueness of the *in situ* coronal measurements. The distribution of the data rates between the instrument suites and within the suites is optimized to the measurement requirements of each phase. Since the entire 20 days of encounter data are stored in each SSR, the data storage capacity is driven by the instrument data rate requirements. For this study, the requirements were developed from a JPL-provided summary of the instrument AO responses. The stored data rate profile is shown in Figure 4-25. The SSR capacity of 128 Gbits offers ample space for science and spacecraft housekeeping data taken during the encounter.

The real-time data rate is determined by the instantaneous capability of the downlink. This rate is affected by many factors including the Sun-Earth-Probe geometry, Earth–Probe distance, elevation angle at the ground station, weather at the ground station, and the downlink band. Hence, the mission operations staff can adjust the real-time data rate to maximize the return depending upon the current operating conditions. The spacecraft has the capability to maintain several science data rate tables corresponding to different real-time data rates. The nominal real-time science data collection rate profile is shown in Figure 4-26. Any unused real-time bandwidth is automatically allocated to playback of the data recorders.

Starting 3 days after perihelion, 2 hours of the real-time link each day are devoted to playback of the most critical encounter data. At the end of the encounter, a full recorder playback is initiated using 16 hours per day of DSMS contact time. Figure 4-27 shows the overall data profile for each encounter. The stored data total reflects the required instrument data rates depicted in Figure 4-25. The total science return line reflects the sum of the real-time data transmitted during the encounter plus the stored science data placed in the recorder. Additional science data can be accommodated, limited only by total capacity of the recorders and the extended operation cost for downlink time.

The onboard data handling approach places the onus for instrument data processing on the instrument DPUs. Once generated, the instrument data are sent to the DPU for that instrument suite. The DPU performs any required data evaluation and compression. Low-rate science data are placed into CCSDS frames and sent to the C&DH component over the 1553 bus. After compression, high-rate image data are converted into CCSDS frames and buffered in the DPU to be sent over the 1553 bus as well.

4.4.6.3 Summary

The data handling subsystem meets requirements and exceeds the expected data return over

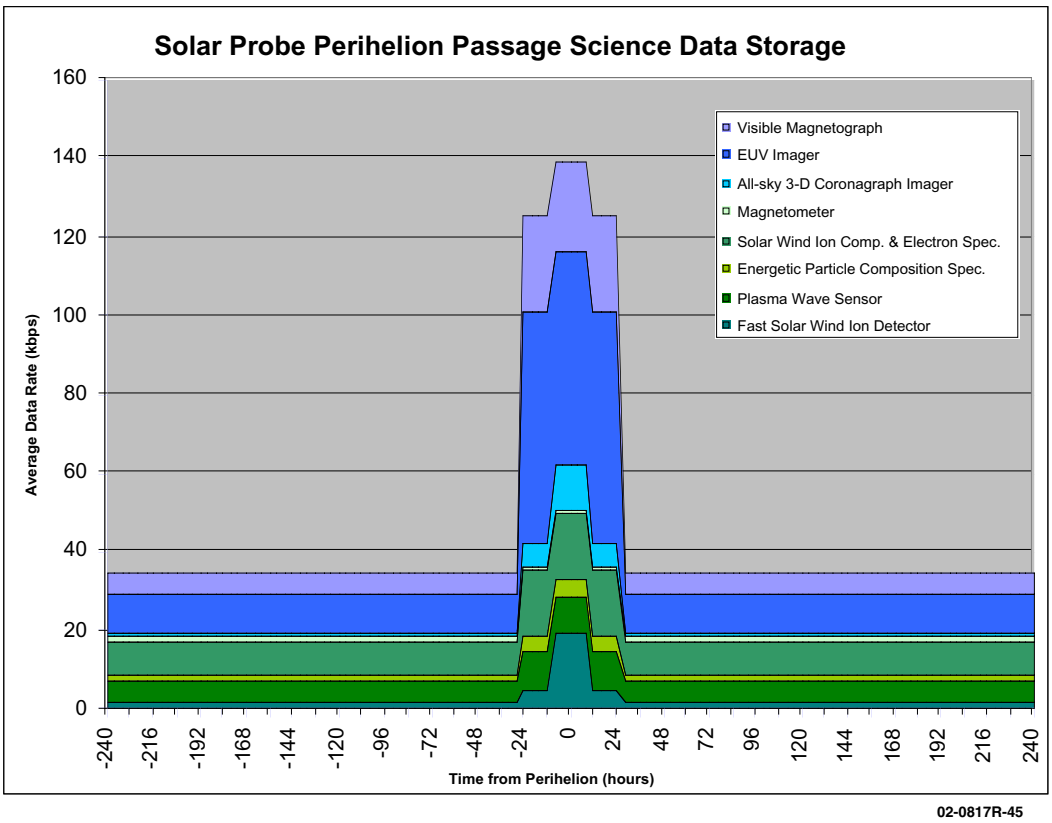

Figure 4-25. Solar encounter instrument stored data rates.

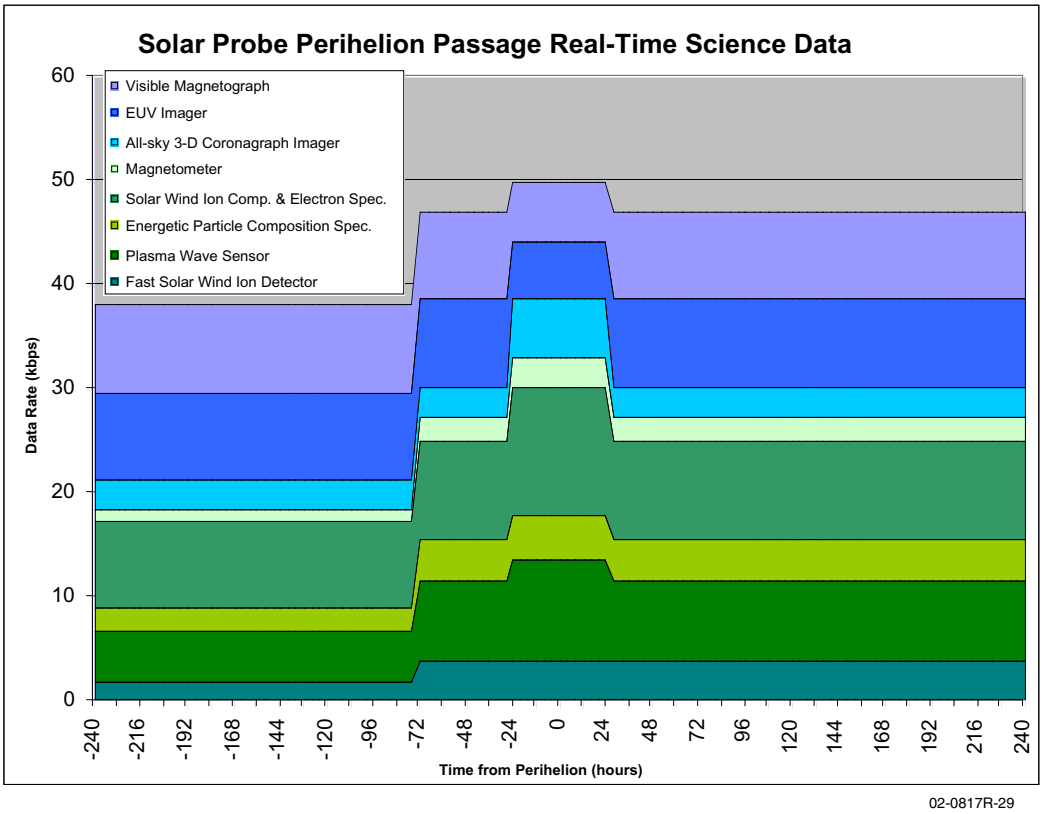

Figure 4-26. Nominal real-time science data collection profile.

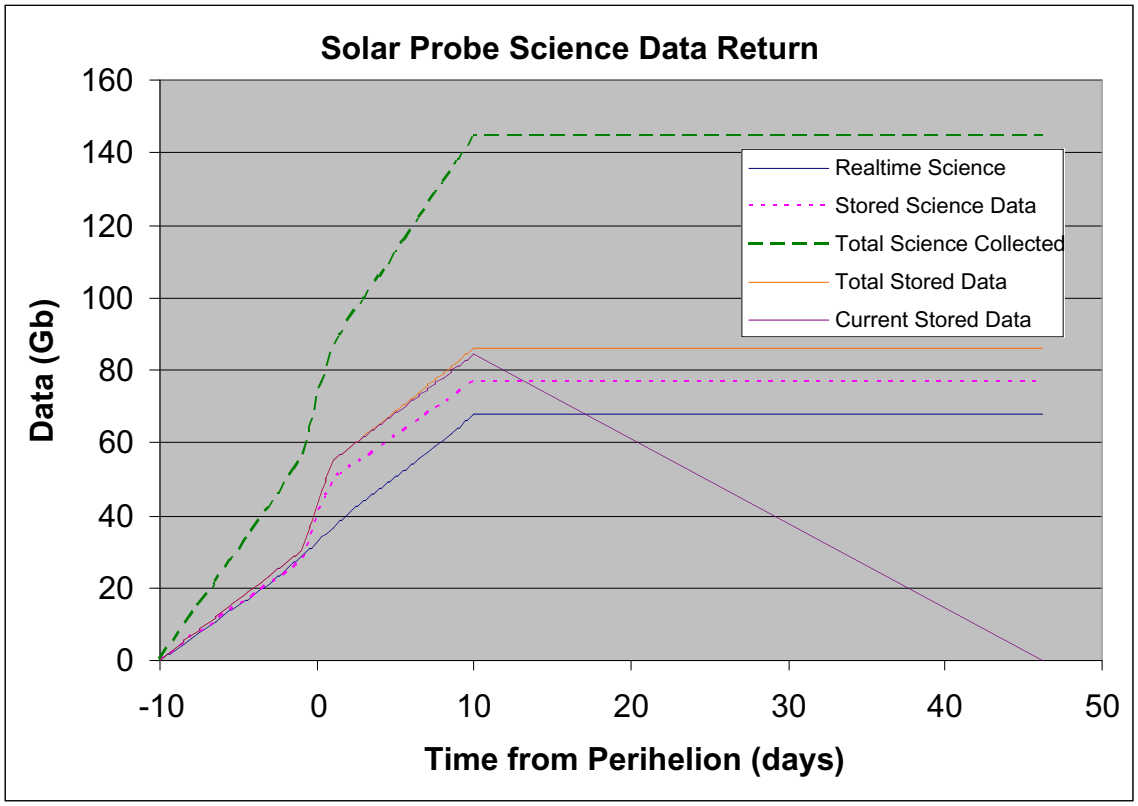

02-0817R-28

Figure 4-27. Solar encounter data collection and storage profile.

the 1999 mission description by a factor of 3. This can be accomplished using established hardware described in Sections 4.4.3 and 4.4.5 with little overall technical risk.

4.4.7 Guidance and Control

4.4.7.1 Requirements

Pointing Requirements. The pointing requirements for Solar Probe come from two basic sources. The first source, the AO documentation, defines the following pointing requirements to support the remote sensing instruments during solar encounter (Table 4-1, requirements 19–22):

- Absolute pointing requirement ≤0.3°
- Absolute attitude knowledge ≤0.05°
- Jitter ≤0.005° in 1 s

For this study we assumed that the nominal boresight was solar nadir and that these requirements would be applied over the entire solar encounter except during brief periods for necessary momentum management. Refinement of these requirements and assumptions will require interaction with the science team.

The second source of pointing requirements is allocated based on the pointing requirements of the HGA. Selection of Ka-band transmission and the limit of a 0.8-m HGA requires a pointing accuracy of 0.2°. Accounting for misalignments and ability to calibrate the antenna on orbit, the attitude control system was allocated 0.025° inertial knowledge accuracy and 0.05° for attitude control.

Environmental Requirements. Several environmental factors were drivers for the Solar Probe G&C design. First, as the spacecraft approaches perihelion, a star tracker looking away from the Sun through the solar corona will see sunlight reflected off dust particles (Klaasen 2002). In addition, the coronal brightness may vary by a factor of 10 due to “local condensations,” and

coronal lighting reduces the S/N ratio on the charge-coupled device (CCD) in the star tracker, thereby reducing the number of detectable stars and degrading the performance of the star tracker. These phenomena considerably limited the choice of star trackers and also drove the design to operate two star trackers throughout the solar encounter.

Next, solar pressure will be very high and will change rapidly during the solar encounter. During this phase, the cone-shaped heat shield is to be pointed toward solar nadir. Because the center of photon pressure is ahead of the center of mass, the solar pressure torque is destabilizing and becomes an important part of the dynamics of the spacecraft near perihelion. The solar pressure torque is 0.08 N·m/radian (0.0014 N·m/degree) at perihelion and decreases with distance r from the Sun as $1/r^2$. Initial analysis (Lisman 2001; Tarditi et al. 2001) shows that without constant attitude control at perihelion, the photon torque causes the attitude to change from 0.2° to 3° in 3 min, thereby exposing the instruments and the spacecraft bus directly to the intense solar flux. In addition, even relatively small misalignments of the heat shield induces significant torque and momentum buildup, potentially forcing more frequent use of thrusters for momentum management.

Solar dust impacts were also an important attitude control consideration. Data extracted from Mann (2001) and Lisman (2002) indicate a 1% chance of encountering a grain 100 μm or larger for each square meter of surface area projected into the relative velocity direction. The dust particles are mostly in a nearly circular orbit within ±30° of the solar equator and are in greater concentration near the equator. The momentum and attitude can be controlled by wheels for <130-μm dust and by warm and ready thrusters for <315-μm dust. There is significant uncertainty in the dust model due to the paucity of *in situ* data, and so a conservative design is was pursued.

Finally, the large velocity of the spacecraft results in significant stellar aberrations due to relativistic considerations. Relativistic effects will cause apparent shifts in the Earth position, solar nadir, and stellar references, requiring correction terms as part of the G&C design.

4.4.7.2 Functional Description

The Solar Probe spacecraft coordinate frame is illustrated in Figure 4-28 and is defined as follows:

- Origin centered at base of adapter ring
- Z-axis through center of adapter ring and apex of heat shield
- $-Y$-axis parallel with nominal boresight of antenna and in the plane of the bottom of the adapter ring
- X-axis formed using right hand rule

Shortly after deployment, the G&C system will need to despin the spacecraft from 60 to 0 rpm. This spin rate is induced by the spin-stabilized Star 48B stage. Despin will be performed by onboard thrusters until the total angular momentum is reduced to 0.1 N·ms. Then the wheels take over and slew the spacecraft to the desired attitude.

For most of the mission the spacecraft will maintain 3-axis pointing control with the $-Y$ axis

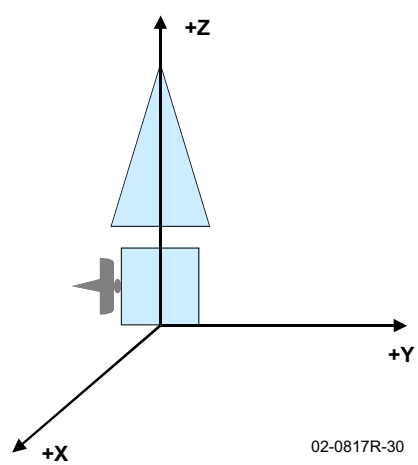

Figure 4-28. Solar Probe coordinate frame.

(nominal HGA/MGA boresight) pointed toward Earth. This attitude can be maintained when the spacecraft at least 0.8 AU from the Sun. While in this cruise attitude mode, a slow rotation of 0.5 rpm will be introduced to reduce angular momentum buildup from solar pressure torque. Occasionally, momentum will build up enough that momentum dumps using thrusters will be needed. Adequate pointing control will easily be maintained to keep the MGA pointed at Earth to within 5° circular error 3σ.

As the spacecraft comes inside of 0.8 AU, it must change attitude so that the TPS points toward the Sun and keeps the instruments and subsystems within its protective umbra. Some off-pointing from solar nadir may be necessary to keep the HGA and MGA pointed at the Earth, as long as sensitive instruments and subsystems are not exposed to the Sun.

During the solar encounter (P ± 10 days), the spacecraft attitude will be maintained so that the *Z*-axis is pointed toward solar nadir and the HGA and science pointing requirements are maintained. As a result of the intense solar pressures, momentum dumping will be much more frequent during this period. For short periods, thrusters will fire to remove angular momentum and the requirements for instrument pointing and control may not be maintained. Each momentum management maneuver will be completed in under 1 min.

An alternative approach is being considered for the periods of most intense solar pressure; this approach involves dynamically controlling the spacecraft so that the photon torque can actually be used to control momentum buildup. Such an approach requires an intentional offset in the heat shield that is controlled automatically by the feedback control system. If this approach is implemented, traditional momentum dumping using thrusters will not be needed during this period. Implementation will require additional analysis and interaction with the science teams to ensure that the intent of the pointing requirements can be met.

4.4.7.3 Hardware

Attitude Determination. Attitude determination will be performed by redundant star trackers and a high-precision IMU. The baseline star tracker selected was the Sodern SED-16. This star tracker meets performance, radiation, and design life requirements, and preliminary data indicate that it will perform adequately in the presence of coronal lighting near the Sun. The star tracker pointing directions (boresights in the *X*-*Y* plane and *Y*-*Z* plane at 45° from the –*Y* axis) were chosen to ensure that the star trackers view different parts of the solar corona at all times, minimizing the chances of both trackers being blinded simultaneously by locally high coronal brightness.

The IMU initially selected as the baseline is the Northrop Grumman Space Inertial Reference Unit (SIRU). This IMU is a derivative of previous IMUs that have significant flight heritage and is designed to meet high radiation and design-life requirements associated with deep-space missions. Although the SIRU gyro has excellent drift stability, the drift itself can be up to 2° per hour estimated to an accuracy of 0.05° per hour. In the absence of star tracker updates and a reliable bias estimate, safe attitude control can be maintained for up to only 20 min. The SIRU unit has 4-for-3 redundancy for both gyros and accelerometers and redundant electronics and interfaces.

To accommodate a safing attitude determination system during cruise, digital Sun sensors are mounted to provide almost 4π steradian coverage and allow an attitude reference relative to the Sun if an attitude determination anomaly occurs. At distances beyond 3.0 AU, simply pointing the –*Y*-axis toward the Sun allows contact with the Earth within the MGA beamwidth of 10°. Inside of this solar distance, a small step

star search pattern will be performed to reestablish contact with the ground.

Because of possible long-duration star tracker blinding, system resets, or other attitude control anomalies, we thought it prudent to baseline a new solar horizon sensor for safing during the time that the spacecraft needs to be protected behind the TPS umbra. One such concept being evaluated is a device mounted to the end of the boom. The detector consists of a conical ring of carbon–carbon material, a mirrored conical reflector, and a detector array with pinhole lens. The detector array resides in a small electronics box, which contains readout electronics for both the detector and a set of thermistors.

If an attitude error reaches a designated threshold, the edge of the conical ring is illuminated and projected on to the detector. The processed signal is used to provide attitude control for safing purposes during the solar encounter. The detector could potentially be based on a micro-DSAD currently being developed for the New Horizons mission. Another option being considered places sensors along the outer ring of the TPS.

Attitude Control. Primary attitude control will be performed using four reaction wheels mounted to provide 4-for-3 redundancy. Due to power constraints, only three wheels will be powered and the fourth carried as a cold spare during the solar encouter. Ithaco TW-4B200 wheels were initially selected to meet the momentum storage and torque requirements to offset dust impacts up to 1.5° off solar nadir within the tight power and mass constraints imposed by the mission.

An alternative approach, use of all-thruster dead-band control, was also considered. This approach uses small minimum-impulse-bit thrusters like those used on Voyager and Cassini, eliminating the need to carry reaction wheels and significantly reducing the spacecraft power requirements. The power reductions could be significant enough to eliminate the battery and charging system, since transient power peaks would be reduced considerably. Preliminary analysis indicates that pointing requirements might be met with thruster control. The reduction in reaction wheel mass is mostly offset by the increase in mission propellant. This approach was not baselined because the current assumption is that 2.5-mg/s outgassing requirement encompasses everything on the spacecraft including thruster exhaust. A single impulse bit using two coupled thrusters expends 11 mg over a 400-ms duration. The thruster control option will continue to be explored once additional inputs from the science community are available to address the outgassing issue in more detail.

Sixteen 4-N thrusters will still be carried for ΔV maneuvers and momentum management. The thrusters have been initially placed to provide redundant coupled pairs about the spacecraft center of mass, providing the capability to maneuver efficiently in any direction while maintaining contact with the ground.

4.4.7.4 Summary

The G&C subsystem meets requirements with a low-risk functional approach and mostly existing hardware. A conservative design overcomes the significant uncertainties in the properties of the unexplored environment that Solar Probe encounters in the solar corona. Better environmental knowledge would enable refinements in the concept and a better estimate of the required resources. Section 5, Risk Mitigation, details a prudent plan for reducing environmental uncertainties and developing a new solar horizon safing sensor to add robustness to the design.

4.4.8 Propulsion

4.4.8.1 Requirements

Propulsion requirements are derived from the mission design and G&C requirements (Table 4-1, requirements 1–3 and 19–22). The function of the propulsion system is to provide thrust for performing ΔV maneuvers and managing angular momentum. A thrust level of 4 N was considered adequate to balance the needs for acceleration during maneuvers, minimum-impulse-bit control to maintain attitude during momentum dumps, and significant margin in torque to overcome expected dust particle impacts during the solar encounter. The initial ΔV estimate of 225 m/s and attitude control budget of 6 kg requires a total available propellant load of 69.1 kg. Sixteen thrusters were needed to provide adequate redundancy and flexibility to maintain contact through the MGA for any ΔV maneuver.

4.4.8.2 Alternatives Considered

Several propulsion system types were considered, including both electrical and chemical options. All electric propulsion systems were immediately discarded, however, because of the limited power available on the Solar Probe spacecraft. A simple blow-down monopropellant system that is fully compliant with the Solar Probe requirements was ultimately selected, though a dual-mode system with bipropellant ΔV thrusters and monopropellant attitude control thrusters might theoretically weigh less. This selection was made for a variety of reasons, including cost, reliability, and packaging advantages. (For example, the bipropellant engines are large and radiatively cooled, and the pointing requirements of the spacecraft combined with the umbra constraints essentially preclude their use.)

4.4.8.3 Concept Description

The baseline propulsion system architecture is shown in Figure 4-29. This design is similar in architecture to almost every hydrazine propulsion system flying today. Sixteen thrusters provide forces in all required directions, and each thruster has series-redundant control valves to protect against leakage. These thrusters are grouped into two redundant sets, which provide ΔV in groups of four and can be used singly or in groups of two to four for momentum management. Hydrazine propellant and nitrogen pressurant are stored in a single tank whose pressure decreases as propellant is depleted. Pressurant is separated from the propellant by an elastomeric diaphragm within the tank. Latching valves isolate the thrusters from the tank for ground safety and system reliability (i.e., in case of a thruster leak), while manual service valves are used for testing and loading the system on the ground. The system's surge suppression orifices keep transient pressures within appropriate levels, and the pressure transducers are used together with temperature telemetry to gauge propellant and monitor system performance in flight. Spacecraft ambient temperatures will be maintained such that the propulsion system requires no heaters except those on the thruster catalyst beds.

Several flight-proven options exist for each component of the Solar Probe propulsion system, resulting in a high level of confidence that no qualification testing will be required for the project. A representative set of heritage components was selected for preliminary performance evaluations and shows that system requirements can be met. The representative thruster selected is the Aerojet MR-111c 4.0-N rocket engine assembly (Figure 4-30). This thruster has an extensive flight and test history, and it meets or exceeds all Solar Probe requirements. Using performance numbers typical of this thruster, a total maximum required usable propellant load of 69.1 kg can be calculated for the mission. This number, together with the range of inlet pressures for which the thruster has been qualified, results in a required a tank volume of at least 90

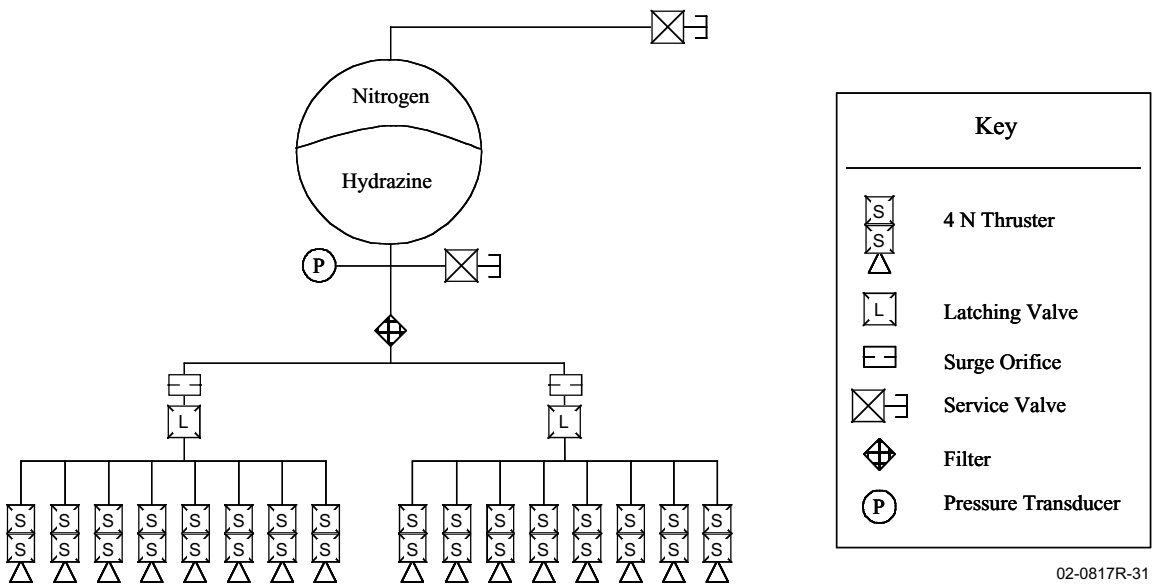

Figure 4-29. Solar Probe propulsion architecture.

liters; at least two commercially available flight-proven tanks exist in this size range, affording flexibility when the final flight propulsion system configuration is selected.

4.4.8.4 Summary

The propulsion subsystem meets its derived requirements with entirely off-the-shelf hardware and represents a very low risk approach.

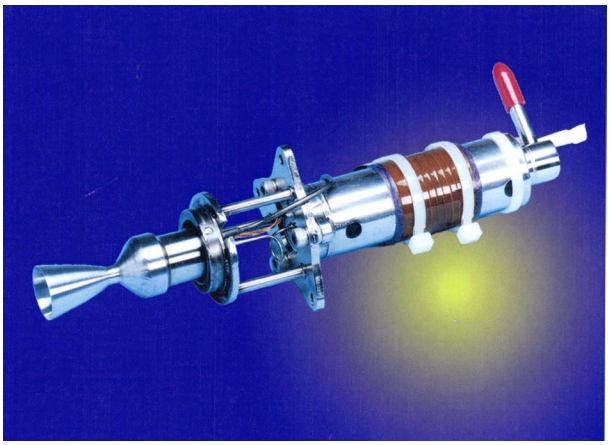

Figure 4-30. Aerojet MR-111c 4.0-N rocket engine assembly, shown with axial nozzle.

4.4.9 Flight Software

4.4.9.1 Requirements

The software supports meeting mission requirements as allocated by the mission, power, ACS, C&DH, communications, and fault protection subsystem areas.

4.4.9.2 Software Development Approach

The Solar Probe spacecraft flight software will have the benefit of significant heritage from MESSENGER and numerous other missions, including JHU/APL's NEAR, TIMED, and CONTOUR. As on MESSENGER, each IEM contains a single processor to carry out the C&DH, G&C, interface communications, and autonomy functions. As for TIMED and NEAR, a separate AIU (Attitude Interface Unit) provides an added level of fault protection during the solar encounter. As was planned for CONTOUR, both processors will be active during the solar encounter to ensure the collection of all data from the two instrument suites.

The five major functional areas addressed by flight software are described below:

- C&DH functions include support of CCSDS protocols for uplink and downlink, command processing (including macros and time-delayed commands), telemetry processing, Mil-Std-1553 bus management, autonomy rules (fault detection and recovery [FDR], management of redundancy, and other operations), SSR management, science data handling (scheduling, sequencing, and compression), thermal management, memory scrubbing, and other FDR algorithms.
- G&C functions include attitude estimation and control via reaction wheels and thrusters, guidance, Mil-Std-1553 bus processing, G&C FDR, memory scrubbing, and telemetry reporting.
- Interface communications within the spacecraft are via the 1553 bus and PCI bus. The 1553 bus is used to communicate between the IEMs and major spacecraft subsystems (including the instrument DPUs, PDU, RF transmitters, and the AIU). In addition, the 1553 bus is used to cross-strap the two IEMs to optimize redundancy and increase reliability. The PCI bus is used to communicate with the SSR, command and telemetry card, uplink and downlink cards, and the instrument interface card. Data flow from the instruments to the SSR in both IEMs.
- Autonomy will be critical to carrying out the operational and safing functions. Sequences of commands stored onboard can be triggered at a specified time or when a specific event occurs. The use of rules and stored command sequences eliminates the need for much special-purpose software and decouples the autonomy (operational and safing) algorithms from the software development. Scheduling and sequencing of instruments will be performed using time-tagged commands and macros. Instrument state-of-health checking and other decision-based tasks will be performed using autonomy rules.
- Fault protection includes a Cruise Safe Mode and a Solar Encounter Safing Mode. In Cruise Safe Mode, the spacecraft turns off nonessential hardware and points the antennas toward Earth. In Solar Encounter Safing Mode, the AIU takes control of the G&C functions to keep the spacecraft pointed toward the Sun. Both modes will be tested independently of the operational software.

Solar Probe software will be developed in strict accordance with the JHU/APL Space Department software development process. Hardware-in-the-loop simulations using engineering models of the flight IEM are used to test flight software designs and algorithms. These tests address each phase of the mission to ensure success and reduce risk prior to launch. Ground support electronics hardware and software are developed to support hardware checkout, software development, spacecraft integration, and mission operations. Independent acceptance testing is performed on mission-critical software.

4.4.9.3 Summary

The flight software will meet all functional requirements, and major portions of the designs have significant flight heritage from previous programs. Software development processes that have been proven successful on several flight programs will be implemented on Solar Probe.

4.5 Integration and Test (I&T)

4.5.1 Requirements

Space system I&T has the following objectives:

- Verify system-level performance
- Identify unexpected interactions among subsystem elements
- Identify failure modes from design weakness, material defects, and workmanship
- Operate components long enough to identify failures due to infant mortality
- Establish standard operating and contingency procedures for mission operations

- Verify that the spacecraft will operate properly through launch and in on-orbit environments

4.5.2 I&T Approach

I&T must reduce risk during both system-level integration and flight operations. Therefore, a methodical, hierarchical approach, designed to uncover potential problems early, must be followed. This section uses JHU/APL practices and facilities as an example of such an approach.

Testing starts at the breadboard level where all designs undergo interface compatibility testing prior to release for flight fabrication. This practice minimizes the number of interface problems encountered during system-level integration. Piece parts, components, and boards are environmentally tested at stress levels higher than those the system will encounter in test or operation. Imposing more stressful test levels at lower integration levels is a proven technique to find problems early and minimize problems at system-level integration. This I&T approach is similar to that used on other JHU/APL spacecraft programs, including NEAR, TIMED, CONTOUR, and MESSENGER.

A protoflight approach (qualification levels for flight duration) would be followed for the Solar Probe spacecraft, payload, and third-stage environmental test programs. Instrument and spacecraft components are fully tested, both functionally and environmentally, before delivery for system integration. All components are vibrated in 3 axes at protoflight levels. They also undergo operational and survival thermal cycling. The design levels used will envelop both the Atlas V and Delta IV launch vehicle environments. Results from the structure qualification testing are then used to correlate the coupled-loads analysis finite element model prior to integration.

The Solar Probe spacecraft would be integrated in JHU/APL's Kershner Space Building. This spacecraft integration and test facility maintains class 100,000, 10,000, and 100 clean rooms. The building also houses a vibration test facility and thermal vacuum chambers in a variety of sizes. When possible, subsystem and instrument mechanical models, data simulators, and engineering models will be integrated early with spacecraft structural or electrical components to provide early mechanical and electrical interface verification. Spacecraft integration (Figure 4-31) begins with delivery of the flight-qualified primary structure, which will already include the propulsion system. The spacecraft harness is then installed and rung out to ensure that flight hardware can be safely integrated.

A Pre-Integration Review will be held for each spacecraft component and instrument. The integration team will review the results of the component or instrument testing program and present plans for mechanical and electrical integration with the spacecraft.

During integration, several special tests will be conducted. These include DSMS RF compatibility tests, time system verification tests, special guidance and control tests, system self-compatibility tests, and mission operations tests.

The three flight RTGs will be integrated after the spacecraft is mounted on the launch vehicle at CCAFS. During the spacecraft test program, thermal, electrical, and mass simulators of the RTGs will be used to verify RTG to spacecraft interfaces and functionality. After integration of all of the spacecraft subsystems and instruments, the baseline performance test will be performed. Then mechanical alignments will be measured using optical cubes mounted on the instruments and G&C components.

After the Pre-Environmental Review, the environmental test program begins. The spacecraft and necessary ground support equipment will be shipped to NASA/GSFC via air-ride van. The spacecraft bus will be in one shipping container,

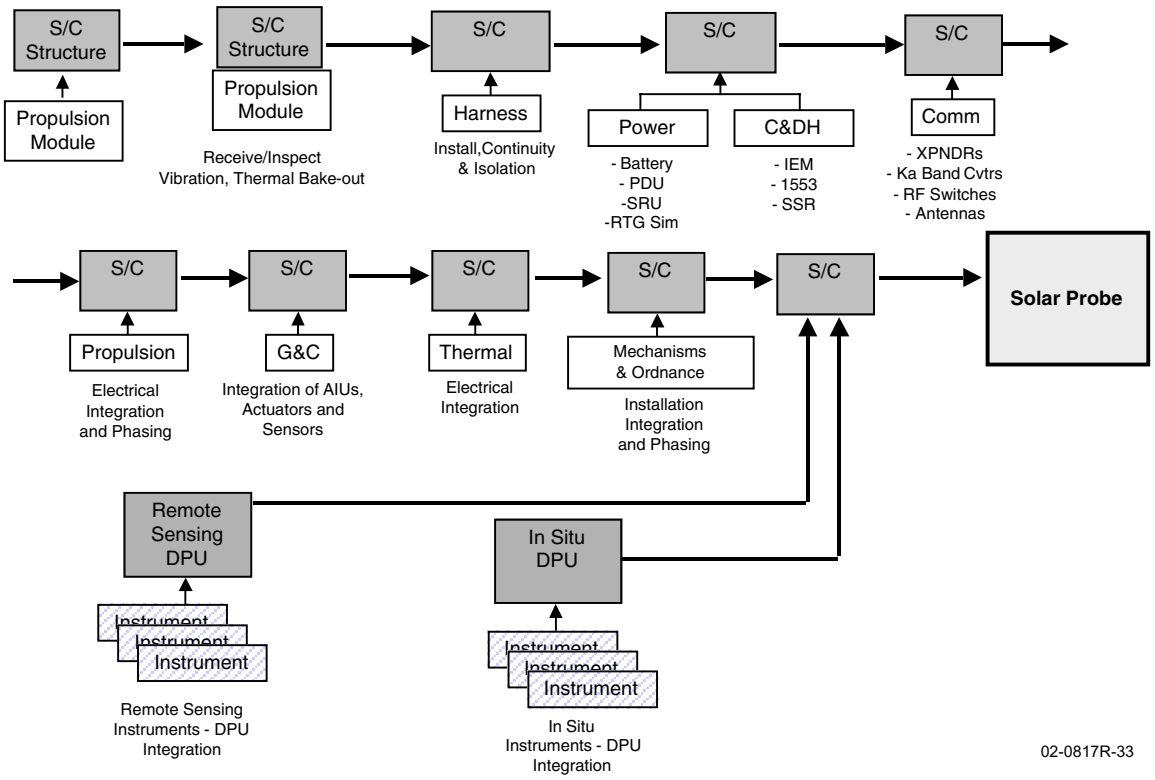

Figure 4-31. Spacecraft integration process.

and the TPS will be shipped in a separate container. The environmental test program starts with the spacecraft vibration tests performed in the GSFC vibration test facility. The spacecraft will be in launch configuration (including the TPS) and will be powered during these tests.

Solar Probe will then be moved to the GSFC acoustic test facility for the acoustics and shock/separation tests. These are followed by mass properties measurements and spin-balancing. Finally, the thermal balance and thermal vacuum cycling tests will be conducted. During the thermal cycling tests, the DSMS Compatibility Test Trailer will be utilized to perform DSMS RF compatibility tests and end-to-end simulations of mission operations. Baseline performance tests will be run prior to the thermal vacuum tests and during and after the thermal cycling test. In addition, mechanical alignments will be verified after completion of the environmental program.

The spacecraft, TPS, and ground support equipment will then be shipped to the KSC launch processing facility. Following initial electrical tests, a final baseline performance test will be conducted. The Mission Operations Team (MOT) will be provided time for mission simulations and DSMS testing, which will use Mil-71 at KSC.

Next, the flight mechanical build is initiated, including ordnance installation, flight blanket installation, TPS installation and alignment, and RTG fit checks and installation rehearsals. After mating with the third stage and installation of the RTG mass models, the final spacecraft spin-balance test will be performed.

Once the spacecraft is moved to the launch pad and mounted on the launch vehicle, final preparations are conducted. These include electrical system functional testing, launch rehearsals, and flight RTG installation. Readiness reviews and

process rehearsals will be part of a comprehensive program to ensure safe and orderly RTG installation.

The final steps prior to launch will be the Launch Readiness Review and red tag item removals.

4.6 Ground and Data Systems Overview

4.6.1 Requirements

The Solar Probe ground system includes all personnel, hardware, software, data links, and facilities used to conduct I&T operations; to conduct flight tests and operations; to generate and uplink commands; and to receive, process, analyze, and disseminate flight data. The ground and data systems are required to support mission requirements (Table 4-1, requirements 23 and 24) as defined by the telecommunications and data handling implementation approaches as well as the defined concept of operations. Requirements are expected to be better defined once instrument teams have been selected and can include their specific requirements. Since the study did not have instrument team input, the model was based on previous experience on other recent flight programs.

4.6.2 Design Approach

Figure 4-32 shows the ground systems architecture. The ground system architecture is inherited from the MESSENGER and New Horizons missions, which in turn were derived from the low-cost CONTOUR and NEAR systems. Software from MESSENGER and New Horizons will be reused wherever feasible. The same COTS control center software will be used, as will the JHU/APL-developed telemetry router, server, and

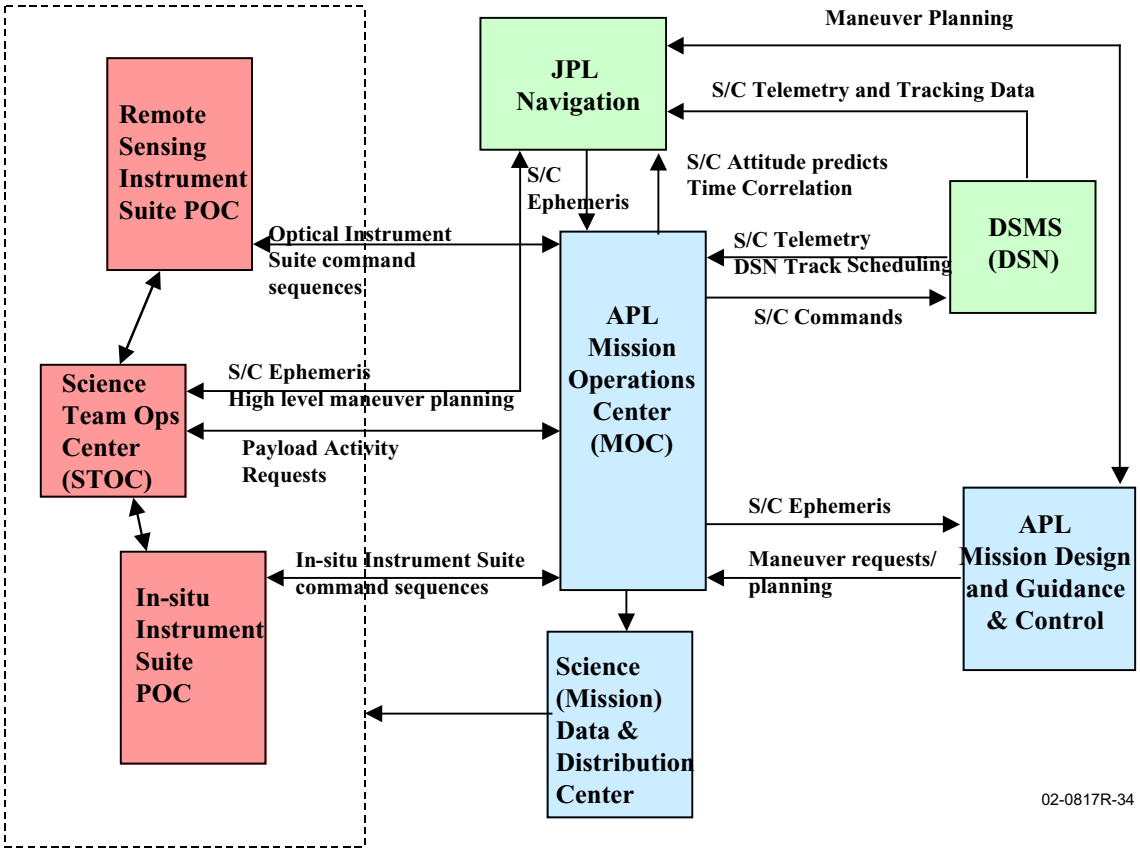

Figure 4-32. Solar Probe ground system architecture.

archive system. As on MESSENGER and New Horizons, SEQGEN software, developed at JPL, will be used for mission planning. Spacecraft health assessment and science data processing software will be developed at JHU/APL based on Solar Probe's specific requirements.

This ground system architecture is based on a common, scalable design that supports bench-level testing, spacecraft I&T, and mission operations. Using a common set of tools to support I&T from bench-level testing to integrated spacecraft testing saves both cost and schedule resources.

The Mission Operations Center (MOC) would be co-located with the MESSENGER and New Horizons MOCs. Because the MOC ground system features the same "look and feel" as those for MESSENGER and New Horizons, and because all three spacecraft have relatively common avionics architecture, mission operations personnel can be shared. This sharing of personnel reduces cost. Facility equipment such as computers, network infrastructure, and peripherals can also be shared.

A high-fidelity hardware-in-the-loop spacecraft simulator, maintained in the MOC, will be used to train controllers and assist in software testing, command load verification, and anomaly resolution. This simulator will be built from spacecraft components that are copies of the flight hardware and contain the actual flight software. Critical command sequences will be tested on this simulator before being uploaded to the spacecraft.

In addition to the hardware-based spacecraft simulator, a software spacecraft simulator will be developed to model system resources and test command sequences. While the hardware-in-the-loop simulator will operate at real-time speeds, the software simulator will run many times faster, allowing the testing of weeks' worth of command sequences in several hours.

JHU/APL's MOC will be connected to the NASA DSMS via leased communications lines. As on MESSENGER and New Horizons, the MOC command workstations, bracketed by network firewalls for security, will be connected to the JHU/APL Space Department network on one side and the DSMS on the other side. The MOC network will adhere to JHU/APL network security guidelines, the security requirements for connecting to the DSMS, and any other NASA security procedures mandated for Solar Probe.

Responsibility for many of the data dissemination activities is to be determined, including

- Receiving, archiving, and analyzing all instrument engineering telemetry
- Receiving, archiving, and reducing all instrument science data to Planetary Data System (PDS) Level 1 format
- Distributing science data and associated engineering/navigation data to co-investigators, participating scientists, the education and public outreach team, and the PDS
- Receiving and archiving higher-level science data products produced by the science team

However, for the purposes of this study, we assumed that the JHU/APL Mission Data Center (MDC) will prepare Level 1 telemetry and distribute it to the Science Team Operations Center (STOC) and the Payload Operations Centers (POCs). Planning for science operations will use applications built on the JHU/APL Science Planning Framework and Toolbox. Clock-correlation processing is performed by the MOC and disseminated to the STOC, the POCs, and the navigation team.

JPL's Navigation Group provides radiometric data conditioning and validation, Doppler data pre-conditioning, orbit determination, ancillary navigation data processing, and verification of JHU/APL-computed maneuvers. It interfaces directly with the DSMS for tracking and acquisition data.

4.6.3 Summary

The ground and data system architecture identified will meet currently identified requirements; it also takes of advantage of significant heritage from previous programs. Once the instrument teams have been identified, this architecture can be refined to suit both these teams' specific needs and those of the Solar Probe mission.

4.7 Mission Operations

4.7.1 Requirements

The Solar Probe Mission Operations System (MOS) consists of the teams and ground facilities required to conduct post-launch operations. It must to support the operational concept defined in Section 4.2.

4.7.2 Approach

Because of the similarities in their missions, Solar Probe builds on the successful experiences and lessons learned from NEAR, CONTOUR, and MESSENGER.

The MOC houses the elements used to conduct the three main functions within space operations—activity planning and scheduling, real-time command and control, and off-line performance assessment. The Solar Probe MOT will take advantage of lessons learned on previous missions and build on the successful experiences from NEAR, CONTOUR, and MESSENGER by capitalizing on existing infrastructure and utilizing the same proven processes and procedures used to conduct the post-launch operations. In addition, software to perform these various functions will be extensively reused, reducing the cost and risk of additional software development. The MOT is also supported by outside organizations in specific areas. As they have done on previous missions, JPL will provide navigation support. The instrument suite POCs will provide the instrument command sequences to meet the detailed science objectives as defined by the science team.

In operations planning, the design, development, test, review, and control of the mission-critical sequences such as science acquisition activities and TCMs adhere to the proven process employed on past missions. Before any sequence is uplinked, it is run both on the real-time hardware-in-the-loop simulator and on the faster-than-real-time software simulator.

During real-time contact with the spacecaft through the DSMS, routine and nonroutine operations are performed to ensure the health and safety of the spacecraft. During such contacts, the telemetry is evaluated for out-of-limit conditions and to verify the spacecraft's overall state of health. Commands are uploaded to the spacecraft for housekeeping functions and for science data acquisition sequences. Also performed during real-time contacts on a less frequent basis are parameter uploads, flight software uploads, and TCMs as required. In the event of non-nominal spacecraft behavior, the MOT implements diagnostic procedures and initiates other prescribed responses where applicable. A summary of the types of activities performed during DSMS contacts in the various mission phases in shown in Table 4-14.

Off-line performance assessment is performed on the spacecraft as well as on the overall operation itself to continually evaluate the efficiency of the operation and to incorporate lessons learned throughout the mission. Assessment of the spacecraft includes both short- and long-term trending and the off-line resolution of anomalous spacecraft behavior. In this area, the engineering development teams remain on the project at a low level to evaluate their subsystems' performance throughout the mission.

The science team defines the science requirements and the science acquisition activities on a monthly basis. From this, the MOT and

Table 4-14. Mission Operations Team activities during mission phases.

Mission Phase	Duration	Contact Frequency	Activities Performed
Spacecraft separation and early checkout	1 week	24 h/day	• Performance monitoring • Initial turn-on and checkout of spacecraft subsystems
Continued spacecraft checkout	12 weeks	3 or 4 to 8 h/week	• Continued performance monitoring • Initial instrument turn-on and checkout • Further checkout of spacecraft functionality and performance • Spacecraft certification
Cruise 1	10 months	1 to 8 h/week	• State-of-health evaluation • Noncoherent ranging • Routine housekeeping functions • Diagnosis and initial response to anomalistic behavior • Collection and downlink of cruise science (approx. 22 Mbits/week)
Jupiter flyby	2 months	3 or 4 to 8 h/week	• Normal cruise functions • Plan, test, implement, analyze navigation burn
Cruise 2	20 months	1 to 8 h/week	• Normal cruise functions
Solar encounter 1 preps	12 weeks	3 or 4 to 8 h/week	• Normal cruise functions • Plan, test, implement, and analyze required TCMs. • Rehearsals of encounter 1 sequence on simulators • Rehearsals of encounter 1 sequence on spacecraft • Updates to sequence based on tests • Additional rehearsals on simulators and spacecraft
Solar encounter 1	20 days	24 h/day	• Normal cruise functions • Maintain continuous downlink • Change spacecraft configuration as required • Change downlink rates as required • Update and retest upcoming sequences as situations arise
Encounter 1 data retrieval	8 weeks	2 to 8 h/day	• Normal cruise functions • Plan, test, implement, and analyze re-targeting burn • Playback SSR data from both SSRs
Cruise 3	46 months	1 to 8 h/week	• Normal cruise functions
Solar encounter 2 preps	12 weeks	3 or 4 to 8 h/week	• Same as encounter 1
Solar encounter 2	20 days	24 h/day	• Same as encounter 1
Encounter 2 data retrieval	8 weeks	2 to 8 h/day	• Same as encounter 1

instrument suite POCs derive the required spacecraft and instrument configurations. The instrument suite POCs construct the required instrument command sequences to perform the science acquisition process for their respective instrument suites. The MOT constructs the spacecraft command sequences for attitude maneuvers, data recording, and any other required spacecraft configuration changes. Prior to and during the flyby encounter, the planning system is designed to allow late changes in command sequences as situations arise, provided there is ample time for test. A 6-month timeline with the solar encounter in the middle of the window (Figure 4-33) shows the

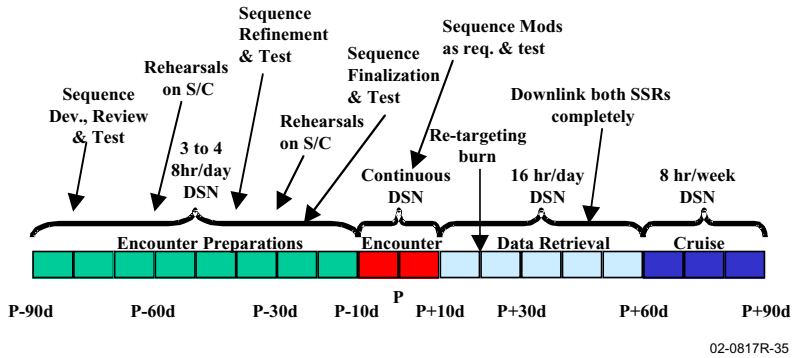

Figure 4-33. Timeline of a 6-month window around a solar encounter.

types of activities performed by the MOT and spacecraft.

The mission design and navigation teams participate with the MOT in maneuver definition and implementation. In addition, the navigation team processes the noncoherent ranging information to compute the spacecraft ephemeris.

As has been the case on prior missions, the MOT staff will increase in size to support the solar encounters and maneuvers and decrease to a small core team during cruise phases. Although the team members will be shared with other ongoing missions, because of the team's waning and waxing nature and because the Solar Probe mission is so long, it is critical that a long-term knowledge management and retention plan be implemented.

To support this important effort, a training program will stress the roles and responsibilities of each member of the MOT. This not only expedites new member training, but also assists in the advancement or cross-training of existing members. The training program will consist of a combination of videotaped classroom lecture sessions and "practical lab" training on the ground simulator to reinforce the classroom training. The training program will conclude with a certification process that must be completed by all MOT members before they are placed into the on-line rotation without assistance.

During the development phase of the mission, the MOT develops the MOS in addition to gaining a detailed understanding of the operation of the spacecraft. Members of the MOT support the I&T effort, and members of the I&T team support the MOS development through assistance with sequence development and test. In the I&T phase, the MOT is allocated spacecraft test time during which mission simulations are conducted in a "test it as you fly it" approach. These mission simulations are conducted with three main objectives in mind. First, they test the capability of the MOS to construct the sequences, load them, and verify execution. Second, the tests provide an excellent full-up spacecraft test where all components except the power system are exercised as they would be post-launch; the power system will be simulated, of course. Third, the testing provides an excellent opportunity for MOT training with the spacecraft. The mission simulations consist of a launch, separation, and early on-orbit checkout simulation, a typical TCM, the Jupiter flyby sequence, and a solar encounter simulation. This solar encounter sequence developed prior to launch is refined after post-launch calibrations. The mission simulation tests are archived for future training opportunities.

4.7.3 Summary

The mission operations approach supports the mission requirements and current operational concept defined in Section 4.2. A key element of the MOS is the emphasis on knowledge management and retention so that cost-driven variations in staffing do not impact performance.

5. RISK MITIGATION

This report has described in detail an optimized engineering solution for a viable Solar Probe mission. The mission design selected maximizes science return by affording multiple quadrature passes of the Sun within one solar cycle. The highly fault-tolerant flight system carries a payload of *in situ* and remote sensing instruments into the harsh environment of the Sun's corona. Science data are both telemetered in real time and redundantly recorded onboard for later downlink, ensuring maximum data return.

As the mission and spacecraft designs developed, trade studies were performed to examine the possible means of achieving the mission objectives and establishing the requirements for each subsystem. In addition to technical and cost considerations, balancing overall risk was a critical element of all trade study evaluations. To arrive at an optimal solution, we included technical risk, cost risk, and improved probability of mission success as discriminators in the decision process. The result is a feasible design that requires modest technology development only where that development is uniquely necessary to achieve the primary mission objectives. Table 5-1 presents the heritage and maturity—as reflected by the technology readiness level (TRL)—for the Solar Probe subsystem components.

The balanced risk approach identified several key technical challenges for Solar Probe. To mitigate these technical challenges, a risk retirement program has been outlined, beginning 2 years prior to mission formulation. Such a schedule allows time for the iteration and revision of processes that are inevitable in technology development activities.

For each required technology development area, a roadmap has been developed that identifies the steps to be taken to bring the system to maturity. In each case, contingency approaches have been identified should the planned development be unsuccessful. The impact of having to implement fallbacks is also identified. Appropriate trigger dates and technical criteria will be identified that specify at what point each development effort must prove successful or the fallback option will be initiated.

From the list in Table 5-1, the systems requiring technology development to advance their readiness level have been identified as those with a TRL rating below 5. These include thermal/structure, telecommunications, dust protection, and attitude control. While the power system also requires maturation, this development is largely out of the scope of the Solar Probe mission implementers, and is being directed by the Department of Energy (DOE) and the NASA Nuclear Systems Initiative.

The remainder of this section addresses the technical areas identified as requiring technology development. The nature of the risk is described, followed by a summary of the relevant state of the art of the technology. The planned steps toward mitigation are laid out, along with a fallback plan and the impact of that contingency action.

5.1 Thermal Protection System (TPS)

The system requiring the most technology development, and whose fallback position has the greatest impact on Solar Probe, is the Thermal Protection System (TPS), which includes the primary heat shield assembly, the secondary shield assembly, and light tubes that penetrate these shields to allow the nadir-pointing remote sensing instruments to see the Sun.

5.1.1 Primary Shield Assembly

A large (2.7-m diameter, 5-m height) primary shield is required to shadow the spacecraft

Table 5-1. Subsystem components, heritage, and technology readiness levels (TRLs).

Subsystem	Vendor	Heritage	TRL	Comments
Integrated Electronics Module				
DC/DC converter	JHU/APL	Modified CONTOUR	7	Modifications for higher efficiency
Solid state recorder	JHU/APL	New development	6	New impl. of existing technology
Flight computer	BAE	First flight with Deep Impact	6	Off-the-shelf procurement
Cmd/TLM card	JHU/APL	New development	6	New impl. of existing technology
Downlink card	JHU/APL	Modified CONTOUR	7	Frequency and control pass-through to mods
Uplink card	JHU/APL	Modified CONTOUR	7	Minor mods, customized for Solar Probe
Attitude Interface Unit				
Processor board	BAE	First flight with Deep Impact	6	Off-the-shelf procurement
Attitude interface electronics	JHU/APL	Slight mod of several JHU/APL built flight units	7	Minor mods., customized for Solar Probe
RF Communications				
USO	JHU/APL	Cassini	9	Build to print
X-band SSPA	JHU/APL	Modified MESSENGER	7	Minor mods, customized for Solar Probe
X to Ka freq converter	JHU/APL	New development	2	Migrate to Ka-band frequencies
Ka-band SSPA	JHU/APL	New development	2	Develop high efficiency 8W RF output
Diplexer	MCC	CONTOUR	9	Off-the-shelf procurement
RF switch assy	Com-Dev	CONTOUR	9	Off-the-shelf procurement
MGA	JHU/APL	Modified CONTOUR	7	Minor mods, customized for Solar Probe
HGA	JHU/APL	New development	2	Design for both Ka & X-band operation
LGA	JHU/APL	Modified CONTOUR	7	Minor mods, customized for Solar Probe
Attitude Control System				
Star trackers	Sodern	20 flight units deli; 3 in flight	9	Off-the-shelf procurement
IMU	Northrop-Grumman	Updated NEAR design; will have flown on MESSENGER	7	Off-the-shelf procurement
DSADs	Adcole	Many flight programs	9	
Solar horizon sensor	JHU/APL	New development	3	Current concept based on μDSAD chip
Power				
Power distr. unit:				
Power switching	JHU/APL	Mod of MESSENGER, STEREO	7	Minor mods, customized for Solar Probe
Cmd decoder	JHU/APL	Mod of MESSENGER, STEREO	7	Minor mods, customized for Solar Probe
1553 Board	JHU/APL	Mod of MESSENGER, STEREO	7	Minor mods, customized for Solar Probe
Shunt regulator unit:				
Shunt regulator	JHU/APL	Mod of NEAR, CONTOUR, New Horizons	7	Minor mods, customized for Solar Probe
Capacitor bank	JHU/APL	New Horizons	7	Mod. capacitance and small mods to electronics
Lithium ion battery	Eagle-Picher	New development	7	New implementation of existing technology
Boost converter	JHU/APL	Modified ACE	7	Customized for Solar Probe
Charge controller	JHU/APL	Based on several JHU/APL flight programs	7	Minor mods, customized for Solar Probe
RTG	GFE	New development	7	MMRTG being developed by DOE. Technology same as previous RTGs
Propulsion				
Tank	Gen Dynamics	EURECA	9	Off-the-shelf procurement
Thrusters	Gen. Dynamics	Many flight programs	9	Off-the-shelf procurement
Valves, filters	VACCO	Many flight programs	9	Off-the-shelf procurement
Pressure transducers	Paine	Many flight programs	9	Off-the-shelf procurement
Mechanical				
Telescoping boom	Astro Aerosp.	Modification of existing designs	7	Modified for Solar Probe application
Rotary actuators	Moog	Many flight programs	9	Off-the-shelf procurement
Dust shield	JHU/APL	New development.	3	Potential use of CONTOUR materials & design approach
Thermal				
Primary TPS	JHU/APL	New development	2	Large carbon–carbon structures have been built for space applications (e.g., shuttle)
Secondary TPS	JHU/APL	New development	2	Need to select insulation material
Light tubes	JHU/APL	New development	2	

systems and science payload from solar radiation while minimizing mass loss due to sublimation at the extreme temperatures of the near-Sun environment. The baseline material selected for the primary heat shield is carbon-carbon (C-C), which is chemically and physically stable in the deep-space environment, is insensitive to hydrogen embrittlement, and has a high strength-to- weight ratio. It is also used for the support struts and other assembly components. The specific risks associated with the primary shield assembly are (1) its manufacturability and (2) its outgassing performance at extreme temperatures.

5.1.1.1 Manufacturability

Because of its size and mass, the primary shield requires a robust system of struts to support it and connect it with the spacecraft bus. The primary shield assembly is a critical component of Solar Probe, and its manufacturing and assembly processes should be demonstrated as early as possible to ensure that they are mature when mission implementation begins.

State of the Art. Large carbon-carbon structures not unlike that proposed for Solar Probe are commonly used for high-temperature applications, such as the Space Shuttle nose cones. These structures are about 2 m in diameter and are subjected to temperatures of approximately 2000 K. The fabrication processes of such structures are largely the same as those required for the Solar Probe primary shield.

The fundamental shield design (a 15° half-angle carbon-carbon cone with a diameter of about 2.5 m) has been studied in depth during previous Solar Probe studies, and a manufacturer of carbon-carbon materials has been involved in the current study specifically to address the feasibility of fabricating the primary shield assembly. A methodology evaluation has been performed and several alternative approaches to assembling the shield and its strut assembly have been laid out.

Mitigation Plan. The risks associated with the fabrication of such a large assembly can most easily be retired by fabricating and testing full-sized prototype units. A qualified vendor will be selected who will work with us on the development of the entire thermal protection system. A detailed approach to the fabrication of the primary shield will be developed, including such decisions as whether to build multiple flat panels that are joined to form a faceted cylinder, or to join larger curved pieces. Such decisions will be based on the capabilities of the selected vendor's facilities as well as the dimensional requirements of the shield.

In parallel with this development, materials testing will be performed to verify the mechanical properties of the samples. Tests will be performed on sample joints and interfaces between the various primary shield assembly components. The results of these tests will be used to develop mature assembly procedures. The current plan is to fabricate two full-scale prototype shield assemblies in series. This conservative approach allows lessons learned during the first manufacturing run to be implemented and proven in the second run.

Fallback and Implications. The true risk associated with the fabrication of the shield assembly is not whether the assembly can be made, but whether the mass estimated for a stiff and survivable structure is adequate. Going to the trouble of building prototypes will not only retire manufacturing risk, but also reduce the uncertainty associated with the mass allocation of a major component, and should improve the overall mass margin. If complications arise during the manufacturing process that are insurmountable within the allotted schedule and budget, then the mass allocation to the shield would be increased at the expense of margin.

5.1.1.2 High-Temperature Behavior

Although it is well known that carbon-carbon materials can withstand the extreme temperatures that Solar Probe will encounter, the actual temperature that the shield reaches will directly affect the extent of outgassing that occurs. A specific mass sublimation limit has been determined, above which the primary science objectives are jeopardized (see discussion in Section 4.4.2.1).

State of the Art. Candidate carbon–carbon materials and manufacturing processes have been extensively evaluated in previous Solar Probe studies, such as that conducted by Lockheed Martin, JPL, and NASA Langley Research Center (Dirling 1998). These studies measured optical properties (in particular absorptivity α and emissivity ε) of carbon–carbon at high temperatures. Mass loss at high temperatures has also been characterized, but the data are sparse, and the tests were limited to small samples and near-normal incidence angles.

The very limited amount of high-temperature test data with these types of materials creates design uncertainty despite significant margin in both design temperature and solar incidence angle.

Mitigation Plan. A detailed plan for high-temperature testing of carbon–carbon material samples must be developed that includes both off-angle optical property measurements and mass loss measurements under the same conditions. Solar furnaces such as that at Sandia National Laboratories are candidate facilities for such tests. Obtaining results consistent with previous studies using targeted samples of carbon–carbon material will provide the needed confidence in the previous experience and design margin.

Fallback and Implications. The 2-year pre-formulation risk reduction period allows time for repeated test series using a variety carbon–carbon samples. If the test results demonstrate that the predicted margin is not representative, then a modification of the shield design will be considered. The primary option would be to decrease the cone angle below 15° to reduce the shield temperature. This would elongate the shield assembly and likely increase its mass.

5.1.2 Secondary Shield Assembly

While the primary shield shadows the spacecraft bus, the secondary shield provides the bulk of the thermal insulation between the hot primary shield and the spacecraft bus. The temperature gradient across this assembly will range from the primary shield temperature of approximately 2200 K down to about 750 K at the base of the secondary shield. As a result, this shield must incorporate low-density materials that can withstand extreme temperatures and exhibit low thermal conductivity. The specific risk associated with this system is the structural integrity of the candidate materials and a mechanical assembly that allows them to be mounted to the primary shield.

State of the Art. High-performance materials such as carbon aerogel, carbon fiber batts, and aerogel-infiltrated foams offer great promise as the high-temperature components of the secondary shield. Thermal conductivity of these materials at high temperatures is low enough to provide efficient thermal isolation, and the low densities help keep the mass allocations down. Thermal analysis of such a secondary shield incorporated into the current Solar Probe design has confirmed the desired performance. Optical and mass loss properties of these materials have yet to be characterized at the extreme temperatures anticipated for Solar Probe, and little has been done with respect to packaging into larger assemblies.

Mitigation Plan. A carefully planned strategy of testing must be developed to characterize both

high-temperature and mechanical properties of candidate materials. The selection and testing of adhesives or other elements of the assembly must be included as well, as the results of these tests will have direct bearing on the assembly design. Full-scale prototype assemblies will be fabricated and tested once the materials and packaging methods have been determined. Mechanical tests of such large structures are straightforward, but high-temperature tests might not be feasible. It is important, therefore, that reliable relationships between material sample data at extreme temperatures and lower, more easily attainable temperatures can be made. With these, the response of full-scale prototypes at the extreme can be validated.

Fallback and Implications. If, after exploring the candidate materials and assembly approaches, it is improbable that the high-performance materials listed above can be incorporated into the secondary shield, lower-performance, commercial materials must be considered. Utilizing such materials in the shield assembly affords less of a challenge, but the resulting shield will be more massive.

5.1.3 Light Tubes

Two of the remote sensing instruments in the science payload require nadir-pointing fields of view (FOVs). For this study, we assumed that nadir-pointing FOVs would be achieved by incorporating carbon–carbon light tubes to create an optical path through the primary and secondary shields. The specific risk associated with the light tubes is the degree to which they will limit the performance of the nadir-viewing imagers or complicate their development and integration. A related e concern is that the alignment of the tubes within the TPS shields cannot be maintained to the satisfaction of the imagers.

State of the Art. Thermal analysis was performed on a variety of tube designs and it was determined that thermal throughput could be limited to about 25 W if the tubes were truncated at the bottom (spacecraft side) of the secondary shield. Heat rejection remained a problem if the tubes extended all the way to the instrument apertures.

Mitigation Plan. Before effort is expended on dealing with fabrication issues, the general concept of imaging through truncated, tapered tubes must be validated through optical tests with representative instrumentation. Once this approach is validated, the fabrication and mechanical integration issues need to be addressed. A fabrication and test plan will be developed and followed to produce prototype tubes and means of attaching them to the primary and secondary shields. Initial mechanical and alignment tests will be conducted with a mockup of the TPS shields, and once primary and secondary shield prototypes have been built, tests can begin with the entire assembly. In the event that the use of truncated light tubes is not viable with the imagers, extending them to the instrument aperture must be pursued, although this adds a formidable thermal control challenge for the instrumenters.

Fallback and Implications. As with the other components of the TPS, mass is at risk. Strengthening the tubes and their supports, which will require increased mass, can mitigate alignment problems. If the truncated tubes cannot provide the imagers the unobscured view they require, then further strengthening might be required to mate the instruments to the tubes.

5.2 Telecommunications

The Solar Probe telecommunications system is dual frequency, employing X-band (for uplink and downlink) and Ka-band (for downlink only). The addition of Ka-band capability allows Solar Probe to overcome the transmission losses associated with coronal scintillation and thereby

to support real-time downlink of science data during solar passes. Given the 20-W power allocation for the telecommunications system and the predicted performance of the 0.8-m dual-frequency high gain antenna (HGA), a relatively healthy solar encounter data rate of ≥25 kbps can easily be achieved with a high-efficiency (approximately 40%) solid-state power amplifier (SSPA). The specific risk associated with this system is the successful development of such a high-efficiency SSPA.

State of the Art. Currently available Ka-band SSPAs achieve efficiencies of only about 20%, whereas 40% efficient X-band SSPAs will soon be obtainable. Ka-band antennas are readily available with efficiencies of 60%, the highest published efficiency currently being 73%. Mars Global Surveyor incorporated a dual frequency X- and Ka-band antenna, but that system was not optimized for efficiency.

Mitigation Plan. The efficiencies of the SSPA, the antenna, and the electronics packaging all contribute to the overall performance of the Ka-band system. The 40% efficient SSPA requirement assumes only average performance from the antenna and packaging. An increase in antenna performance relaxes the efficiency requirement for the SSPA, so improvements in that development will also be pursued. It is currently conservatively assumed that the dual-frequency antenna can achieve only 50% efficiency, although better performance is likely. If an antenna efficiency of 70% can be attained, then the required Ka-band SSPA needs to be only about 25% efficient to afford the desired 25 kbps data rate.

The development process for the Ka-band system begins with the down-selection of a preferred technology, such as gallium arsenide (GaAs), gallium nitride (GaN), indium phosphide (InP), or silicon carbide (SiC). Once the preferred technology is chosen, parts are selected that best suit the technology, and the fabrication and test of a prototype amplifier can ensue. In parallel, a prototype dual-frequency antenna will be developed and its performance characterized. As with the other technology development efforts, time is allotted to accommodate redesigns and repeated tests in both of these efforts.

Fallback and Implications. In general, the lower the peak telecommunications system efficiency achieved, the lower the data rate available during solar encounters. As a result, the fallback position is to accept a lower data rate at perihelion. If the SSPA development only accomplishes 25% efficiency and the dual-frequency antenna cannot be optimized above 60%, then the resulting data rate will be 75% of the desired value. The impact of such a fallback is the reduction of real-time data downlink, but there is no associated science loss, since the real-time downlink itself is redundant. All science data collected will be transmitted after the solar pass.

5.3 Dust Protection

A dust protection system must be incorporated into Solar Probe to shield the spacecraft from particulates of varying sizes and velocities. Specific risks associated with small particles include the pitting of optics, degradation of cable insulation, and abrasion of thermal surfaces. Larger particles could cause more severe damage to the spacecraft, since collisions of 450 km/s are possible.

State of the Art. The solar dust environment is not well understood, due to limited data and models based on 1-AU observations. Analytical models (hydrocodes) exist only for velocities of about 30 km/s and cannot reliably be extrapolated to the 400 km/s regime.

Mitigation Plan. To clarify the current state of understanding of the solar dust environment, a workshop can be convened that will focus on the Solar Probe environment. The purpose will be to consolidate and interpret data, update

models, and propose additional measurements to be made.

Additionally, a model validation program needs to be developed to assess the effectiveness of dust mitigation approaches. A national survey of state-of-the-art equipment and facilities for laser damage effects testing should be conducted. A test plan will be devised that combines analytical model development with dust impact experiments to verify those models. The effects of dust impacts on spacecraft components and coatings can be assessed, and a dust protection system can be evolved that incorporates a discrete shield, localized shielding, and embedded packaging concepts.

Fallback and Implications. Due to the uncertainty of this environment, spacecraft protection must be maximized within the mass constraints of the program. If analyses and models indicate a harsher environment and greater threat than currently assumed, then the mass margin will decrease as more mass is allotted to dust protection.

5.4 Attitude Control

To augment the star trackers and the inertial measurement unit (IMU), a solar horizon sensor is proposed as an added precaution to maintain a Sun-pointing attitude regardless of the state of primary or redundant attitude system sensors during a solar pass. The specific risk associated with this system is the loss of an additional safeguard if this technology is not developed. While there is ample heritage for this sensor approach, the application and environment are new.

State of the Art. Sensors performing the tasks required of this unit have been developed for previous missions, e.g., the Sun gates on Viking, Voyager, and Galileo. A variety of sensor technologies exist that might be applicable to this development.

Mitigation Plan. More than one design concept for this sensor will be developed. One approach is to detect the solar horizon optically, using variations of digital solar attitude sensors or similar devices. A method that does not rely on imaging the horizon directly incorporates thermistors located around the base of the primary shield that indicate when the shield begins to point away from Sun center. Prototypes of these sensors will be fabricated and validated through representative tests.

Fallback and Implications. If a complex system incorporating digital Sun sensors cannot be developed for moderate cost, the simpler thermistor system should be utilized. If this approach cannot be validated, the risk of relying on the redundant attitude control system devices must simply be accepted.

5.5 Radioisotope Power System

Using a radioisotope power system enables Solar Probe to operate reliably throughout its mission life and at distances where solar power is not feasible (farther than 2 AU and closer than about 0.3 AU). Due to the extremely limited availability of traditional radioisotope thermoelectric generator (RTGs), Solar Probe will utilize the new, smaller multi-mission radioisotope thermoelectric generators (MMRTGs) that are being developed by NASA and the Department of Energy (DOE) for a wide range of future space missions. The performance of general-purpose heat source (GPHS) RTGs and issues related to their safety are well understood and pose little technical risk to Solar Probe. The specific risks to the mission are programmatic in nature, and concern the timely development of the MMRTGs and completion of the launch approval process.

Current Status. RTGs have been used on more than 15 NASA missions over the past 30 years, and the design has remained unchanged since the

Galileo mission. The MMRTG currently being developed is a modification of this design that uses a shorter housing holding only eight GPHS modules. The MMRTG development is part of NASA's Nuclear Systems Initiative, and is being coordinated with the DOE. A competitive procurement has been initiated for the design, development, and qualification of MMRTGs, and the development schedule calls for the first flight unit to be available in early 2008.

Mitigation Activities. Representatives of the Solar Probe team will work closely with DOE, NASA, and the MMRTG developer to ensure that mission requirements are adequately represented and that the details of the spacecraft design remain fully compatible with the design of the MMRTG. The overall development schedule will also be closely monitored.

In addition, the significant effort that is anticipated to meet all safety requirements typically associated with RTG missions will begin in the pre-formulation phase. Solar Probe will have the great benefit of leverage from the experience of the New Horizons mission team, which has been actively engaged in these activities. An early start is the best mitigation against delays associated with the documentation preparation and approval processes.

Implications. The Solar Probe mission concept is based on a strawman launch date in May 2010, which is well matched to the current MMRTG development schedule. The launch opportunity recurs every 13 months with only minor changes to the mission profile, but the later in the mission development that such a slip occurs, the more costly that delay becomes. Early and close participation in the MMRTG development effort can help reduce such risk.

5.6 Risk Mitigation Activity Schedule

Figure 5-1 shows a high-level timeline of Solar Probe risk mitigation activities. Phase A and Phase B are consistent with the strawman mission launch date of May 2010, and are included here simply to illustrate that risk reduction activities continue into mission implementation. Two years of technology development prior to Phase A is considered sufficient to perform the tasks outlined above and to achieve the goal of retiring risk early.

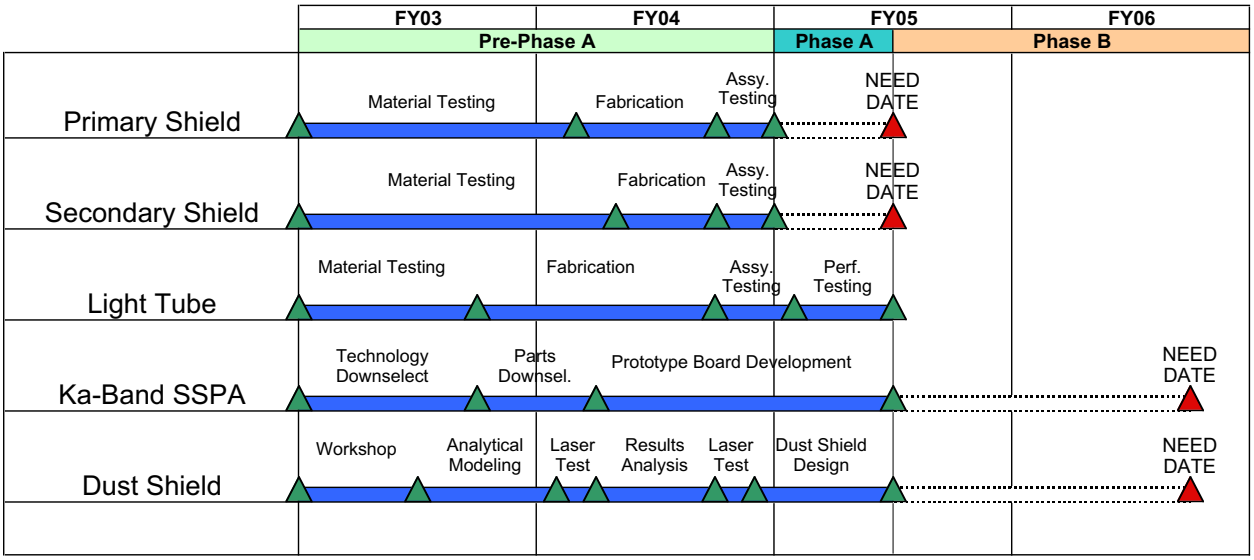

Figure 5-1. Risk mitigation schedule.

APPENDIX A

SOLAR PROBE MASS, POWER, AND SPACECRAFT DIMENSIONS

Table A-1. Solar Probe Equipment List and Detailed Mass Breakdown						
Subsystem Name	**Qty.**	**CBE Mass Each (kg)**	**CBE Mass Total (kg)**	**Growth Allowance (Reserves)**	**Total Mass Not to Exceed (incl/Growth Allowance)**	**Notes and Heritage**
Instruments						
CBE Instrument Mass Total			**39.70**		54.58	
Remote Sensing Instruments						
Remote Sensing, Data Unit	1	3.00	3.00	40%	4.20	Drawn from AO responses, 1997 NRA
Remote Sensing,Power Unit	1	3.00	3.00	40%	4.20	Drawn from AO responses, 1997 NRA
EUVI (Requires Light Tube)	1	3.00	3.00	40%	4.20	Drawn from AO responses, 1997 NRA
EUVI Light Tube	1	0.50	0.50	40%	0.70	APL Structures Estimate
ASC	1	2.80	2.80	40%	3.92	Drawn from AO responses, 1997 NRA
VMH (requires Light Tube)	1	3.00	3.00	40%	4.20	Drawn from AO responses, 1997 NRA
VMH Light Tube	1	0.50	0.50	40%	0.70	APL Structures Estimate
Insitu Instruments						
Insitu, Data Unit	1	3.00	3.00	40%	4.20	Drawn from AO responses, 1997 NRA
Insitu, Power Unit	1	4.50	4.50	40%	6.30	Drawn from AO responses, 1997 NRA
PWS, DPU and Search Coils	1	3.50	3.50	40%	4.90	Drawn from AO responses, 1997 NRA
EPCS, EPD Sensor head and electronics	1	0.70	0.70	40%	0.98	Drawn from AO responses, 1997 NRA
FSWD, Electronics and Sensor Head	1	1.00	1.00	40%	1.40	Drawn from AO responses, 1997 NRA
SWICES Instrument Total Allocated	1	4.40	4.40	40%	6.16	Drawn from AO responses, 1997 NRA
MAG, DPU and Sensor	1	1.80	1.80	40%	2.52	Drawn from AO responses, 1997 NRA
Science Boom	1	5.00	5.00	20%	6.00	Astro-Aerospace telescoping composite boom, 5 m long
Telecommunications						
Tellecommunications System Current Total			**16.920**		**20.30**	
High Gain Antenna	1	4.00	4.00	20%	4.80	APL RF System Estimate, .8 m antenna
HGA Antenna Drive Motor	2	1.30	2.60	20%	3.12	Moog Rotary Actuator Type 2
HGA Mechanical Support Structure	1	1.50	1.50	20%	1.80	APL Structures Estimate
HGA Motor Electronics	1	1.00	1.00	20%	1.20	Stereo Heritage
Ultra Stable Oscillators	2	1.50	3.00	20%	3.60	New Horizons Design
Low Gain Antennas	2	0.35	0.70	20%	0.84	NEAR, ACE, Contour Heritage
Medium Gain Antenna	1	0.56	0.56	20%	0.67	APL RF System Estimate
X-Distrubution	1	0.80	0.80	20%	0.96	APL RF System Estimate
Cables, etc.	1	2.76	2.76	20%	3.31	APL RF System Estimate
Guidance and Control (G&C) System,						
CBE G&C System Current Total=			**40.58**		**48.24**	
IMU	1	6.60	6.60	10%	7.26	Litton
Reaction Wheel	4	5.70	22.80	20%	27.36	ITHACH-TW-4A120
Reaction Wheel Bracket	4	0.50	2.00	20%	2.40	TIMED Heritage, scaled
Star Cameras	2	3.01	6.02	20%	7.22	SODERN, SED-16
DSAD's	2	0.26	0.52	20%	0.62	Stereo Design
DSAD Electronics	1	0.64	0.64	20%	0.77	Stereo Design
Horizon Sensors	1	1.00	1.00	40%	1.40	APL System Engineering Estimate
Star Camera Bracket	1	1.00	1.00	20%	1.20	APL Structures Estimate
Power System,						
CBE Power System Total=			**95.80**		**114.96**	
RTG	3	24.00	72.00	20%	86.40	Multi-Mission Module Baseline, BEST case mass, Emg, 5/23/02
Shunts	2	0.50	1.00	20%	1.20	Based on New Horizons, 282 watts BOL
SRU (Capacitor Bank)	1	6.30	6.30	20%	7.56	New Horizons, mod based on Uno Carlsson inputs
Battery Charger	1	0.50	0.50	20%	0.60	Uno Carlsson Estimate
Battery Boost Converter	1	1.00	1.00	20%	1.20	Uno Carlsson Estimate
Battery(s)	1	2.50	2.50	20%	3.00	SAFT V34570 D, 4.6 Ahr. Case estimate DE
PDU/AIU	1	12.50	12.50	20%	15.00	New Horizons, based on 282 watts, 1 RTG.

Table A-1. Solar Probe Equipment List and Detailed Mass Breakdown

Subsystem Name	Qty.	CBE Mass Each (kg)	CBE Mass Total (kg)	Growth Allowance (Reserves)	Total Mass Not to Exceed (incl/Growth Allowance)	Notes and Heritage
Thermal						
CBE Thermal Sub System Total=			**148.80**		**190.96**	
Primary Heat Shield	1	39.00	39.00	20%	46.80	APL Structures Estimate, 2.8 meter diameter
Primary Heat Shield Support System	1	10.90	10.90	20%	13.08	APL Structures Estimate
Secondary Heat Shield Aerogel	1	62.00	62.00	40%	86.80	APL Structures Estimate, 19 cm .06 gm/cm^3
Secondary Heat Shield face sheets	3	5.70	17.10	20%	20.52	APL Structures Estimate,
SC MLI	1	18.90	18.90	20%	22.68	in**2 area)
Heaters	1	0.00	0.00	20%	0.00	APL Thermal Estimate
Diode Heat Pipe	1	0.90	0.90	20%	1.08	Messenger Design
C&DH						
CBE C&DH System Total=			**14.41**		**17.30**	
Integrated Electronics Module (IEM)	2	6.85	13.70	20%	16.44	Contour/Messenger/STEREO Heritage
TRIOS	14	0.05	0.71	20%	0.86	Contour/Messenger/STEREO Heritage
Propulsion						
CBE Propulsion System Total=			**21.83**		**24.42**	
Tank	1	10.89	10.89	10%	11.98	PSI P/N 80409-1, Centaur Upper Stage Heritage
Piping	1	2.27	2.27	20%	2.72	APL Propulsion System Estimate / Pluto Heritage
Thrusters, 1 lb	16	0.36	5.79	10%	6.37	Heritage
Filter	1	0.16	0.16	10%	0.18	Vacco P/N FOD10635, CONTOUR/Pluto Heritage
latch Valves	2	0.34	0.68	10%	0.75	Vacco P/N V1E10747, CONTOUR/Pluto Heritage
Pressure Transducer	1	0.22	0.22	20%	0.26	Paine P/N 213-76-260-02, CONTOUR/Pluto Heritage
Electrical Connectors	10	0.02	0.23	20%	0.27	APL Propulsion System Estimate
Cabling	1	1.36	1.36	20%	1.63	APL Propulsion System Estimate
Fill and Drain Valves	2	0.11	0.23	10%	0.25	Vacco P/N V1E10433, CONTOUR/Pluto Heritage
Allocated Items						
Primary Structure			85.60	20%	102.72	15% of CBE wet mass allocated
Dust Shield			12.00	20%	14.40	Eng/Willey Allocation, matches with JPL Memo
Harness			21.55	20%	25.86	Allocation based on Timed/Contour/Messenger heritage
Sub Totals						
Best Estimate SC Dry Mass			**497.19**		**613.73**	
Useable Propellant			69.10		69.10	
Residual Propellant			1.37		1.37	
Pressurant			0.60		0.60	
Total consumables			**71.07**	**0%**	**71.07**	
CBE SC Mass Wet			**568.26**		**684.80**	
CBE Max Dry Mass			641.93		641.93	
Max SC Launch Mass			713.00		713.00	
Mass Margin Wet			25.47%		4.12%	
Mass Margin Dry			**29.11%**		4.59%	
Unalocated Reserves (Kg.)			144.74		**28.20**	

Table A-2. Solar Probe Power Budget.

Subsystem/Component	Average EOL Power	Growth-Allow	Power NTE	Ascent - Launch Duty Cycle	Ascent - Launch Avg. Power	Ascent - Launch Peak Power	Ascent - Post Deployment Duty Cycle	Ascent - Post Deployment Avg. Power	Ascent - Post Deployment Peak Power	Maneuver Mode Duty Cycle	Maneuver Mode Avg. Power	Maneuver Mode Peak Power	Ready Mode Duty Cycle	Ready Mode Avg. Power	Ready Mode Peak Power	Ready Mode- Mom. Dump Duty Cycle	Ready Mode- Mom. Dump Avg. Power	Ready Mode- Mom. Dump Peak Power	Science Mode Duty Cycle	Science Mode Avg. Power	Science Mode Peak Power	Science Mode- Mom. Dump Duty Cycle	Science Mode- Mom. Dump Avg. Power	Science Mode- Mom. Dump Peak Power
Instruments	**39.2**	**20%**	**47.0**	0%	**0.0**	**0.0**	0%	**0.0**	**0.0**	100%	**47.0**	**100.0**	100%	**47.0**	**100.0**	100%	**47.0**	**100.0**	100%	**47.0**	**100.0**	100%	**47.0**	**100.0**
Power Subsystem	**25.6**	**17%**	**30.0**		**30.0**	**30.0**		**30.0**	**30.0**		**30.0**	**30.0**		**30.0**	**30.0**		**30.0**	**30.0**		**30.0**	**30.0**		**30.0**	**30.0**
PDU (Includes AIU functions)	18.5	20%	22.2	100%	22.2	22.2	100%	22.2	22.2	100%	22.2	22.2	100%	22.2	22.2	100%	22.2	22.2	100%	22.2	22.2	100%	22.2	22.2
SRU	6.1	10%	6.7	100%	6.7	6.7	100%	6.7	6.7	100%	6.7	6.7	100%	6.7	6.7	100%	6.7	6.7	100%	6.7	6.7	100%	6.7	6.7
Battery Trickle Charge	1.0	10%	1.1	100%	1.1	1.1	100%	1.1	1.1	100%	1.1	1.1	100%	1.1	1.1	100%	1.1	1.1	100%	1.1	1.1	100%	1.1	1.1
G&C Subsystem	**73.8**	**10%**	**81.2**		**32.8**	**0.3**		**64.7**	**196.2**		**64.7**	**82.7**		**64.7**	**79.7**		**73.5**	**64.7**		**73.5**	**200.4**		**73.5**	**73.5**
IMU	29.5	10%	32.5	100%	32.5	0.0	100%	32.5	32.5	100%	32.5	32.5	100%	32.5	32.5	100%	32.5	32.5	100%	32.5	32.5	100%	32.5	32.5
RWAs (4) (max. speed)	28.0	10%	30.8	0%	0.0	0.0	75%	23.1	150.0	75%	23.1	23.1	75%	23.1	38.1	75%	23.1	23.1	75%	23.1	150.0	100%	23.1	23.1
Star Trackers (2)	16.0	10%	17.6	0%	0.0	0.0	50%	8.8	13.4	50%	8.8	26.8	50%	8.8	8.8	100%	17.6	8.8	100%	17.6	17.6	100%	17.6	17.6
Sun Sensors	0.3	10%	0.3	100%	0.3	0.3	100%	0.3	0.3	100%	0.3	0.3	100%	0.3	0.3	100%	0.3	0.3	100%	0.3	0.3	100%	0.3	0.3
Propulsion Subsystem	**90.9**	**10%**	**100.0**		**10.5**	**10.5**		**28.6**	**66.0**		**46.8**	**46.8**		**2.0**	**2.0**		**19.5**	**46.8**		**10.5**	**46.8**		**19.5**	**46.8**
1 lb Thrusters (16, max 4 firing)	33.0	10%	36.3	0%	0.0	0.0	50%	18.2	36.3	100%	36.3	36.3	0%	0.0	0.0	25%	9.1	36.3	0%	0.0	36.3	25%	9.1	36.3
Cat Bed Heaters (16)	30.9	10%	34.0	25%	8.5	8.5	25%	8.5	0.0	25%	8.5	8.5	0%	0.0	0.0	25%	8.5	8.5	25%	8.5	8.5	25%	8.5	8.5
Latch Valves (2)	25.2	10%	27.7	0%	0.0	0.0	0%	0.0	27.7	0%	0.0	0.0	0%	0.0	0.0	0%	0.0	0.0	0%	0.0	0.0	0%	0.0	0.0
Pressure Transducers (2)	1.8	10%	2.0	100%	2.0	2.0	100%	2.0	2.0	100%	2.0	2.0	100%	2.0	2.0	100%	2.0	2.0	100%	2.0	2.0	100%	2.0	2.0
RF Subsystem	**26.1**	**18%**	**30.8**		**6.8**	**6.8**		**30.8**	**30.8**		**30.8**	**30.8**		**30.8**	**30.8**		**30.8**	**30.8**		**30.8**	**30.8**		**30.8**	**30.8**
Transmitter	20.0	20%	24.0	0%	0.0	0.0	100%	24.0	24.0	100%	24.0	24.0	100%	24.0	24.0	100%	24.0	24.0	100%	24.0	24.0	100%	24.0	24.0
Ka-Converter	1.1	20%	1.3	100%	1.3	1.3	100%	1.3	1.3	100%	1.3	1.3	100%	1.3	1.3	100%	1.3	1.3	100%	1.3	1.3	100%	1.3	1.3
USOs	5.0	10%	5.5	100%	5.5	5.5	100%	5.5	5.5	100%	5.5	5.5	100%	5.5	5.5	100%	5.5	5.5	100%	5.5	5.5	100%	5.5	5.5
Avionics Subsystem	**47.8**	**10%**	**52.6**		**52.6**	**52.6**		**52.6**	**52.6**		**32.3**	**52.6**		**32.3**	**52.6**		**32.3**	**52.6**		**52.6**	**52.6**		**52.6**	**52.6**
IEM 1	29.4	10%	32.3	100%	32.3	32.3	100%	32.3	32.3	100%	32.3	32.3	100%	32.3	32.3	100%	32.3	32.3	100%	32.3	32.3	100%	32.3	32.3
IEM 2 (downlink card off)	18.4	10%	20.2	100%	20.2	20.2	100%	20.2	20.2	0%	0.0	20.2	0%	0.0	20.2	0%	0.0	20.2	100%	20.2	20.2	100%	20.2	20.2
Thermal Subsystem	**0.0**	**20%**	**0.0**	0%	**0.0**	**0.0**	0%	**0.0**	**0.0**	0%	**0.0**	**0.0**	100%	**0.0**	**0.0**	100%	**0.0**	**0.0**	0%	**0.0**	**0.0**	0%	**0.0**	**0.0**
Subtotal	303.4	13%	341.6	3%	132.7	100.2		206.7	375.6		251.7	342.9		206.9	295.1		233.2	324.9		244.4	460.6		253.5	333.7
Harness Losses	**4.6**	**13%**	**5.1**		**2.0**	**1.5**		**3.1**	**5.6**		**3.8**	**5.1**		**3.1**	**4.4**		**3.5**	**4.9**		**3.7**	**6.9**		**3.8**	**5.0**
Total	**307.9**		**346.7**		**134.7**	**101.7**		**209.8**	**381.2**		**255.4**	**348.0**		**210.0**	**299.5**		**236.7**	**329.7**		**248.1**	**467.5**		**257.3**	**338.7**
Available Power 3 MMRTG (BOL)					**153 W**			**330 W**																
Available Power 3 MMRTG (3.1 yr)											**293.7 W**			**293.7 W**			**293.7 W**			**293.7 W**			**293.7 W**	
Available Power 3 MMRTG (7.1 yr)														**273.9 W**			**273.9 W**			**273.9 W**			**273.9 W**	
First Pass																								
Power Reserves (W)					18.3	51.3		120.2	-51.2		38.3	-54.3		83.7	-5.8		57.0	-36.0		45.6	-173.8		36.4	-45.0
Power Reserve Margin (%)					13.6%			57.3%			15.0%			39.9%			24.1%			18.4%			14.2%	
Overall Power Margin (%)					**26.9%**			**76.4%**			**30.6%**			**60.0%**			**41.2%**			**34.6%**			**29.5%**	
Second Pass																								
Power Reserves (W)														63.9	-25.6		37.2	-55.8		25.8	-193.6		16.6	-64.8
Power Reserve Margin (%)														30.4%			15.7%			10.4%			6.5%	
Overall Power Margin (%)														**49.2%**			**31.7%**			**25.5%**			**20.8%**	

APPENDIX B

REFERENCES

Armstrong, J. W., and R. Woo, *Contribution to Starprobe Report,* Inter-Office Memorandum no. 3331-80-070, Jet Propulsion Laboratory, Jet Propulsion Laboratory, Pasadena, CA, Dec. 15, 1980.

Banjeree, D., L. Teriaca, J. G. Doyle, and P. Lemaire, Polar plumes and inter-plume regions as observed by SUMER on SOHO. *Solar Phys., 194,* 43–58, 2000.

Beyer, P. E., D. J. Mudgway, and M. M. Andrews, The Galileo Mission to Jupiter: Interplanetary Cruise Post-Earth-2 Encounter Through Jupiter Orbit Insertion, *The Telecommunications and Data Acquisition Progress Report 42-125, 1996*, Jet Propulsion Laboratory, Pasadena, CA, pp. 1-16, May 15, 1996.

Bokulic, R. S., and W. V. Moore, Near Earth Asteroid Rendezvous (NEAR) Spacecraft Solar Conjunction Experiment, *J. Spacecraft Rockets*, *36(1),* 87–91, 1999.

DeForest, C. E., S. P. Plunkett, and M. D. Andrews, Observation of polar plumes at high solar altitudes, *Astrophys. J.*, *546,* 569–575, 2001.

Dirling, R. B. Jr., *Solar Probe Thermal Shield Design—Carbon-Carbon Characterization,* SAIC Technical Report 98/1039, Sept. 4, 1998.

Divine, N., and H. Garrett, Charged particle distributions in Jupiter's magnetosphere, *J. Geophys. Res.*, *88,* 6689, 1983.

Frazer, R. K., *Solar Probe Secondary Heat Shield Material Options*, Technical Memorandum, A1C-02-116, The Johns Hopkins University Applied Physics Laboratory, Laurel, MD, Oct. 21, 2002.

Giacobbe, F., *Thermal Analysis and Conceptual Design of the Solar Probe*, Technical Memorandum SAI-ANYS-385, SWALES Aerospace, Inc., Beltsville, MD (in preparation), 2002.

Gloeckler, G., et al., *Solar Probe: First Mission to the Nearest Star*, *Report of the NASA Science Definition Team for the Solar Probe Mission,* published for NASA by The Johns Hopkins University Applied Physics Laboratory, Laurel, MD, Feb. 1999.

Jensen, J. R., and R. S. Bokulic, Experimental verification of noncoherent Doppler tracking at the Deep Space Network, *IEEE Trans. Aerospace Electron. Sys, 36*(4), Oct. 2000.

Jensen, J. R., and R. S. Bokulic, Highly accurate, noncoherent technique for spacecraft Doppler tracking, *IEEE Trans. Aerospace Electron. Sys., 35*(3), 963–973, July 1999.

Klaasen, K., *Star Detection from Within the Solar Corona*, Jet Propulsion Laboratory, Pasadena, CA, Feb. 14, 2002.

Koerner, M. A., *Telemetry and Command Degradation caused by the RF Signal Amplitude Scintillations Produced by the Near Sun Plasma During the Period Near VRM Superior Conjunction,* Inter-Office Memorandum no. 3392-84-64, Jet Propulsion Laboratory, Pasadena, CA, May 21, 1984.

Lee, S.-C., and C.-J. Lee, *Solar Probe Light Tube Thermal Analysis,* Status Report 2002-1, prepared for D. Lisman under CWO#156, Applied Sciences Laboratory, Inc., Hacienda Heights, CA, June 10, 2002.

Lisman, D., *Design Dust Particle Update*, JPL Interoffice Memo, Solar Probe Project, June 24, 2002.

Lisman, D., *Photon Torque Analysis,* Project Action Item #11, JPL Technical Memorandum to Dave Lehman, Solar Probe Project, Nov. 7, 2001.

Mann, I., *Dust Environment Near the Sun*, Institute of Planetology, Münster, Germany, November 2001 (draft report).

Morabito, D. M., S. Shambayati, S. Butman, D. Fort, and S. Finley, *The 1998 Mars Global Surveyor Solar Corona Experiment,* Telecommunications and Mission Operations Progress Report TMO PR 42-142, Aug. 15, 2000.

Morabito, D. M., S. Shambayati, S. Finley, D. Fort, J. Taylor, and D. Moyd, Ka-Band and X-band observations of the solar corona acquired during superior conjunctions using interplanetary spacecraft, 7th Ka Band Utilization Conference, Genoa, Italy, September 26–28, 2001.

Morabito, D. M., S. Shambayati, S. Finley, and D. Fort, The Cassini May 2000 solar conjunction, *IEEE Trans. Antennas Propagation*, submitted 2002.

NASA, *Announcement of Opportunity: Europa Orbiter/Pluto-Kuiper Express/Solar Probe,* AO 99-OSS-04, Space Science Support Office, Langley Research Center, 1999a.

NASA, *Solar Probe Mission and Project Description*, Space Science Support Office, Langley Research Center, 1999b.

National Academy of Sciences, *The Sun to the Earth—And Beyond, A Decadal Research Strategy in Solar and Space Physics*, Space Studies Board, 2002.

Neugebauer, M., and R. Davies (eds.), *A Closeup of the Sun*, JPL publication 70-78, Jet Propulsion Laboratory, Pasadena, CA, September 1, 1978.

Page, D. E., Exploratory journey out of the ecliptic plane, *Science*, *190*, 845–850, 1975.

Sheeley, N. R., et al., Measurement of flow speeds in the corona between 2 and 30 R_S. *Astrophys. J., 484,* 47–478. 1997.

Strachan, L., R. Suleiman, A. V. Panasyuk, D. A. Biesecker, and J. L. Kohl, Empirical densities, kinetic temperatures, and outflow velocities in the equatorial streamer belt at solar minimum, *Astrophys. J., 571,* 1008–1014, 2002.

Tarditi A., et al., *Photon Pressure Torque from Off-Nadir Pointing*, SAIC Technical Memorandum TM 01-4222-21 to D. Lisman and J. Randolph, Jet Propulsion Laboratory, Pasadena, CA, Oct. 26, 2001.

Webster, J., *Magellan Spacecraft Performance During Solar Conjunction,* Inter-Office Memorandum no. 3395-94-44, Jet Propulsion Laboratory, Pasadena, CA, Aug. 4, 1994.

Xapsos, M. A., G. P. Summers, P. Shapiro, and E. A. Burke, New techniques for predicting solar proton fluences for radiation effects applications, *IEEE Trans. Nucl. Sci., 43*(6), 2772–2777, 1996.

APPENDIX C

ACRONYMS AND ABBREVIATIONS

α	Absorptivity
ε	Emmissivity
µDSAD	Micro Digital Solar Aspect Detector
ACS	Attitude Control System
AIU	Attitude Interface Unit
AO	Announcement of Opportunity
APL	The Johns Hopkins University Applied Physics Laboratory
ASCI	All-Sky Coronagraph Imager
BOL	Beginning of Life
bps	Bits per Second
C&DH	Command and Data Handling
C_3	Maximum Required Launch Energy
C-C	Carbon–Carbon
CCAFS	Cape Canaveral Air Force Station
CCD	Charge-Coupled Device
CCSDS	Consultative Committee for Space Data Systems
CD	Cumulative Distribution
CONTOUR	Comet Nucleus Tour
COTS	Commercial-Off-The-Shelf
DC	Direct Current
DEIS	Draft Environmental Impact Statement
DLA	Declination of Launch Asymptote
DOE	Department of Energy
DPU	Data Processing Unit
DS-1	Deep Space 1
DSAD	Digital Solar Aspect Detector
DSMS	Deep Space Mission System (formerly the Deep Space Network, DSN)
EEPROM	Electrically Erasable Programmable Read-Only Memory
EIT	Extreme Ultraviolet Imaging Telescope on SOHO
ELV	Expendable Launch Vehicle
EMC	Electromagnetic Compatibility
EMI	Electromagnetic Interference
EPCS	Energetic Particle Composition Spectrometer
ESA	European Space Agency
EUVI	Extreme Ultraviolet Imager
FDR	Fault Detection and Recovery
FOV	Field of View

FPGA	Field-Programmable Gate Array
FSWID	Fast Solar Wind Ion Detector
G&C	Guidance and Control
GE	General Electric
GFE	Government-Furnished Equipment
GIS	Graphite Impact Shell
GPHS	General Purpose Heat Sources
GSFC	NASA Goddard Space Flight Center
HGA	High-Gain Antenna
I&T	Integration and Test
IEM	Integrated Electronics Module
IMU	Inertial Measurement Unit
INSRP	Interagency Nuclear Safety Review Panel
JGA	Jupiter Gravity Assist
JHU/APL	The Johns Hopkins University Applied Physics Laboratory
JPL	Jet Propulsion Laboratory
kbps	Kilobits per Second
KSC	Kennedy Space Center
LASCO	Large Angle and Spectrometric Coronagraph on SOHO
LGA	Low-Gain Antenna
LMA	Lockheed Martin Astronautics
LOS	Line of Sight
LVPC	Low Voltage Power Converter
LWRHU	Light Weight Radioisotope Heater Unit
LWS	Living With a Star
MAG	Magnetometer
MDC	Mission Data Center
MESSENGER	MErcury Surface, Space ENvironment, GEochemistry, and Ranging
MGA	Medium-Gain Antenna
MGS	Mars Global Surveyor
MIPS	Millions of Instructions per Second
MLI	Multilayer Insulation
MMRTG	Multi-Mission Radioisotope Thermal Generator
MOC	Mission Operations Center
MOS	Mission Operations System
MOT	Mission Operations Team
MPD	[Solar Probe] Mission and Project Description
N/A	Not Applicable
NASA	National Aeronautics and Space Administration
NEAR	Near Earth Asteroid Rendezvous
NEPA	National Environmental Policy Act

NTE	Not-to-Exceed
PCI	Peripheral Component Interconnect
PDS	Planetary Data System
PDU	Power Distribution Unit
POC	Payload Operations Center
PSAR	Preliminary Safety Analysis Report
PWS	Plasma Wave Sensor
RDM	Radiation Design Margin
REM	Rocket Engine Module
RIO	Remote Input/Output
RF	Radio Frequency
RHCP	Right Hand Circular Polorization
R_J	Radius of Jupiter
rpm	Revolutions per Minute
R_S	Solar Radius
RTG	Radioisotope Thermal Generator
S/C	Spacecraft
S/N	Signal-to-Noise Ratio
SDT	Science Definition Team
SEC	Sun-Earth Connection
SEP	Sun-Earth-Probe
SIRU	Space Inertial Reference Unit
SOHO	Solar and Heliospheric Observatory
SPDT	Single-Pole-Double-Throw
SRG	Stirling Radioisotope Generator
SRI	Southern Research Institute
SRM	Solid Rocket Motor
SRU	Shunt Regulator Unit
SSPA	Solid-State Power Amplifier
SSR	Solid-State Recorder
STEREO	Solar-Terrestrial Relations Observatory
STOC	Science Team Operations Center
STP	Solar-Terrestrial Probe
SWICES	Solar Wind Ion Composition and Electron Spectrometer
SWOOPS	Solar Wind Plasma Experiment on Ulysses
TAC	Thruster and Attitude Control
TCM	Trajectory Correction Maneuver
TID	Total Ionizing Dose
TIMED	Thermosphere, Ionosphere, Mesosphere Energetics and Dynamics
TLM	Telemetry
TPS	Thermal Protection System

TRL	Technology Readiness Level
TtNUS	Tetra Tech NUS, Inc. (subcontractor to JHU/APL)
USO	Ultrastable Oscillator
UVCS	Ultraviolet Coronagraph Spectrometer on SOHO
VEEGA	Venus-Earth-Earth Gravity Assist
VMH	Visible Magnetograph–Helioseismograph
VVEJGA	Venus-Venus-Earth-Jupiter Gravity Assist
XFER	Transfer

JOHNS HOPKINS
UNIVERSITY
Applied Physics Laboratory